ISBN 978-82-471-1408-7 (printed ver.)
ISBN 978-82-471-1408-0 (electronic ver.)
ISSN 1503-8181

Doctoral theses at NTNU, 2009:19

Torunn Smevik

The impedance of brass instruments, with special attention to numerical simulations analyzing the possible influence of wall vibrations

NTNU
Norwegian University of
Science and Technology

Thesis for the degree of
doktor ingeniør
Faculty of Information Technology, Mathematics
and Electrical Engineering
Department of Electronics and Telecommunications

NTNU
Norwegian University of
Science and Technology

Doctoral theses at NTNU, 2009:19

NTNU

The impedance of brass instruments, with special attention to numerical simulations analyzing the possible influence of wall vibrations.

Thesis for the degree of doktor ingeniør

Trondheim, January 2011

Norwegian University of
Science and Technology
Faculty of Information Technology,
Mathematics and Electrical Engineering
Department of Electronics and Telecommunications

NTNU
Norwegian University of Science and Technology

Thesis for the degree of doktor ingeniør
Faculty of Information Technology, Mathematics
and Electrical Engineering
Department of Electronics and Telecommunications

ISBN 978-82-471-1408-7 (printed ver.)
ISBN 978-82-471-1408-0 (electronic ver.)
ISSN 1503-8181

Doctoral Theses at NTNU, 2009:19

Printed by Tapir Uttrykk

Contents

1 Introduction **4**

2 Numerical and experimental methods **8**

2.1 Definitions 8

2.1.1 Glossary of symbols 8

2.1.2 Instantaneous fundamental frequency 9

2.2 The Norwegian birch bark lur 11

2.3 Numerical methods 14

2.3.1 The wave equation 14

2.3.2 The finite element method 15

2.3.3 The transmission line model 20

2.4 Measurements and sound recordings 24

2.4.1 Acoustical input impedance measurements 24

2.4.2 Sound recordings 25

3 Brass instruments **29**

3.1 Playing a brass instrument 29

3.2 The acoustic impedance of a straight cylinder 31

3.3 Impedance of more complicated geometries 34
3.3.1 The bell 35
3.3.2 The valves 41
3.3.3 The mouthpiece 41
3.3.4 The whole instrument 43
3.4 Impedance of the driver 45
3.5 Some comments on different playing techniques 47
3.5.1 Slurs 50
3.5.2 Lip trills 50
3.5.3 Stopped horn 51
3.5.4 Mutes 51

4 Wall vibrations **55**

4.1 Introduction 55
4.2 Theory 56
4.3 Literature review 57
4.4 Finite element simulations 58
4.4.1 2-D simulations 59
4.4.2 3-D simulations 63
4.4.3 Materials 65
4.5 Results 66
4.5.1 Cylindrical tubes 66
4.5.2 3-D cylinders 78
4.5.3 Various other forms 89

4.6 Discussion and conclusion 104

A Matlab files **110**

A.1 TLM simulation 110

A.2 Lur recordings analyzis 115

A.3 Instantaneous frequency 117

B Material parameters **119**

C Comsol resolution **120**

Chapter 1

Introduction

Man has made music for a very long time. Bones with lateral holes assumed to be flutes has been found on a number of Stone Age sites, and the musical tradition of China, India and Ancient Greece goes thousands of years back. The knowledge about how to make music and of instruments has throughout most of the history of music been based on the experience and traditions of musicians and instrument makers. The development from animal horns and sea shells, probably mainly blown for signalling purposes, to today's modern orchestral instruments has come along in leaps and bounds driven forward by the demands of musicians, composers and audience. Changes in music style have demanded more of the musicians, making it necessary to make better or new instruments. These changes in the instruments often make it possible to produce music with wider variety then what originally started the improvements.

Most of the brass instruments of natural origin have a nearly conical bore, making it possible to play parts of a more or less harmonic series. Reproducing these instruments in metal or wood made it possible to get instruments of any length and for example add a flared bell for better sound radiation. Producing as much sound as possible was important for an instrument group often used during war or hunt. In Europe, depictions of instruments of varying size and shape have been found in paintings and carvings throughout the Middle Ages. As very few instruments have been found, their development must be found through pictures and written sources and it can often be difficult to find details in bore or construction (for example whether the instrument had a detached or lose mouthpiece). War trumpets and hunting horns have been used by many European cultures, and during the first part of the 2. millennia after Christ their importance as musical instruments increased. However, compared to for example the string instruments they were confined by their inability to produce chromatic scales, even in the high register.

For the brass instruments, the most important change to take them from a signal instrument to a fully integrated member of today's orchestras was the ability to play chromatic. From the 14. century there are written records of trumpets being used for dance music in Europe. For the high register the overtones would be close enough to be musically

useful, and as there is diatonic music written for the deep register for trumpets, it can be assumed that they were fitted with a slide to make it possible to play. Woodwind-like holes on brass instruments can be traced back to the tenth century, and one of the most popular instruments of the Renaissance and the Baroque periods, the cornett, was a conical instrument with finger holes. As the finger holes needed to be of the same dimension as the bore at the position of the holes to maintain the harmonic relationship between the modes, the size and form of the instruments that could give a satisfying musical result were restricted by the size of the musicians fingers until the inventions of keys and pads in the 19th century.

Some instruments, like the cornett, were developed gradually and their origin can't be dated. Others, like the serpent [1], saxophone and Wagner tuba [2], were invented to meet a specific need from musicians or composers. Other inventions are just for a part of the instrument, but have influenced the development of whole instrument groups. For brass instruments without a conical bore, finger holes can't be used to get a chromatic scale and the musician is stuck with the harmonic series given by the instruments geometry. This led to the invention of crooks [3] of different lengths that could be added to the instrument so it could be played in different keys. However, changing the crooks was time-consuming, so the composers had to make sure the musicians had time between key-changes. Horn players had to have up to 11 crooks to be able to play in all keys, which could lead to certain confusion. The hand-in-bell technique made it possible to play chromatically on the horn, but the timbre of the open and stopped tones were very different. When the first successful valve was patented in 1814, it meant that chromatic brass instruments with nearly any bore could be constructed.

These changes were all based mostly on experience and technical finesse. Although Pythagoras' discovery of the numerical intervals in musical scales and the following discussion about why some sounds are more pleasing than others are about 2000 years old, most agree that the field of acoustics (including musical acoustics) was established some 150 years ago, when Hermann von Helmholtz published his *Die Lehre von den Tonempfindungen als physiologische Grundlage für die Theorie der Musik*. Since then, much research have been done on musical instruments, both by amateurs and professionals, covering most of the physical aspects of why instruments sound as they do, performance practice etc.

In the middle of the 18th century, Daniel Bernoulli, Leonhard Euler and Joseph Louis Lagrange first discussed how acoustical waves behave in horns. Their work wasn't continued, although several scientists worked with the problem in the 19the century. In 1919, the American physicist A. G. Webster published a report about second-order partial differential equation for the velocity potential as a function of time and of distance along an acoustic horn, the so-called horn equation or Webster's equation. It can be used to calculate the propagation of pressure waves in a horn assuming that no transverse modes

[1] Most probably invented by Edme Guillaume in 1590 [2]

[2] The saxophone was patented by Adolphe Sax in 1846, and the Wagner tuba was invented by Wagner after he visited Sax's workshop in 1853 [2]

[3] Invented around 1700 in Vienna by a Herr Leichnamschneider

exist.

Because of the continuously increasing capacity of computers for numerical calculations, the recent years have seen rapid improvement when it comes to analyzing many of the problems linked with the understanding of why instruments sound as they do. However, accurate models of whole instruments are still normally too memory demanding. A numerical model of a brass instruments would for example have to include the whole bore (including boundary layers, temperature gradients and interaction between the vibrating air and the instruments walls), the players lips and mouth cavity, the surrounding air and possibly the musician and would require a very fine mesh in parts of the instrument, making the task quite enormous. Luckily it is possible to model only parts of the instrument at the time, which is what this thesis attempts to do.

Some of the main areas of research on brass instrument acoustics are the behaviour of the vibrating lips, non-linear propagation and input impedance. The modelling of the brass players lips and their interaction with the air column have been influenced by studies done in the recent years on the mechanical reed woodwind instruments (models with 1 degree of freedom) and the human vocal folds (models with more than one degree of freedom). These models have come up with useful information concerning for example the excitation of brass instruments.

As the brass instruments are played on frequencies very close to the resonances of the bore, many studies on how to measure the acoustical input impedance accurately and find it theoretically have been done. Commercially available measuring equipment to reconstruct the bore from impulse responses (for for example instrument makers) have been made based on the devices used for scientific research. For instruments with flares that increase rapidly the plane-wave approximation isn't very good, and to improve the theoretical results multi-modal approaches have been tried successfully. It has been found that at fortissimo shock-waves are generated in some brass instruments, a phenomenon associated with the brightness of the sound of trombones and trumpets.

A brass instrument can be divided into two main parts when played, the instrument itself and the lips. This thesis will focus on the instrument and what changes in the shape and make of the bore can influence. Chapter 2 consist of 4 parts. The first part is definitions, the second part is a presentation of the Norwegian birch bark lur, a traditional, valve less Norwegian brass instrument made of wood that has been used for some of the analysis. The third part is a short introduction to finite elements and the transmission line method used in chapter 6 and 7 and the fourth and overview of recordings and measurements methods used in this thesis. Chapter 3 is an introduction to brass instruments, mainly concentrating on how the shape of the instrument (the bore) influences the sound. The influence of the mouth piece and the bell on the acoustical input impedance is analyzed, both with measurements on real instruments and simulations.

Chapter 4 deals with wall vibrations and FEM (finite element) simulations of instruments made of different materials. The influence of wall vibrations on the sound of the instrument is one of the fields in musical acoustics where opinions among scientists are

divided, although most musicians and instrument-makers agree that instruments of different materials differ when played. The wall vibrations can influence the instrument in different way, either by changing the acoustical input impedance or by directly radiating sound. It is also possible that the musician can be influenced by vibrations transmitted to the lips trough the mouthpiece. FEM simulations of the wall vibration induced by the vibrating air column or a shaker are studied to see whether they can shed some light on the problem.

This thesis was founded by the Norwegian Research Council and the work was done mainly at the Acoustics research group at NTNU. Thanks to my supervisors Ulf Kristiansen and Jan Tro, and to Øvind Lervik for always having the right microphone. Also thanks to Geir Solum, Marit Bøttcher and Irene Ruud for providing sound samples.

Chapter 2

Numerical and experimental methods

2.1 Definitions

2.1.1 Glossary of symbols

- p Acoustic pressure
- ρ Intstantaneous density (kg/m^3)
- ρ_0 Equilibrium density
- f Frequency
- ω Angular frequency

$$\omega = 2\pi f \tag{2.1}$$

- λ Wavelength
- c Speed of sound, if not mentioned otherwise $c = 343m/s$.
- k Wave number

$$k = \frac{\omega}{c} = \frac{2\pi}{\lambda} \tag{2.2}$$

- Z Impedance
- Z_m Mechanical impedance
- Z_r Radiation impedance
- $\vec{u}$ Particle velocity

- u Particle speed
- **Young's modulus** is a measure of the stiffness of a material. For small strains it is defined as the rate of change of stress with strain.
- **Poisson's ratio** is the ratio of the relative contraction strain to the relative extension strain.

2.1.2 Instantaneous fundamental frequency

One of the techniques used to analyze musical signals in chapter 6 is a time-domain method that finds the instantaneous fundamental frequency. This can be used to find oscillations in the frequency that are too rapid to be found with for example Fourier analysis without re-sampling the signal at a higher sampling frequency. A similar, more robust method was developed by Tucker and Bates [42]. If a signal has a stable waveform with a clear maximum or minimum per period in the time domain , this can be used to find the instantaneous fundamental frequency as a function of time. A matlab algorithm [1] finds the maxima shown in figure 2.1.

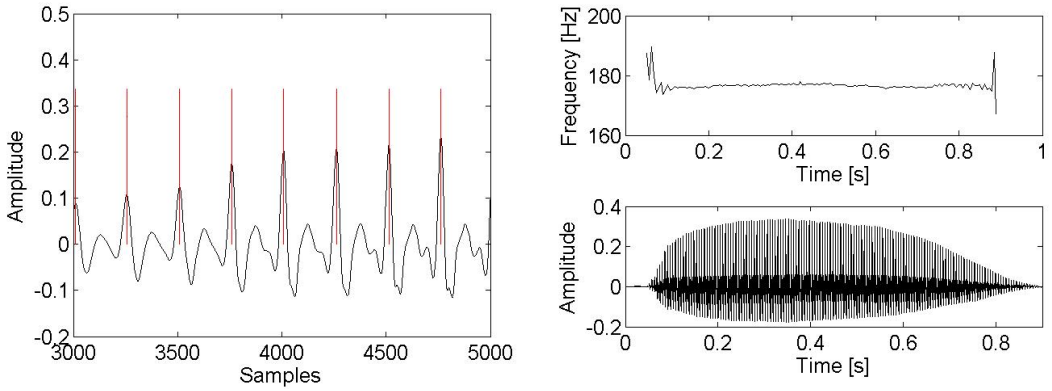

Figure 2.1 *The left figure shows a close-up of a sound signal in the time domain, the horizontal lines depict the maxima of each period. The right figure shows a signal in the time domain (bottom) and its instantaneous fundamental frequency (top). The instantaneous fundamental frequency varies with nearly 15 Hz before it becomes stable.*

If s is the number of samples per period in the time domain and f_s the sampling frequency, the time t_{inst}per period is $\frac{s}{f_s}$ and the instantaneous fundamental frequency f_{inst} equals $\frac{1}{t_{inst}} = \frac{f_s}{s}$.

The accuracy of f_{inst} is given by the accuracy of s, which equals ± 1 and gives an upper frequency for $s - 1$ and a lower frequency for $s + 1$.

[1] In Appendix A.3

$$\Delta^{+} f_{inst} = \frac{f_s}{s} - \frac{f_s}{s+1} = \frac{fs}{s(s+1)} \tag{2.3}$$

$$\Delta^{-} f_{inst} = \frac{f_s}{s} - \frac{f_s}{s-1} = \frac{fs}{s(s-1)} \tag{2.4}$$

If $s >> 1$, which it should be if the signal is recorded with a high enough sampling rate for the frequency range in question, this reduces to

$$\Delta f_{inst} = \frac{fs}{s^2} \tag{2.5}$$

Since $s \propto \frac{1}{f_{inst}}$, the accuracy is better for lower instantaneous fundamental frequencies. If the sampling frequency f_s is changed, the numbers of samples per period s changes as well. Assuming that s is much bigger than the ratio of the new sampling frequency to the old one,$s_{new} \approx s_{old} * \frac{f_s^{new}}{f_s^{old}}$. Together with equation 2.5 this gives that the accuracy as a function of the sampling frequency is proportional to $\frac{1}{f_s}$.

$$\Delta f_{inst}\left(f_s\right) \propto \frac{1}{s} \propto \frac{1}{f_s} \tag{2.6}$$

2.2 The Norwegian birch bark lur

Most of the instrument mentioned in this thesis (for example the horn and the trumpet) are common modern instruments that don't need further introduction. The Norwegian birch bark lur is a traditional Norwegian brass instrument made of wood, and as it is not as common or well known a presentation of the instrument is in place. It was used partly because its simple geometry and the fact that it is made of wood made it possible to insert a probe microphone half way into the instrument.

Figure 2.2 *Modern reconstruction of a bronze lur*

The lur or neverlur is a Norwegian folk instrument in the same family as the alphorn. Lurs both of metal and wood have been used in Norway, the metal lurs are made of bronze and date from the Bronze Age. It is the instrument from the Nordic prehistory that has been given the most attention. The majority of finds are from Denmark, but bronze lurs are also found in Norway, Sweden and Russia. They were probably ceremonial instruments used in pairs. The most developed instruments consist of an S-shaped conical tube, 1.5 to 2.25 m long, with a circular, ornate end-plate and mouth-piece. A modern reconstruction of a bronze lur can be seen in figure 2.2. In addition to the actual instruments, several depictions in rock carvings have been found. The wooden lurs are more recent, although that can be due to the fact that none has survived from before the Migration Period. The lur is the instrument most often mentioned in the Norse sagas [40], often used for summoning people to war. Sverre Sigurdsson (King of Norway 1177-1202) summoned his men to fight with one called Andvake, an old word for insomnia.

Most scientists agree that a hollow wooden tube found in the Oseberg ship burial [2] is some sort of wooden trumpet or lur. It is a tube put together by to half cones and has five ring shaped carvings, possibly to give support to what kept the two halves together. Lurs made today are made in about the same way. In Denmark two whole instruments and parts of two others have been found in wells. Both resemble the modern lurs, except they don't have a clear cup inside the mouthpiece. They are about 80 cm long and date to early Germanic Iron Age (375 - 530 AD). The upper 17 cm of another instrument with

[2]The Oseberg ship is a Viking ship in a burial mound in Vestfold, Norway. It was excavated in 1904-1905 and the burial is dated to around 850, parts of the ship to around 800.

a mouthpiece like a trumpet was found in a big excavation in Denmark in the fifties [41]. It is from sometime between 200 to 500 AD and was found together with a considerable amount of weapons, enough for an army of about 1000 men.

Figure 2.3 *Lur in C made by Magnar Storbækken, Tolga, Norway in 1997. The whole instrument is 120 cm, the bell 70 cm. The walls are made of two pieces of Norwegian spruce that have been glued together and then bound with birch bark.*

More recently the instruments were used as a communication device by dairy maids in the mountains and fishers on the coast of Western Norway, especially the shorter instrument known as stuttlur (short lur). Modern lurs are normally made of Norwegian spruce (Picea Abies) and birch bark, the Danish instruments were made of hazel (Corylus) wound with ash (Fraxinus) or alder (Alnus). Unlike the alphorn it is normally straight and so short it can be held up while playing. The length is normally between 1.2 and 2 meters.

There are three different ways of making a lur. Either the instrument can be made of only birch bark, it can be cut out of one piece or wood or put together by two halves that are glued together and then bound with birch bark. Some instrument makers use one piece whereas others make a bell, a mid-section and a separate mouthpiece, thus making it possible to change the tuning of the instrument by using a longer or shorter mid-section similar to the crooks used on for example valve-less horns.

For the shorter lurs, about half of the instrument consists of a conical bell, the other half is the mouthpiece and a tapered mid-section, which typically will increase from about between 5 and 8 mm at the mouthpiece throat to about 2 cm where the conical bell starts. The bell has a max radius of ca 10 cm. The near conical shape gives impedance peaks close to a harmonic series, the lowest harmonics being a bit too high due to the influence of the mid-section. The lurs normal playing range is from the third harmonic to the sixth or seventh, possibly higher for longer instruments. It is possible to play the lower harmonics but they are normally not used very much since they are difficult to play and out of tune with the rest of the useful overtones. The lower harmonics are dominated by the first overtone and the higher harmonics by their fundamental, giving the lur a quite piercing sound.

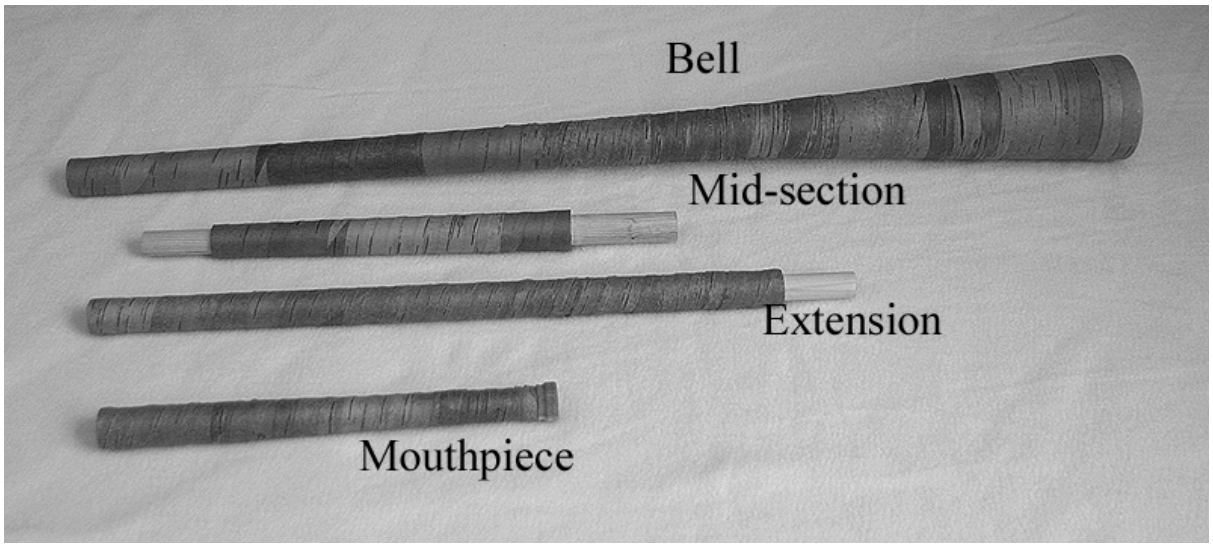

Figure 2.4 *B/F lur in 3/4 pieces made by Magnar Storbkken, Tolga, Norway in 2006. The B-lur consists of the bell, mid-section and mouthpiece, by adding the extension the instrument becomes an F-lur. The instrument is made of spruce and wound together with birch-bark. The mouthpiece rim is similar to that of a French horn mouthpiece (since the B/F tuning is what most French horn players are used to).*

2.3 Numerical methods

The sound field in and around a brass instrument is governed by equations that are usually too complicated for exact solutions, especially when interactions with the instruments walls are being considered. There exist several numerical methods to find approximate solutions, both in the time-domain and in the frequency-domain. Two numerical methods were used in this thesis, the Finite Element Method and the Transmission Line Model. The former has been used with the software COMSOL multiphysics, the later with a Matlab program (Appendix A.1).

2.3.1 The wave equation

To analyze the whole instrument, including for example viscosity and temperature gradients, the relevant equation would be the nonlinear Navier-Stokes equation [3]

$$\rho\left(\frac{\partial\vec{u}}{\partial t}+\left(\vec{u}\cdot\nabla\right)\vec{u}\right)=-\nabla p+\left(\frac{4}{3}\eta+\eta_B\right)\nabla\left(\nabla\cdot\vec{u}\right)-\eta\nabla\times\nabla\times\vec{u} \tag{2.7}$$

where η is the coefficient of shear viscosity and η_B the coefficient of bulk viscosity. In linear the acoustics, the term $\eta\nabla\times\nabla\times\vec{u}$ is normally ignored, as it represents dissipation of energy associated with turbulence, laminar flow etc and is normally only of importance near boundaries.

Equation 2.7 can be simplified : when the left side of the equation is linearized using the linearized equation of continuity and the adiabat, the result is a wave equation including losses

$$\left(1+\tau_S\frac{\partial}{\partial t}\right)\nabla^2 p=\frac{1}{c^2}\frac{\partial^2 p}{\partial t^2} \tag{2.8}$$

where $\tau_s=\frac{\left(\frac{4}{3}\eta+\eta_B\right)}{\rho_0 c^2}$ is the relaxation time and c the thermodymanic speed of sound. With monofrequency motion, equation 2.8 is reduced to a Helmholtz equation

$$\nabla^2 p+\mathbf{k}^2 p=0 \tag{2.9}$$

The simplifications include:

[3] Chapter 8.2 in [3]

- It is assumed that the fluctuations in p and ρ are much smaller than the atmospheric equilibrium values.
- Heat conduction, viscosity, vorticity and gravity are neglected.
- All mean flow related terms are zeroed.

In many situations it will be of interest to find solutions for a discrete set of frequencies instead of a solution in the time domain. It can be easier to interpret than a complicated pulse scattering, and is often less computationally demanding. Solutions in the frequency domain can be found from the Helmholtz equation 2.9 and have been the main focus of the part of this thesis concerned with numerical simulations (especially chapter 7).

Several methods for solving the Helmholtz equation numerically or computing the scattering of waves in the time domain exist. The methods used in this thesis are Finite Element Method (FEM) for the frequency domain and Transmission Line Matrix method (TLM method) for the time domain. The finite element method is a numerical technique used for finding approximate solutions for partial differential equations and integral equations. In this thesis, is has been used to compute the impedance and sound radiation from more or less instrument-like tubes, with and without the vibration of the walls influencing the system. The TLM method is based on Huygens' model of wave propagation and was originally developed for electromagnetic fields but has been adapted to acoustic propagation too. In this thesis, the TLM method was used to calculate wave propagation to see how different bells will reflect the outgoing wave.

2.3.2 The finite element method

The finite element method (FEM) [14] is a numerical method to solve partial differential equations (PDEs). One of the central ideas behind FEM is to divide the area to be examined into smaller elements, and to approximate an equation that is close to the equation that needs to be solved, but is numerically stable on each element. The corners on the elements are called nodal points. The values for the nodal points are calculated and then used to find the values for the rest of the area by using form functions. The form functions are determined by the shape of the elements.

To show how the solution to the acoustical problems can be found, the Helmholtz equation is a logical way to start. Substituting $k = \frac{\omega}{c}$, equation 2.9 can be written

$$\nabla^2 p + \frac{\omega^2}{c^2} p = 0 \tag{2.10}$$

Assuming that the boundaries are all hard surfaces gives the boundary condition

$$\frac{\partial p}{\partial n} = 0 \tag{2.11}$$

If the Helmholtz equation is satisfied in the domain Ω and on the boundary Γ, then for any functions W and $\bar{W}$

$$\int_\Omega W \left(\nabla^2 p + \frac{\omega^2}{c^2} p \right) d\Omega = 0 \tag{2.12}$$

$$\int_\Gamma \bar{W} \frac{\partial p}{\partial n} d\Gamma = 0 \tag{2.13}$$

The two equations 2.12 and 2.13 can be combined to

$$\int_\Omega W \left(\nabla^2 p + \frac{\omega^2}{c^2} p \right) d\Omega + \int_\Gamma \bar{W} \frac{\partial p}{\partial n} d\Gamma = 0 \tag{2.14}$$

This is a good place to start the finite element discretization. For each element a set of nodes are defined, and a shape function. If a geometry have a total of M nodes, the pressure p can be approximated as

$$p = \sum_{i=1}^{N} N_i p_i = \mathbf{Np} \tag{2.15}$$

where $\mathbf{N}$ and $\mathbf{p}$ are the matrices for the shape functions and nodal pressures. The shape functions are chosen so that they are zero everywhere except on one element. Writing equation 2.14 for a set of functions W_j and $\bar{W}_j$ gives a set of N equations :

$$\int_\Omega W_j \left[\nabla^2 (\mathbf{Np}) + \frac{\omega^2}{c^2} (\mathbf{Np}) \right] d\Omega + \int_\Gamma \bar{W}_j \frac{\partial \mathbf{Np}}{\partial n} d\Gamma = 0 \tag{2.16}$$

Replacing $W_j = N_j$ and $\bar{W}_j = -N_j$, where N_j are the shape functions, equation 2.16 can be written

$$\int_\Omega N^T \left(\nabla^T \nabla N d\Omega \right) p + \omega^2 \left(\frac{1}{c^2} \int N^T N d\Omega \right) + \left(\int_\Gamma -N^T (n \nabla N) \, d\Gamma \right) p = 0 \tag{2.17}$$

The first part of equation 2.17 cancels by integrating by parts, and only two terms remain.

$$\left(\int_\Omega (\nabla N)^T (\nabla N)\, d\Omega\right) p + \omega^2 \left(\frac{1}{c^2}\int_\Omega N^T N d\Omega\right) p = 0 \tag{2.18}$$

By chosing the shape functions N_j equation 2.18 can be solved and the pressure found.

Software : COMSOL multiphysics

The software used for the FEM simulations was COMSOL Multiphysics, formerly known as FEMLAB. COMSOL Multiphysics is a finite-element based software for simulating multiphysics and single-physics applications, and incorporates application interfaces, drawing, meshing and solvers. COMSOL Multiphysics has several different modules, the Acoustics module contains the tools to model acoustic wave propagation in solids and stationary and moving fluids [49]. The Structural Mechanics Module models classical stress-strain analyses, deformation and contact abilities etc, and was used to model the instrument walls [50].

The acoustics module contains several different applications.

- **Pressure acoustics** The dependent variable is the pressure p.
- **Pressure Acoustics, Boundary modal analysis** The dependent variable is the pressure p.
- **Aeroacoustics**
- **Aeroacoustics, Boundary modal analysis**
- **Structural mechanics, Plane strain/Solid stress-strain**

The pressure acoustics application solves the Helmholtz equation

$$\nabla\left(-\frac{1}{\rho_0}(\nabla p - \mathbf{q})\right) - \frac{\omega^2 p}{\rho_0 c^2} = Q \tag{2.19}$$

where $\mathbf{q}$ is a dipole source and Q a monopole source. Both are optional, and when both equals zero, the resulting homogeneous equation becomes an eigenvalue PDE to solve for eigenmodes and eigenfrequencies.

Boundary conditions In *pressure acoustics* the dependent variable is the pressure p.

Boundary conditions for the acoustic pressure domain

- Impedance boundary condition:

$$\mathbf{n} * \left(- \left(\frac{1}{\rho_0} \right) (\nabla p - q) \right) - \frac{i\omega\rho}{Z} = 0 \tag{2.20}$$

When impedance Z is set to that of air (1.25 * 343 Pa s/m) the boundary represents the surrounding air, this works well as the outer boundary of the simulated area when the direction the waves hit the boundary is known and it can be made sure that the incident is normal. $\mathbf{n}$ is the outward bound normal vector.

- Radiation condition

For 2 dimensional geometry

$$\mathbf{n} * \left(\frac{1}{\rho_0} (\nabla p - q) \right) = -i \left(kp + \frac{(k - \mathbf{kn}) \, p_0 e^{-i(\mathbf{kr})}}{\rho_0} \right) \tag{2.21}$$

For 2 dimensional, axi-symmetric geometry

$$\mathbf{n} * (\left(\frac{1}{\rho_0} (\nabla p - q) \right) + \frac{ikp}{\rho_0} + \frac{i}{(2k)} \nabla_T p \tag{2.22}$$

$$= \frac{i}{(2k)} \nabla_T p_0 e^{-i(\mathbf{kr})} + \left(ik - \frac{i \, (\mathbf{kn}) \, p_0 e^{-i(\mathbf{kr})}}{\rho_0} \right) \tag{2.23}$$

$$-i \left(kp + \frac{(k - \mathbf{kn}) \, p_0 e^{-i(\mathbf{kr})}}{\rho_0} \right) \tag{2.24}$$

For both

$$\mathbf{k} = k \mathbf{n}_k \tag{2.25}$$

The radiation condition creates a plane wave.

- Hard wall

$$\mathbf{n} * \left(\frac{1}{\rho_0} (\nabla p - q) \right) = 0 \tag{2.26}$$

This boundary condition is used when the wall is reflecting and rigid.

- Normal acceleration

$$\mathbf{n} * \left(\frac{1}{\rho_0} (\nabla p - q) \right) = a_n \tag{2.27}$$

This boundary condition is used when the walls are vibrating because of the influence from the vibrating air inside and outside the instrument, and is set equal to the normal acceleration of the wall.

- Axial symmetry, $r = 0$, the symmetry axis
- PML (perfectly matching layers)

  A PML is not really a boundary condition but a extra domain that absorbs the incoming waves without creating reflection. With a PML it is not that important that the wave hits the boundary perpendicular as for the impedance boundary condition, it works well for a wide range of incidence angles and wave shapes. The models solves the following equation

$$\nabla(-\frac{1}{\rho_0}\nabla p) - \frac{\omega^2}{\rho_0 c_s^2} = 0 \tag{2.28}$$

  on the PML domain.

Eigenfrequency analysis If all the sources are removed from the frequency domain equation, the only possible solutions with a value other than zero corresponds to a discrete set of angular frequencies ω_n. The solutions have a well defined shape but not a defined amplitude. The solutions are known as the eigenmodes, their corresponding frequencies as eigenfrequencies and they identify the resonance frequencies of the structure.

2.3.3 The transmission line model

Huygens ' Principle says that a wave front consists of several secondary radiators which give rise to spherical wavelets. The envelope of these wavelets forms a new spherical wave front. As a consequence of the repetition of this mechanism, Huygens explained wave propagation. To implement this process on a computer, the field has to be discretized in time and space. The discrete Huygens' model is a synonym for the Transmission-line Matrix method or Transmission-Line Matrix model (TLM) [10] [11] [12] [13]. The TLM method operates in the time domain, and therefore requires no solution of the differential equation.

The TLM method was first applied to electromagnetic waveguide problems, but has later also been used to solve problems with acoustical wave propagation. The name derives from the fact that the lines connecting the nodes in the studies of electromagnetic wave propagation are modelled as electrical transmission lines.

Discretizing of Huygens' wave principle

Assuming a two-dimensional sound space with Cartesian coordinates, divided in nodes separated by the distance δl, the sound propagation takes place between isolated nodes in the matrix. An energy impulse arriving at one of the nodes is normally split in 4, and is reradiated in the north, south, east and west directions. Each shattered pulse has one fourth of the incident energy, and thus the magnitude of the scattered pulse is 1/2, since the pressure values are related to the square root of the energy values.

This is equivalent to the travelling of pulses over an orthogonal mesh made of pairs of transmission lines, or thin acoustic tubes. The junction will represent a discontinuity in the impedance, so the same sort of scattering as at the nodes takes place. In this study, the field and the individual transmission line velocities are chosen to be directly related to the speed of sound, so it is unnecessary to go into detailed modelling of the transmission lines.

When four impulses are incident to the four branches at the same time $t = k\delta t$ (where δt is the time required for a pulse to travel the distance δl, c the propagation speed along the branch and k is an integer), the response can be obtained by superposing the contribution from all the branches. The transmitted pressure pulses will have a positive sign, while the reflected pulse will have a negative sign as it meets a parallel of three similar lines.

The scattered impulse S^n at branch n at time $t + \delta t = (k + 1)\delta t$ is given as

$$S^n_{k+1} = \frac{1}{2} \sum_{m=1}^{4} P^m_k - P^n_k \tag{2.29}$$

where P_k^n is incident impulse at the branch n at time $t = k\delta t$.

In matrix form, this equation becomes

$$\begin{bmatrix} S^1 \\ S^3 \\ S^3 \\ S^4 \end{bmatrix}_{k+1} = \frac{1}{2} \begin{bmatrix} -1 & 1 & 1 & 1 \\ 1 & -1 & 1 & 1 \\ 1 & 1 & -1 & 1 \\ 1 & 1 & 1 & -1 \end{bmatrix} \begin{bmatrix} P^1 \\ P^3 \\ P^3 \\ P^4 \end{bmatrix}_k \tag{2.30}$$

Pressure $P_{i,j}$ at the node is given by

$$P_k^{i,j} = \frac{1}{2} \sum_{n=1}^{4} P_k^n \tag{2.31}$$

where the subscripts i, j represents the node position $(x, y) = (i\delta l, j\delta l$

The scattered pulses travel along the branches in the reverse directions, and become incident pulses to the adjacent elements at whose node the scattering again takes place. The arriving pulses on a node at position (i, j) are represented by the scattered pulses at the adjacent nodes as

$$P_{i,j}^1 = S_{i-1,j}^3 \tag{2.32}$$

$$P_{i,j}^3 = S_{i+1,j}^1 \tag{2.33}$$

$$P_{i,j}^2 = S_{i,j-1}^4 \tag{2.34}$$

$$P_{i,j}^4 = S_{i,j+1}^2 \tag{2.35}$$

where the P^1 are a pulse travelling east, while S^1 is pulse reflected east. In the same way, 2 denotes north, 3 west and 4 south.

Modelling of the boundaries

In the TLM modelling, the boundaries are usually placed halfway between two nodes or at the ends of an element's branch arms. This can be achieved by introducing the reflection coefficient R.

For a rigid wall, the reflection coefficient R equals 1. To implement this condition, the following relation is applied:

$$P_k^n = S_k^n \tag{2.36}$$

For the sound absorbing wall, the reflection coefficient is defined as

$$R = \frac{Z_a - Z_0}{Z_a + Z_0} \tag{2.37}$$

where $Z_0 (= \rho_0 c_0)$ is the characteristic impedance of the branch or the medium when ρ_0 is the density of the medium and c_0 the speed pf sound. However, R does not equal the reflection coefficient for the wave reflected at the wall of the TLM network where the sound speed is different from the one over a single arm or a branch. In this case for the wave perpendicularly incident into the wall, the reflection coefficient equals

$$\Gamma = \frac{Z_a - Z_\tau}{Z_a + Z_\tau} \tag{2.38}$$

where $Z_\tau (= \rho_0 c_\tau)$ is the characteristic impedance for the sound c_τ propagating in the network. The relation between R and Γ is given by combining equations 2.37 and 2.38

$$R = \frac{(1+\Gamma) - \sqrt{2}(1-\Gamma)}{(1+\Gamma) + \sqrt{2}(1-\Gamma)} \tag{2.39}$$

In the special case of the non-reflective boundary in which Γ is set to 0, R is given as

$$R = \frac{1-\sqrt{2}}{1+\sqrt{2}} = -0.1716 \tag{2.40}$$

The non-reflective boundary condition is only exact for the case of perpendicular incidence.

Simulation

The method was implemented in matlab, the program can be found in Appendix A. To ascertain a perpendicular incidence and achieve the right solution in length, the instrument or part of the instrument was modelled as several cylindrical pipes set end to end. This gave the outline of the instrument wall a form as a step function.

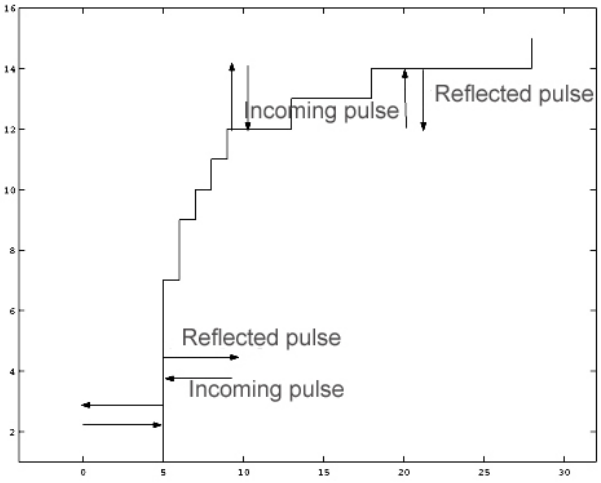

Figure 2.5 *Horn outline as a step function with reflected waves, one unit on the axes equals one step in the chosen resolution*

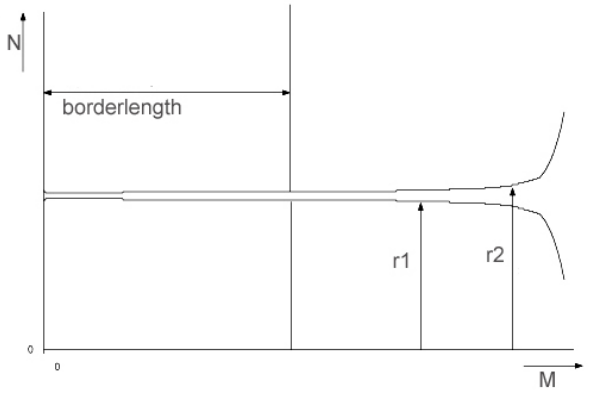

Figure 2.6 *Geometry of the calculated area*

The parameter *borderlength*, shown in figure 2.6 sets how far back the sound propagation should be calculated for cases where parts of the air surrounding the instrument is omitted. The other parameters in the figure, r1 and r2, show how the outline of the horn was given in the program, as the number of steps from N=0 to the horn wall. The horn wall was thought as lying between two nodes, thus placing r1[k] inside the horn and r1[k-1] outside the horn. The horn walls were modelled as rigid walls while the borders of the calculated area were treated as totally absorbing with a reflection coefficient $r = -0.1716$.

2.4 Measurements and sound recordings

To analyze how a brass instrument works, how the different parts influence the sound and how different playing techniques work, both impedance measurements and sound recordings were analyzed.

2.4.1 Acoustical input impedance measurements

The acoustical input impedance [4] is often used to describe an instrument. The maxima of the acoustical input impedance decide which tones can be played on the instrument, so analyzing it can give information on for example tuning. It is usually assumed that the acoustical input impedance is determined by the inner dimensions of the instrument, and that bends and material of the instrument don't influence it. Several systems have been developed to measure it, both time-domain and frequency-domain methods [38], [43] . The device used in this thesis, the Brass Instrument Analyze System (BIAS), is a frequency-domain system developed by the Institut für Wiener Klangstil in Vienna. It is an compact system that is easy to use, fairly fast and easily commercially available. For bore reconstructions, higher resolution can be obtained with time-domain methods [43], but as the purpose was mainly to compare different instrument, the resolution and frequency range were sufficient.

Figure 2.7 *Kitchen funnel used for BIAS measurements in figures 3.11 and 3.12. The funnel has a diameter of about 8 cm at the widest openening, and 8 mm at the narrow end.*

The instrument is connected with the measuring device by the mouthpiece 2.8) and excited with a frequency sweep. To reduce the signal/noise ratio, the measurements should be made in an anechoic chamber or place with similar acoustics. A special microphone picks up the signal, which then is analyzed to find the impedance and impulse response of the instrument. The diagnosis analysis allows the user to choose between un-weighted and weighted impedance curves, pulse response and evaluation of the intonation. There is also an optimizing software for for example improvement of intonation or cloning of an instrument.

[4] For more on the acoustical input impedance see chapter 6.1.2

(a) BIAS (b) With mouthpiece (c) Fastening the mouthpiece

Figure 2.8 *BIAS measuring device. The capillary tubes are connected to a speaker inside the measuring device, the USB cable to a PC. The mouthpiece is placed over the microphone and fastened so that the instrument can be connected with to the BIAS measuring device via the mouthpiece.*

2.4.2 Sound recordings

3 different microphone arrangements have been used for the recordings, one for just recording the sound from the instrument, one for recording the sound at the musicians ear and one for recording the sound inside the instrument.

The former recordings are, if not otherwise mentioned, made in the anechoic chamber with either a DAT recorder or hard-disk recorder (Sound Devices), one or two Brüel and Kjær free-field 1/2 " condenser microphones Type 4190, a Norsonic pre-amplifier (type 1201) and a Norsonic amplifier (type 336). If not mentioned otherwise, the microphone was placed at about the same height as the mouth of the player, 1.5 meters in front of the musician. Some of the recordings were re-sampled at a higher sample-rate using the re-sample function in Cool Edit Pro. The recordings at the ear of the musician were made using the outer microphone on the earplug PARAT made by SINTEF. PARAT is designed as an intelligent hearing protector, which has an ear-piece with , among other things, an inner and an outer microphone. A Brüel and Kjær free-field 1/2 " condenser microphone Type 4190 was used to record the reference sample.

Figure 2.11 shows the experimental setup for recordings of the standing wave inside the lur (see chapter 5 for more on the instrument). The instrument was mounted to a table to make sure it didn't move during the measurement. A probe microphone (a Brüel and Kjær 1/2 " condenser microphone Type 4134 with a 80 cm long probe with inner diameter 3.5 mm and outer diameter 4 mm) was inserted in the instrument, making it possible to record the sound field in about half of the instrument before literally hitting the wall. A similar microphone was used to record a reference signal 10 cm in front of the instrument.

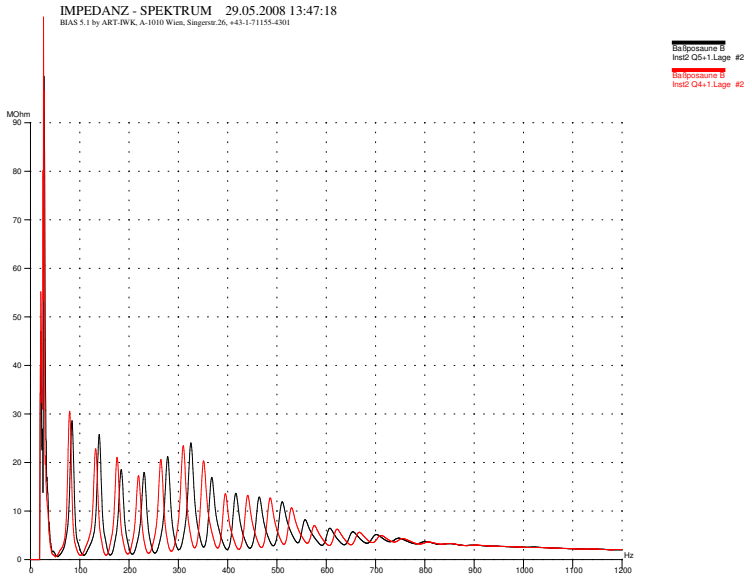

(a) Impedance

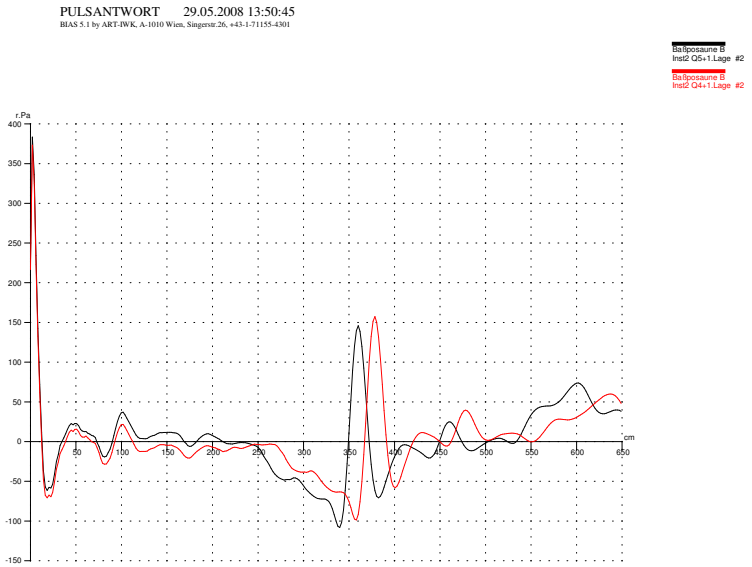

(b) Impulse response

Figure 2.9 *BIAS measurement of the impedance of a trombone. Figure a shows the impedance of two positions, figure b the impulse response of the same two positions. Inside the mouthpiece the sound the two impulse responses are identical, but since the length of the tubing is changed, the bell is not located at the same place. The data can also be retrieved as text files (for the BIAS51 version up to 4000 Hz with a resolution of 0.5 Hz)*

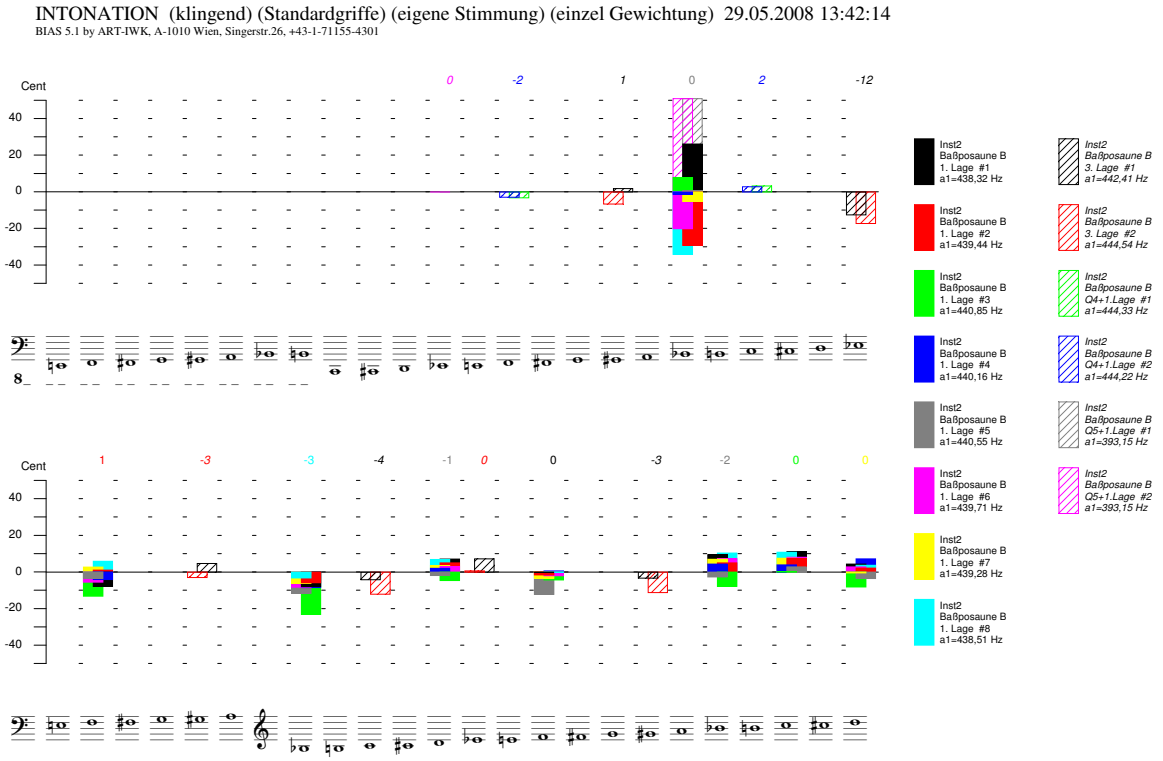

Figure 2.10 *By measuring all the positions or valve combinations the intonation can be calculated as deviation in cent from a perfect harmonic series, for all possible slide positions or valve combinations. The figure shows the intonation for a bastrombone, when one note has several columns it means that it can be played with different slide positions.*

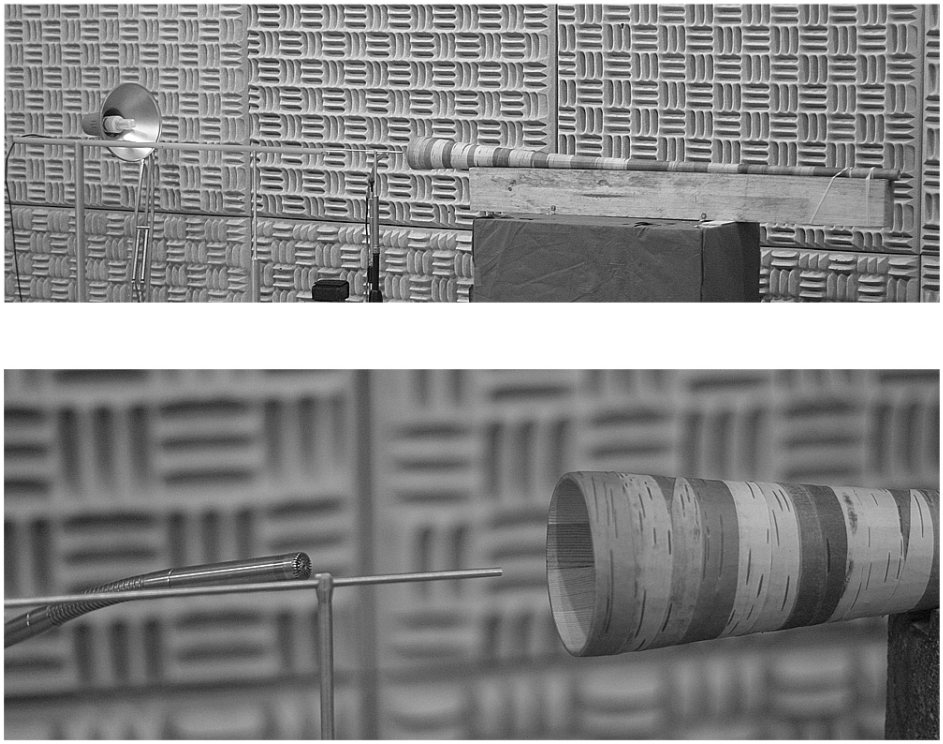

Figure 2.11 *Measuring the standing waves inside the lur. The instrument was fastened to a table to stop it from moving when being played. A measuring microphone was placed right outside the bell for reference recordings. The probe microphone was inserted into the bell and pulled out during playing. The probe covered about half of the instrument. The recordings where made in the half anechoic chamber of the Acoustics group at NTNU.*

Chapter 3

Brass instruments

Despite the name, the common denominator for the brass instruments is not that they are made of brass. They can be made of nearly any material, just as some of the woodwinds, f.ex. the flute and the saxophone are made of metal. Several older brass instruments, like the cornett and the serpent, were made of wood, as are today's alphorns. They can also be made of horn, like the Jewish shofar, or shell. When it comes to shape, size and material, the brass instruments form a diverse group of a great variety. Some brass instruments, like the alphorn, nearly have the shape of a cone with mouthpiece. Others, like today's modern orchestral brass instruments, have far more complicated bores. The length also varies, for modern brass instruments from the 46 cm long pocket-trumpet to the 5.5 meter long BB-flat tuba [48].

According the Hornbostel-Sachs system [44], the brass instruments are classified as aerophones, meaning the sound is produced by a vibrating air column. For the sub group non-free aerophones (wind instruments proper), which includes the brass instruments, the excited air column is inside the instrument unlike the free aerophones, f.ex. the bull-roarer. The brass instruments form a sub-group of the non-free aerophones, as do the woodwinds. The woodwinds are divided in edge-blown instrument and reed instruments, dependent on how the air flow is inserted into the instrument. The brass instruments all have that in common that the vibrating lips modulate the DC air flow from the lungs, so they are also called lip-reed instruments or labrosones (lip-vibrated instruments). They are divided into two sub-groups, although they have the same form of excitation, one for natural instruments like the alphorn and bugle and one for chromatic instruments like the trombone and the trumpet.

3.1 Playing a brass instrument

As a simplification, assume a wind instrument with its internal air column containing only one single, longitudinal standing wave (monofrequency)[5]. The wave gets reflected

both at the open end and at the closed end where the lips are. If no energy is supplied from outside to the air column, the traveling wave will die out due to losses both in the air, in the boundary layers along the walls and at the two ends. For brass instruments, this energy comes in the form of the air blown into the instrument by the player. A steady flow will not work, as the energy must be added the right time: when the pressure in the mouthpiece is at its highest. If it is added when the mouthpiece pressure is at its lowest it will only serve to even out the pressure, not add to the traveling wave. This decides at which frequencies a standing wave can be easliy sustained. The standing wave usually does not consist of only one frequency, as can be seen in figure 3.1, showing the standing waves inside a lur. The sound pressure inside the instrument forms a standing wave, with an amplitude that decreases closer to the opening of the instrument. Figure 3.1(b) shows the normalized amplitude of the 3 first harmonics.

A brass instrument has an antinode at the mouthpiece, the lips of the player can be approximated to a closed end, creating a pressure maximum. Pressure in the mouthpiece fluctuates above and below a mean value, and to add to the wave, the air flow created by the player must flow strongly while the pressure is high and close when it is low. In other words, the standing wave must have a frequency so that the bore equals the wavelength times $\frac{2*n+1}{4}$. Then, because of the phase shift at the open end, the reflected wave will be in phase with the incoming wave the second time it comes back to the lips. The pressure at the pipe entrance and the air flow velocity into the pipe must be in phase. The phase difference between the opening of the lips and the pressure variation goes from 0 degrees to 180 with increasing frequency. To be able to play, the standing wave frequency must be higher than the natural resonance frequency of the lips, at which the pressure variation and the opening of the lips are 90 degrees out of phase.[5]

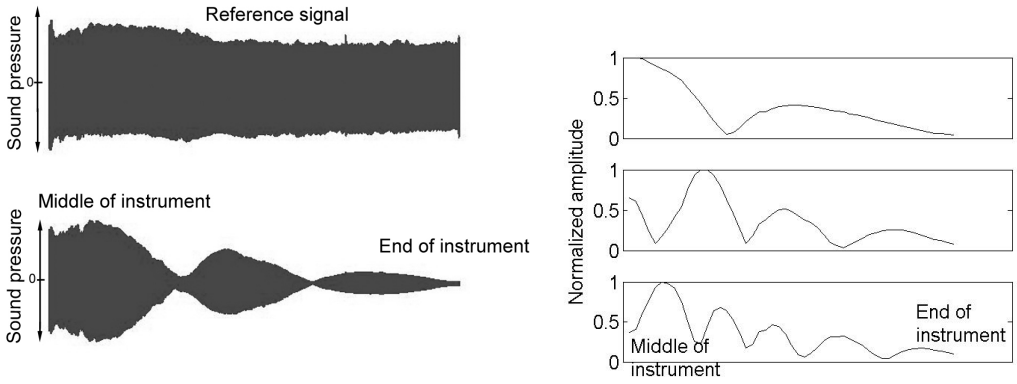

(a) 650 Hz (b) 380 Hz

Figure 3.1 *The left figure shows the reference signal 1 meter outside the instrument, a lur tuned in C, and the standing wave pattern in the bell for a 650 Hz tone. The bell is conical and about 70 cm long, the whole instrument is 120 cm long. The right figure shows the normalized amplitude of the 3 first harmonics inside the bell of the instrument.*

3.2 The acoustic impedance of a straight cylinder

To decide for which frequencies the conditions for a sustainable standing wave are met for a cylinder, it is necessary to find the acoustical input impedance. The mechanical impedance $\mathbf{Z}_m$ is the ratio between the complex driving force $\mathbf{f} = Fe^{j\omega t}$, and its resultant complex speed $\mathbf{u}$ at the point where the force is applied [1].

$$\mathbf{Z}_m = \frac{\mathbf{f}}{\mathbf{u}} \tag{3.1}$$

The acoustic impedance for a plane wave equals $\frac{p}{vS}$, where S is the surface area through which the acoustic wave propagates. The specific acoustic impedance z is the ratio of the sound pressure to the particle velocity.

$$z = \frac{p}{v} = ZS \tag{3.2}$$

where Z is the acoustic impedance.

The impedance is often given as the sum of the mechanical reactance X_m and the mechanical resistance R_m, $Z_m = R_m + jX_m$. In for example Kinsler and Frey [3] the resonance angular frequencies are defined as the frequency or frequencies where X_m vanishes so that the impedance is pure real and equals R_m, its minimum value. This is also the frequencies at which the driving force supplies maximum power to the oscillating system. The driving force f is assumed constant, so at the frequencies when Z_m reaches a minimum, the complex speed reaches a maximum. As brass instruments have an antinode at the closed end, we are interested in the frequencies for which Z_m reaches a maximum (which from now on will be called resonances), since the notes that can be played are slightly above these. An example of this can be seen in table 3.1, the mean frequencies of the notes played on the lur are all slightly higher than the resonance frequencies.

For a pipe with length L that is driven at $x = 0$ and terminated in a mechanical impedance Z_{mL} at $x = L$, the continuities of force and particle speed require that the mechanical impedance of the wave at $x = L$ equals Z_{mL}. Assuming only plane waves, input mechanical impedance Z_{m0} can be expressed as a function of Z_{mL} and the wavenumber k

$$\frac{Z_{m0}}{\rho_0 cS} = \frac{\frac{Z_{mL}}{\rho_0 cS} + j\tan kL}{1 + j\left(\frac{Z_{mL}}{\rho_0 cS}\right)\tan kL} \tag{3.3}$$

Substituting $\frac{Z_{mL}}{\rho_0 cS}$ with $r + jx$ results in

[1] Chapter 10.2 in [3]

Table 3.1 *Impedance peaks of a lur tuned in C measured with BIAS compared to the mean frequencies of the notes played on the instrument.*

Harmonic	Frequency in Hz	Mean frequency of **played** notes in Hz
		75
1	139.0	140
2	279.5	280
3	386.5	400
4	516.0	530
5	647.0	660
6	781.0	790
7	918.0	940

$$\frac{Z_{m0}}{\rho_0 c S} = \frac{r + j\,(x + \tan kL)}{(1 - x\tan kL) + jr\tan kL} \tag{3.4}$$

which can be used for finding the resonance and antiresonance frequencies of the system. If the resistance is zero ($r = 0$), the input impedance disappears at resonance frequencies for which $\tan kL = -x$ and is infinite at antiresonance when $\tan kL = \frac{1}{x}$. When $r \neq 0$,the input impedance (equation 3.4) has minimum reactance when the phases of the numerator and denominator are the same.:

$$\frac{x + \tan kL}{r} = \frac{r\tan kL}{1 - x\tan kL} \tag{3.5}$$

Equation 3.5 can be rewritten quadratic and solved for $\tan kL$ for a pipe with radius r and length L, driven at $x = 0$ and closed at $x = L$ so that $\left|\frac{Z_{mL}}{\rho_0 c S}\right| \to \infty$. The input impedance is then given as $\frac{Z_{m0}}{\rho_0 c S} = -j\cot kL$. For an open ended pipe with the same dimension the easiest assumption is that the mechanical impedance $Z_{mL} = 0$ which would lead to $\frac{Z_{m0}}{\rho_0 c S} = -j\tan kL$ and impedance minima at $f_n = \frac{n}{2}\frac{c}{L}$ for $n = 1, 2, 3...$, but since sound is radiated from the end of the pipe $Z_{mL} = Z_r$, where Z_r is the radiation impedance of the open end of the pipe.

The impedance for a flanged, cylindrical pipe with a radius r and length L, assuming $\delta >> r$

$$\frac{Z_{mL}}{\rho_0 c S} = \frac{1}{2}(kr)^2 + j\frac{8}{3\pi}kr \tag{3.6}$$

Solving equation 3.6 gives $\tan kL = -\frac{8kr}{3\pi}$ for resonance frequencies. Since $\frac{8kr}{3\pi} << 1$, $\tan n\pi - k_n L = \frac{8}{3\pi}ka \approx \tan\frac{8ka}{3\pi}$, therefore $n\pi = k_n L + \frac{8}{3\pi}k_n a$ and impedance minima are:

$$f_{n,min} = \frac{n}{2}\frac{c}{L + \frac{8}{3\pi}r} \tag{3.7}$$

For an unflanged pipe with the same dimensions

$$\frac{Z_{mL}}{\rho_0 c S} = \frac{1}{2}(kr)^2 + j0.6kr \tag{3.8}$$

with impedance minima at

$$f_{n,min} = \frac{n}{2}\frac{c}{L + 0.6r} \tag{3.9}$$

and impedance maxima at

$$f_n = \frac{2n+1}{4}\frac{c}{L + 0.6r}, n = 0, 1, 2, 3... \tag{3.10}$$

As a rule, the effective length L_{eff} can be written as a function of the length L and the radius r of the pipe

$$L_{eff} = L + corr_{end} * r \tag{3.11}$$

assuming that the radius of the pipe is much smaller than the wavelength. If the resonance frequencies f_n are known, the end correction can be calculated from

$$corr_{end} = \frac{1}{r}(\frac{cn}{2f_n} - L) \tag{3.12}$$

If fN can be measured as $f\text{N} \pm \Delta f$, the end correction can be calculated with a resolution $\Delta corr_{end}$

$$\Delta corr_{end} = \frac{cn}{r}\left(\frac{1}{2\left(f_n \pm \Delta f_n\right)} - \frac{1}{2f_n}\right) \tag{3.13}$$

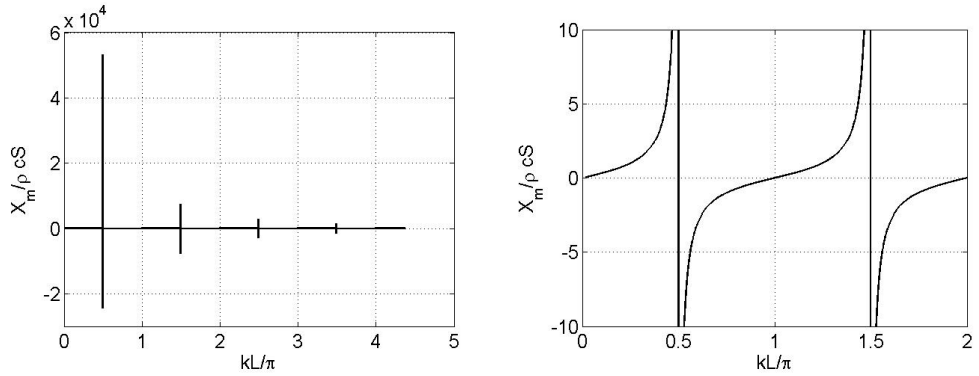

(a) Input mechanical reactance X_m (b) Close-up of X_m

Figure 3.2 *Input mechanical reactance X_m of a 3 meter long air-filled cylindrical pipe with open termination and radius = 1 cm.*

3.3 Impedance of more complicated geometries

Cylinders and cones are the only two forms for which exact solutions of the wave equation can be calculated. As the resonances in cylinders don't form a harmonic series (equation 3.10) but have the ratio 1:3:5:7 etc, and the notes that can easily be played will be just above the resonances, cylinders don't make good instruments if the goal is an harmonic series. A perfect cone would make a harmonic series if it was possible to play it. As it is closed in one end, that could prove difficult, so for nearly conical instruments like the alphorn the mouthpiece must compensate for the part of the cone that is cut off. A conical instrument would also face other problems like f.ex. radiation efficiency and placement of the valves. Some older brass instruments, like the cornette and the serpent, are nearly conical and played with finger holes to produce a whole chromatic series. To have valves a part of the instrument must be cylindrical and so other parts of the bore will have to compensate for the cylindrical part breaking up the harmonic series of the cone.

Most modern brass instruments consists of four major parts

- The bell
- A cylindrical section with valves
- A conical leadpipe
- The mouthpiece + a tapered backbore

3.3.1 The bell

Flares in older instruments were probably made to radiate the sound effectively rather than shifting the resonance frequencies. In modern instruments, the flared bell shifts the resonances of the pipe, and is normally chosen so that the resonances from the 2nd upward come as close to a harmonic series as possible. The 1st is left flat, up to a fifth flatter than the fundamental of the harmonic series made up by the rest of the resonances, and is normally not used. [5] The frequency shift is due to the shift of the reflection point where the wave is reflected back in the bell. In a straight cylinder, the wave is reflected more or less at the opening of the tube. For a flared bell, the situation is more complicated. Figure 3.3 shows a Gauss pulse traveling in 3 different pipes, one cylindrical pipe and two with flared end sections. In the flared sections, the pulses are reflected earlier and their shaped distorted compared to the reflection in the cylindrical pipe.

Figure 3.4(c) shows how the frequencies of a 2 meter long cylinder are shifted upwards by the flares in figures 3.4(a) and 3.4(b). The higher resonances in the widest bell have low amplitudes. When the wavelength can't be considered small compared to the dimension of the bell the reflection coefficient decreases and the standing wave get increasingly difficult to sustain.

The transmission coefficient T_Π of a unflanged cylinder is quite small and depends on the frequency [3].

$$T_\Pi \approx (ka)^2 \tag{3.14}$$

If the pipe ends in a wide flange, the radiated acoustic power is approximately doubled. A gradual flare, like a bell, will increase the low-frequency power transmission even more. This means that the bell not only shifts the resonances, it also changes the radiation of the pipe. A bell radiates the higher harmonics much more efficiently than a cylindrical tube, thus contributing to the harmonic spectrum that characterize the instrument. A wide, steep flare radiates more and makes the instrument louder than a smaller flare. When the wavelength is of the same size as the bell, nearly no wave is reflected, the resonances flatten out and it becomes increasingly difficult to support the standing wave. Over this cut-off frequency the sound is radiated effectively but intonation gets increasingly difficult because of the lack of clear resonances.

Compared to the cylinder, bells are rather directional at higher frequencies and radiate most of the energy straight forward, a fact well known for everyone who has been sitting in front of the brass section in an orchestra. As can be seen in figure 3.5, the sound radiated from a straight cylinder is more evenly distributed around the opening of the instrument then the sound from a bell. Also, the sound level differs more for different frequencies for the cylinder than for a cylinder with a bell attached.

The directivity of the bell means that the sound from the instrument sounds different

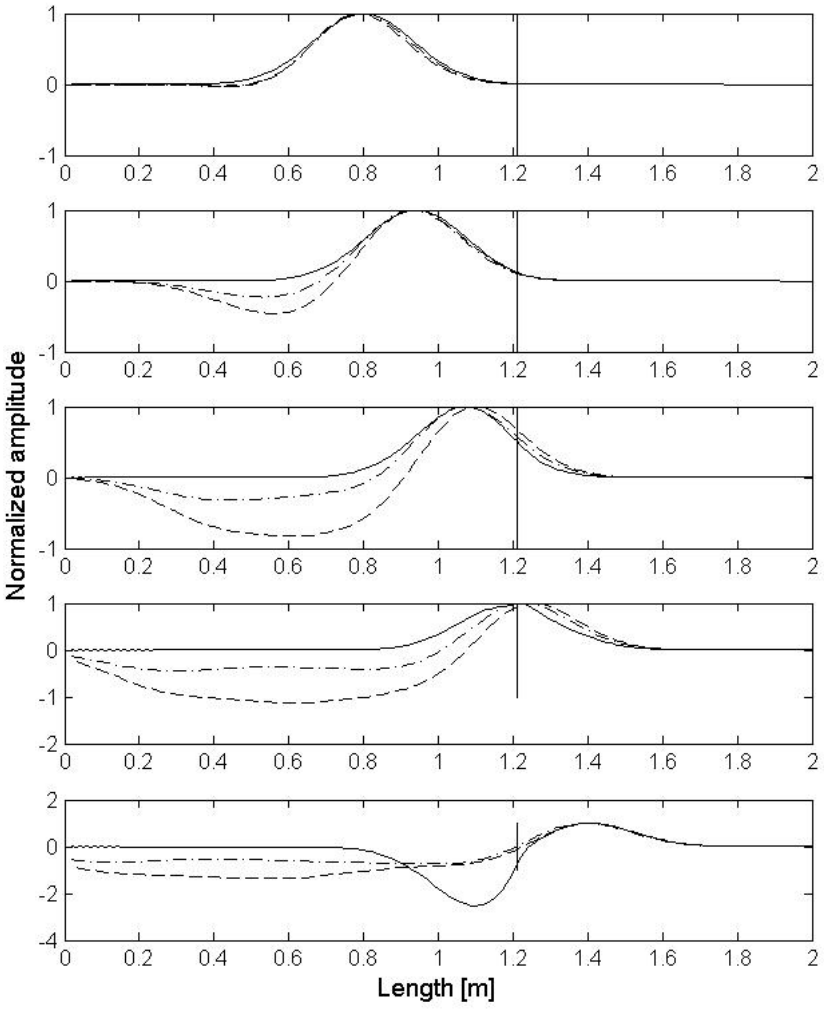

Figure 3.3 *The normalized amplitude of a Gauss pulse (found with TLM simulation) with middle frequency 400 Hz traveling down 3 different tubes with the same length and the same bore the first 70 cm, one 121 cm long cylinder, a 70 cm cylinder with a 51 cm long flared and wide bell (dashed line) and a 70 cm cylinder with a 51 cm long flared and narrow bell (dotted and dashed line). The wave is shown after (from top to bottom) 0.0071, 0.0076, 0.0082, 0.0088, 0.0094 seconds, (one time step equals 2.94e-5 seconds). The widest bell is large compared to the wavelength so no clear reflections occur and it would be hard to maintain a standing wave.*

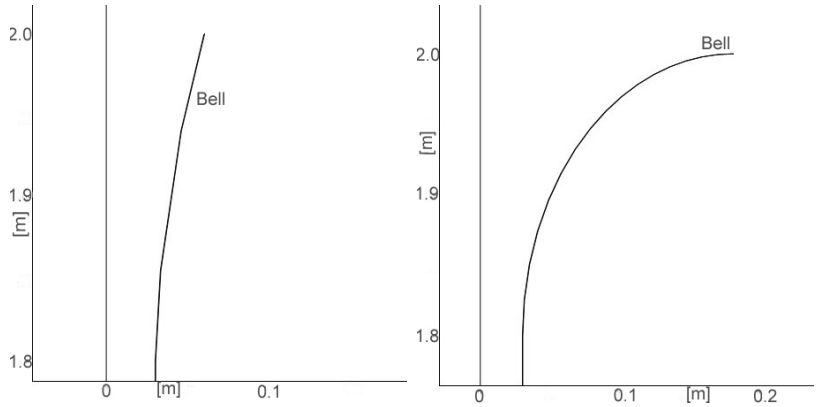

(a) Bell A

(b) Bell B

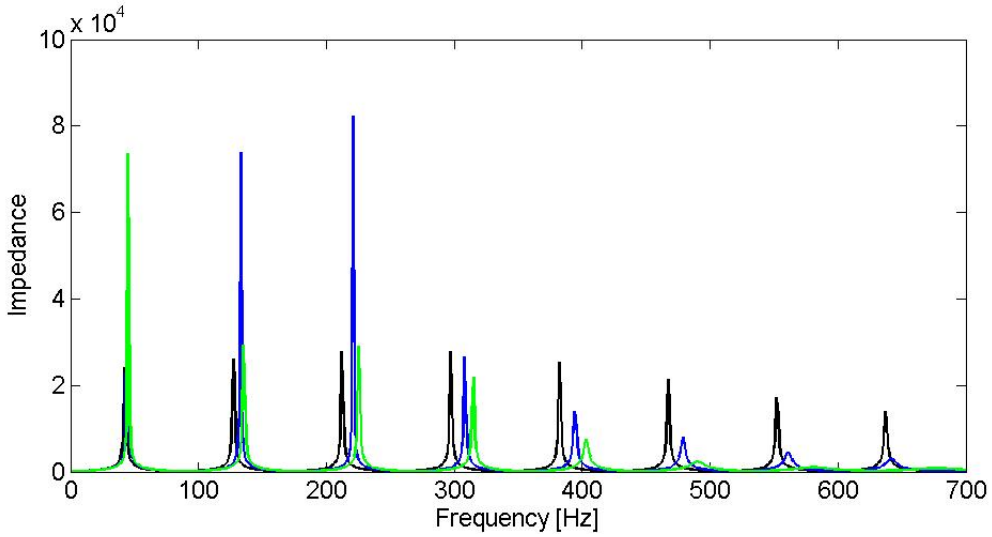

(c) Impedance

Figure 3.4 *Figures a and b show the geometry of two bells which are placed on 1.8 m long cylindrical tube so the instruments have a total length of 2 meters. In figure c the acoustical input impedance (found wit COMSOL multiphysics) of both the instruments (Bell a is blue and bell B is green) and of a 2 meter long cylindrical tube (black) are plotted. The maxima for the instruments with bell are shifted upwards compared to the cylinder, more so for the wider bell.*

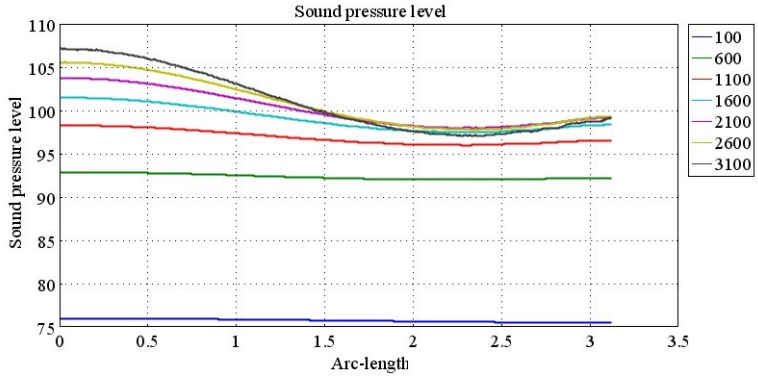

(a) Cylinder

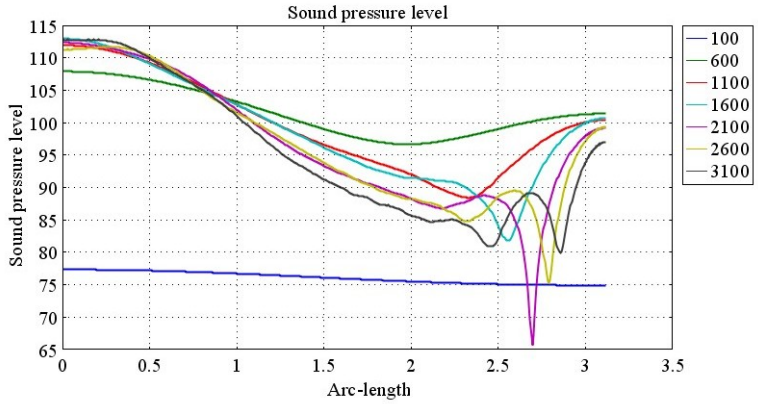

(b) Cylinder + Bell B from figure 3.4(b)

Figure 3.5 *The sound pressure level (calculated with COMSOL multiphysics)sampled at a half circle with radius = 1 meter and center in the middle of the cylinder/bell for 7 different frequencies, starting straight in front of the instrument and ending 1 meter down from the bell/opening. For most frequencies, the bell has a more varying directivity with higher sound pressure straight in front of the instrument compared to sideways and backwards than the cylinder. The sound pressure levels from the different frequencies (except 100 Hz) have about the same amplitude straight in front of the instrument for the flared horn and vary more for the cylinder. Both instruments were placed in a circle with radius 4 meters, the simulations had approximately 13000 elements.*

from different angles. Figures 3.6 and 3.7 show the frequency spectra of a French horn (figure 3.6) and a trombone (figure 3.7). Since the high-register radiates strongest straight out from the bell, the trombone has more high register straight in front of the musician whereas the hornist (or anyone sitting on the right hand of the player) will hear more of the high register than listeners in front the musician, especially on the right ear.

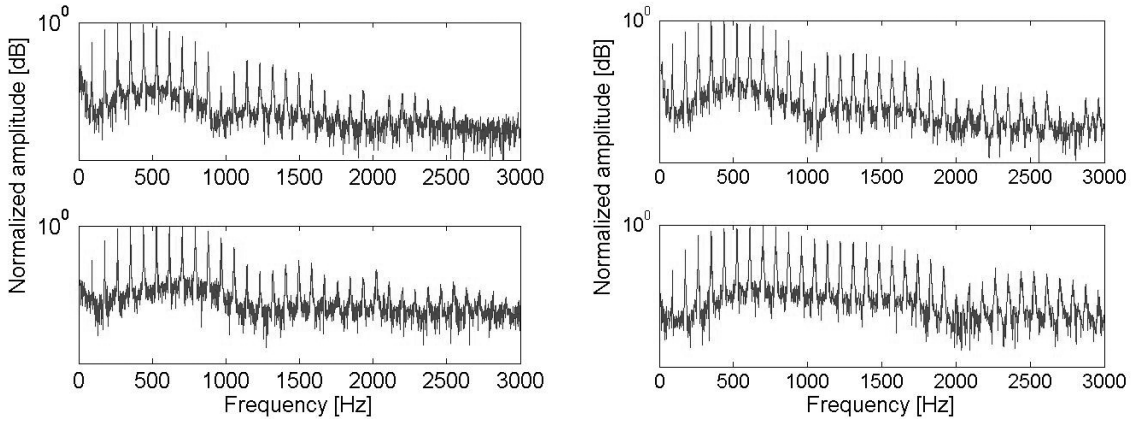

(a) Left ear

(b) Right ear

Figure 3.6 *Frequency spectra for an F played on a tripple Alexander horn recorded at the left ear (left figure) and the right ear (right figure) compared to the frequency spectra of the same note recorded 2 meters in front of the player (top graph in each figure). As the bell of the horn points sidewards, the higher frequencies are relatively stronger for the player, especially at the right ear, than for an audience in front of the musician.*

Modern French horns are played with the right hand inserted into the bell of the instrument even though it no longer is necessary to use the hand to get a full scale. Figure 3.8 shows the impedance of the French horn with and without the hand in the bell. The hand in has several effects on the sound of the instrument.

- The cut-off frequency becomes considerably higher, giving the instrument a wider range.
- The radiation in the high register is decreased, giving the instrument a more mellow sound.
- The resonance peaks are shifted downwards, especially the higher ones.
- Several resonance peaks are added in the higher register, making it easier to get the right intonation.

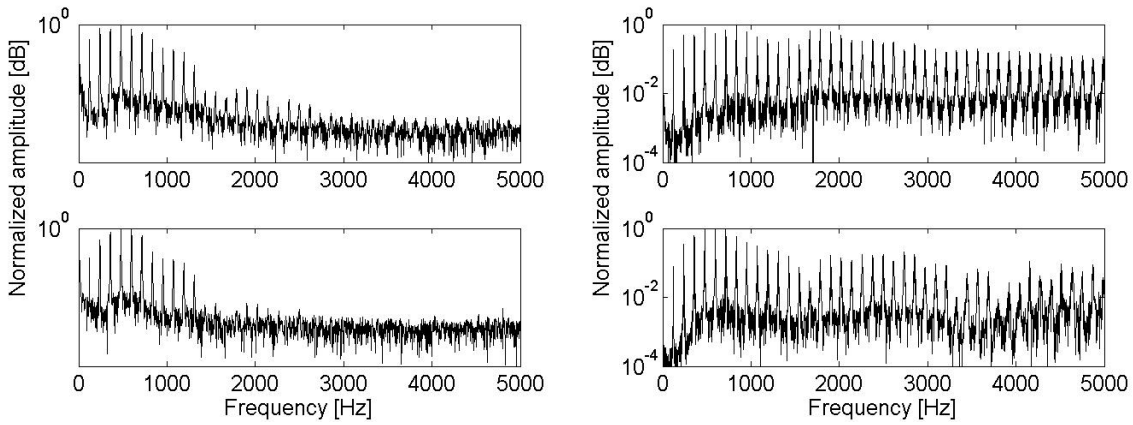

(a) Left ear (b) Right ear

Figure 3.7 *Frequency spectra for a B played on a trombone recorded playing softly (left figure) and loudly (right figure) compared to the frequency spectra of the same note recorded 2 meters in front of the player (top graph in each figure). As the bell of the trombone points straight forward, the frequency spectra have a higher percentage of high harmonics in front of the instrument.*

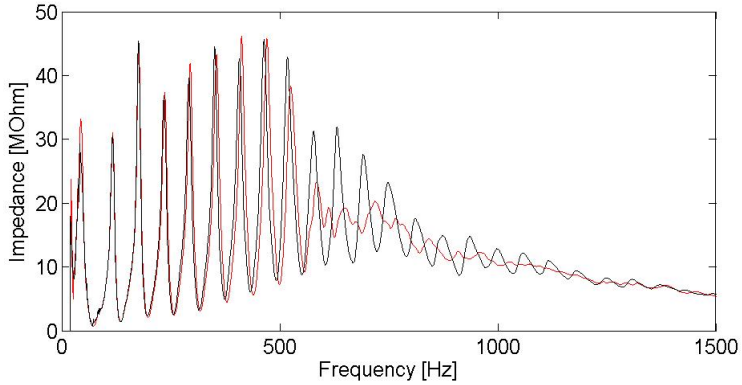

Figure 3.8 *Impedance of a French horn measured with BIAS without the hand in the bell (blue line) and with the hand in the bell (black line).*

3.3.2 The valves

The valves open an additional set of tubing for the air to pass through to make all the notes in the harmonic series available. There are three types of valve in use today, the piston valve (usually used for trumpets and tubas), the rotary valve (usually used in horns) and the Vienna valve (now only used on Vienna horns). The Vienna valves are slower than the piston valves and rotary valves, but have less sharp angles and corners and don't break up the air stream as much as the other two. The valves lower the fundamental by 1 tone (1st valve), 1 semitone (2nd valve) and 3 semitones (3d valve), and can be used in combinations. Some instruments have 4 or 5 valves, for example to add additional tubing, switch between two complete sets of tubing (double or trippel horns) and some horns are equipped with a stop valve so the musician don't have to transpose when playing stopped horn.

Having a conical bore with valves would mean that the valves couldn't just add tubing but had to switch between different ends, so each valve would have a flared end bell. Instruments like this have been made and played (and one is seen by the Quidditch pitch in the Harry Potter films) but they will necessarely be quite heavy and unpractical .

Using the valves together makes the intonation more difficult. When using only the 2nd valve, the added length increases the total length of the instrument with 6 %. If the 1st or 3d valve already is in use, the extra length added by the 2nd valve will not increase the total length of the instrument sufficiently to shift it by one semitone. The musician then have to compensate for the instrument being to high. The more valves are used at the same time, the bigger the problem, so when it is possible to choose between different fingerings it usually best to pick one that involves using as few valves as possible.

3.3.3 The mouthpiece

Mouthpieces vary in size and bore too, but most consist of 4 major parts.

- Rim
- Cup
- Narrow constriction
- Taper that widens out to meet the bore

The rim allows for a comfortable connection with the player's lips. Everyone who has tried to play a trumpet or a horn without the mouthpiece knows that it is a rather uncomfortable experience as the bore is too small to allow the lips to vibrate efficiently. The form of the cup varies from instrument to instrument, from the distinct cup shape in for

example trumpet mouthpieces to the funnel shape of the horn mouthpieces. However, all mouthpieces put a volume of air between the player's lips and the rest of the instrument. This volume of air acts as a Helmholtz resonator and if the size is chosen correctly, the mouthpiece will amplify the impedance peaks in the middle register of the instrument. Figure 3.9 shows the acoustical input impedance of 3 different mouthpieces, the horn mouthpieces Helmholtz resonance is lower both in amplitude and frequency than those of the trumpet mouthpieces, since the horn mouthpiece is slightly bigger and with a more funnel-like bore.

The mouthpiece will also shift the frequencies of the very highest resonances downwards, as opposed to the bell. Some players have several mouthpieces that they use for different playing styles or different parts, often with a detachable rim so that the lips don't have to adjust to a different rim size when the mouthpiece is changed. Figure 3.10 shows the acoustical input impedance of a trumpet mouthpiece and of a signal trumpet with the mouthpiece attached. The main resonances of the trumpet are concentrated around the Helmholtz resonance of the mouthpiece. The second peak in the acoustical input impedance of the mouthpieces is probably due to a resonance whose frequency is decided by the length of the mouthpiece.

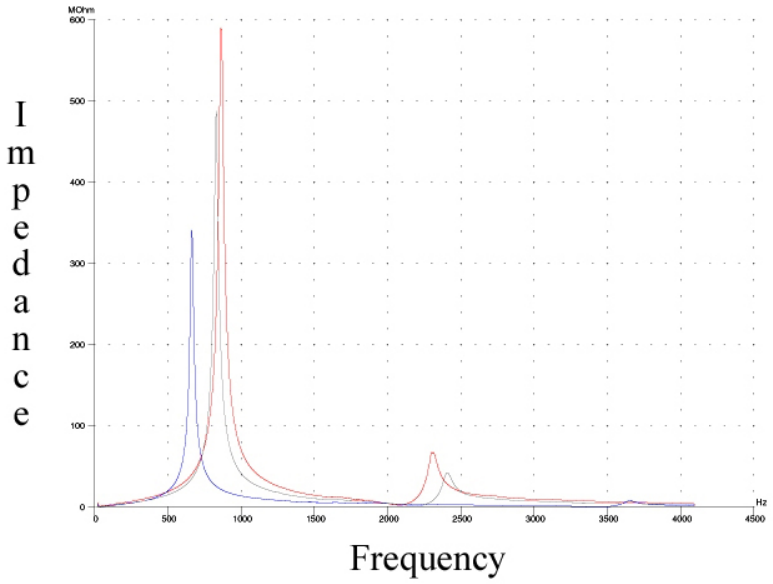

Figure 3.9 *Acoustical input impedance of 3 different mouthpieces, one horn mouthpiece (blue), the mouthpiece of a modern trumpet (red) and the mouthpiece of a signal trumpet measured with BIAS.*

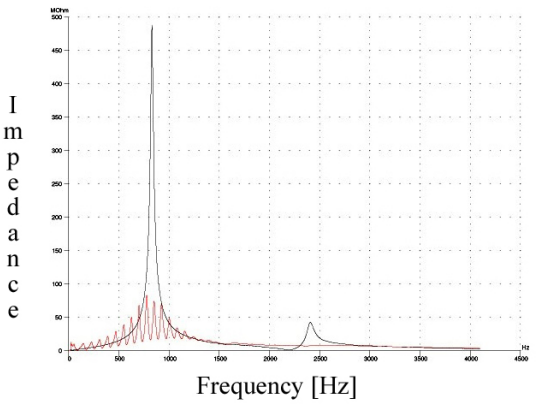

(a) Impedance of trumpet with mouthpiece and trumpet alone

(b) The trumpet (photo Ringve museum).

Figure 3.10 *The left figure shows the acoustical input impedance of the signal trumpet in the right picture (blue) with mouthpiece and the acoustical input impedance of its mouthpiece (red). The acoustical input impedance of the whole instrument is amplified by the mouthpiece, defining in which frequency range the instrument is easiest to play.*

3.3.4 The whole instrument

Figure 3.11 shows how a mouthpiece and a bell (a spherical kitchen funnel with diameter about 6 cm, figure 2.7) influences the impedance of a garden hose and how they compare to the impedance of a lur with the same length as the garden hose. The hose on itself is a cylindrical pipe, adding the bell raises the frequencies of the resonances (see close-up in figure 3.12(a)). The Q-values of the higher frequencies decrease with the bell, but the radius of the bell isn't big enough to affect the cut-off frequencies. The fundamental isn't changed much, as the dimensions of the kitchen funnel serving as bell isn't big enough compared to the wavelength to affect it. Adding the mouthpiece amplifies the resonances where the mouthpiece has its resonances. The lur has a long conical bell, ensuring that the resonances used for playing (harmonics 3-7) are in tune (3.12(b)).

Figure 3.13 shows the acoustical input impedance of a horn in F with no valves compressed and a basstrombone in the first position. The horn and trombone both have the same fundamental, the offset in the horn's impedance is probably due to the funnel shape of the horn's mouthpiece, whereas the trombone's mouthpiece is shaped like a cup. The horn's mouthpiece is considerably smaller than the trombone's, and as the instruments have the same length, it accounts for the higher amplitude of the horn's impedance since it amplifies more. Just above 1200 Hz, the trombone's impedance is amplified by the second peak of the impedance of the mouthpiece. Figure 3.14 shows the acoustical input impedance of a trumpet in C and a lur in C. The lur has a longer flare than the trumpet, about half the instrument consists of the conical bell. Therefor the trumpets' harmonic is

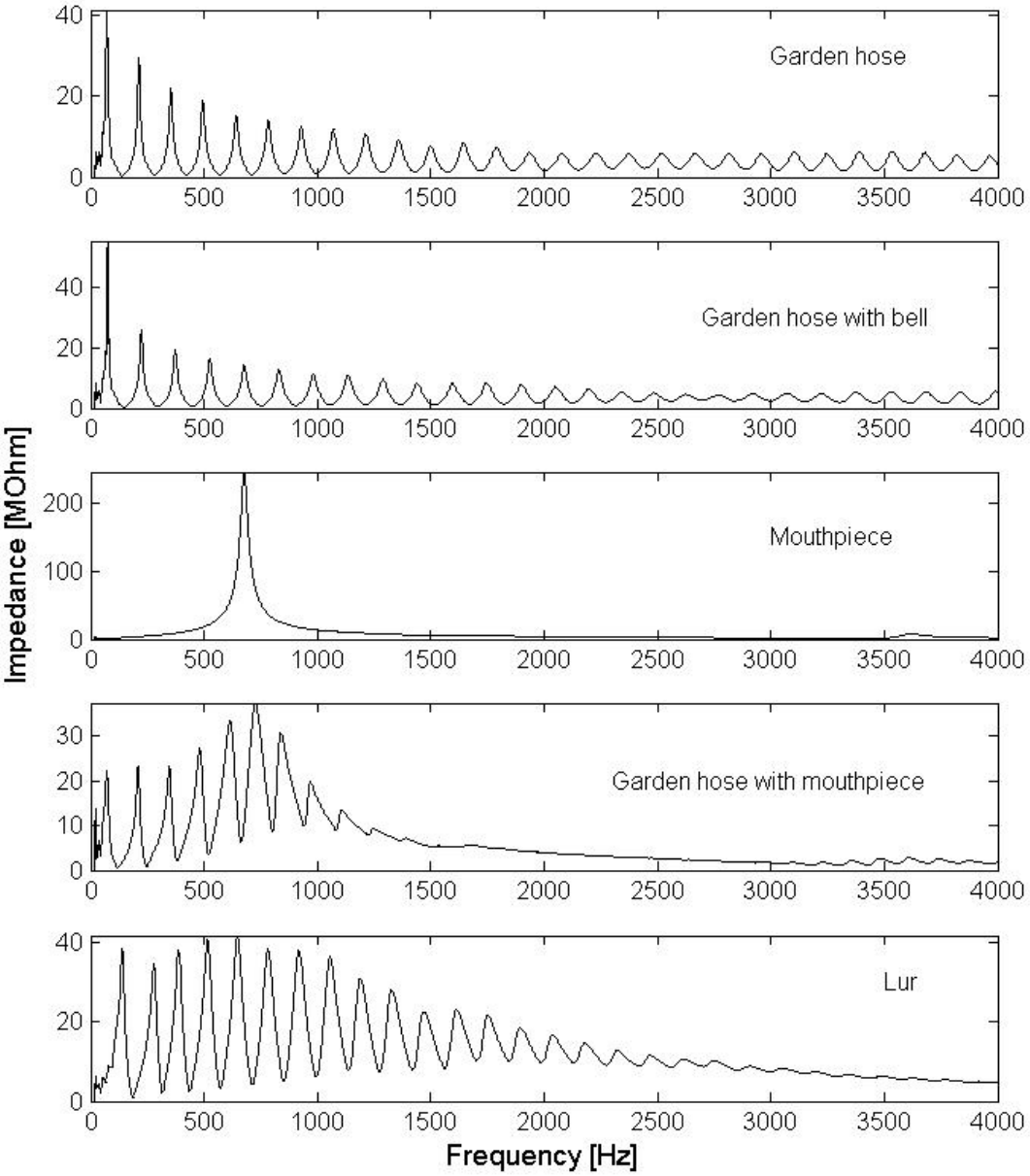

Figure 3.11 *Impedance (measured with BIAS) with (from top to bottom) a garden hose, a garden hose with a bell, a horn mouthpiece, a garden hose with the horn mouthpiece attached and a lur. All the instruments are 1.20 m long, the garden hose as a diameter of 0.6 cm and the bell used on the garden hose has radius 3 cm.*

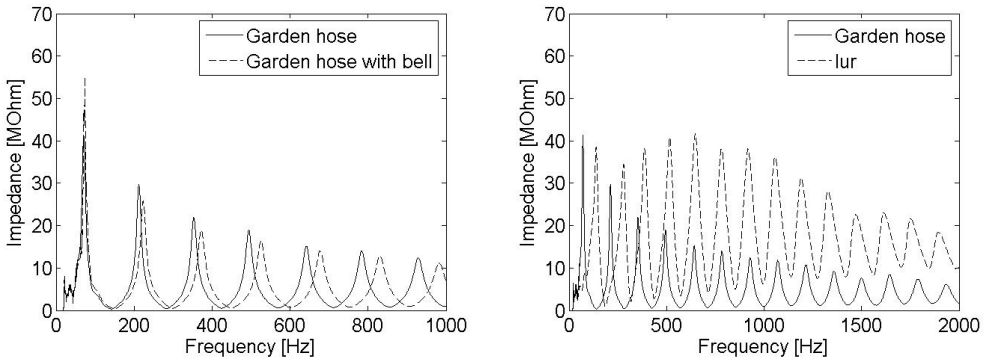

(a) Garden hose with and without bell (b) Garden hose and lur.

Figure 3.12 *Close-up of the acoustical input impedance of the garden hose with and without the bell (left figure) and close-up of the acoustical input impendace of the garden hose and the lur (right figure), all of them measured with BIAS.*

lower than that of the lur, and the lur has more clear resonance peaks than the trumpet.

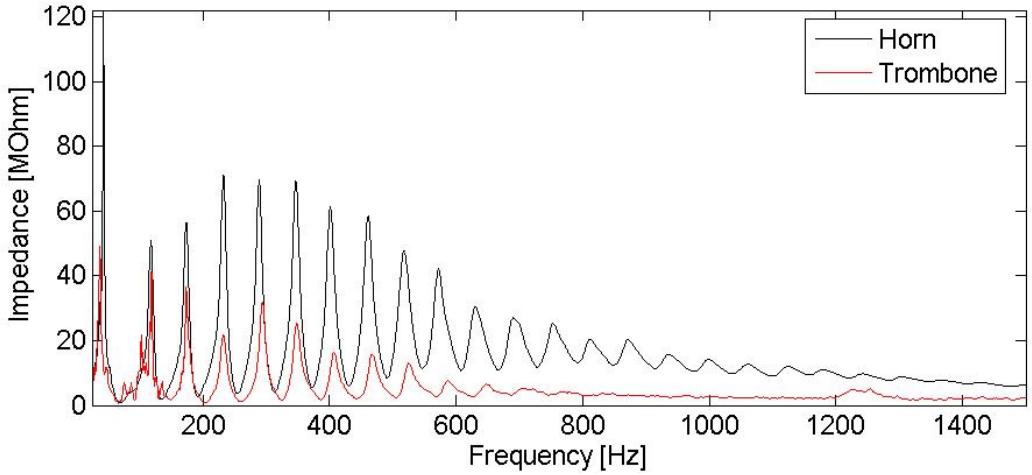

Figure 3.13 *Acoustical input impedance (measured with BIAS) of a horn in F (black line) with no valves compressed and of a basstrombone (red line) in the first position.*

3.4 Impedance of the driver

Setting the end where the lips are as a closed end is an approximation. The vibrating lips also have an impedance. Assuming that they behave like a damped harmonic oscillator, the input mechanical impedance Z_{md} of the driver is

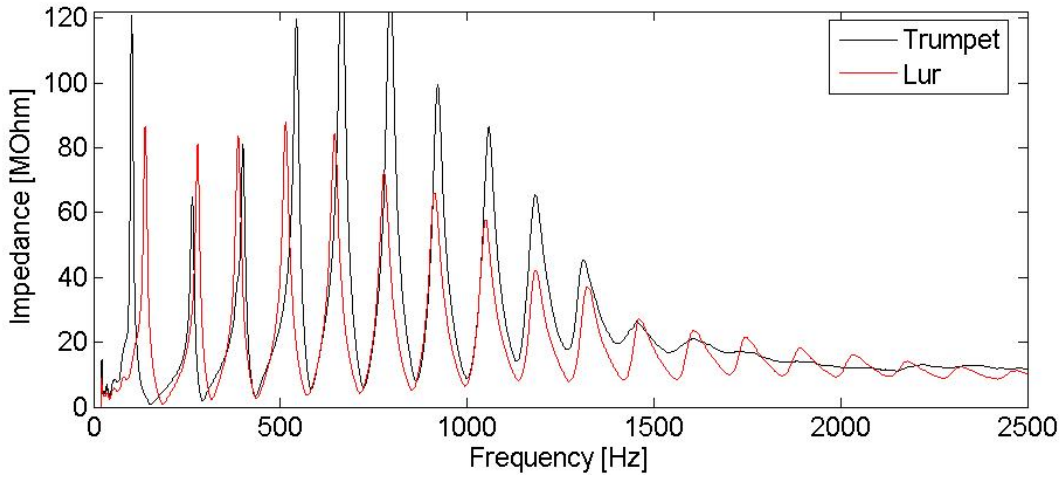

Figure 3.14 *Acoustical input impedance (measured with BIAS) of a trumpet in C (red line) with no valves compressed and a lur in C (black line).*

$$Z_{md} = R_m + j\left(\omega m - \frac{s}{\omega}\right) \tag{3.15}$$

where s is the stiffness of the driver and m the mass of the driver. The mechanical input impedance of the whole system is the sum of the mechanical input impedance of the driver and of the pipe (Z_{m0}), so that the anti-resonances are found from

$$Im\left\{Z_{md} + Z_{m0}\right\} = 0 \tag{3.16}$$

Using equations 3.15 and 3.3 we get

$$Im\left(R_m + \omega m - \frac{s}{\omega} + \frac{\frac{1}{4}(ka)^2 + j0.6ka + j\tan kL\rho_0 cS}{\rho_0 cS + j\left(\frac{1}{4}(ka)^2 + j0.6ka\right)\tan kL}\right) = 0 \tag{3.17}$$

for the resonances. Figure 3.15 shows the complex part of the acoustical input impedance of a 3 meter long air-filled open-ended tube with different drivers. The zero-crossings can be moved away from the multiples of $\frac{L}{\pi}$ by changing the drivers stiffness and mass (for brass instruments, the tension of the lips). The general shape of the impendance curve also changes.

When the musician plays the instrument, the frequency and amplitude of the lips vibration decide the frequency and amplitude of the tone the instruments produces. For low amplitudes, especially in the high register, the lips don't close totally and the vibrations are more or less sinusoidal. When the amplitude decreases, the lips close and cut of the

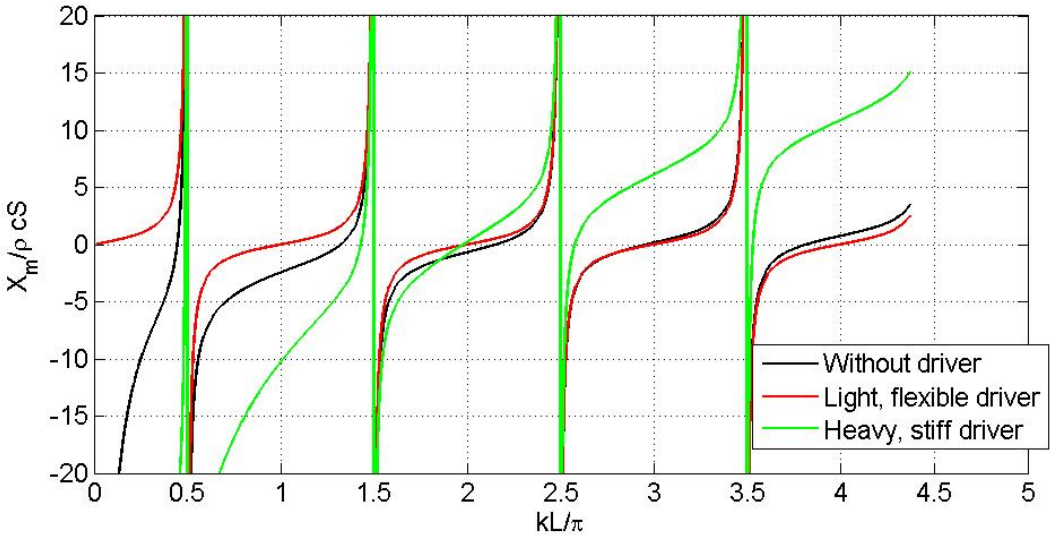

Figure 3.15 *Close-up of the mechanical input reactance X_m of a 3 meter long air-filled cylindrical pipe with open termination and radius = 1 cm and 3 different drivers (equation 3.17). One driver has mass and stiffness = 0 (the same as no driver), one driver is light and flexible and one driver is heavy and stiff.*

air stream thus creating the a richer harmonic spectrum as can be seen in figure 3.16. From medium loud to very loud, the waveform changes from near sinusoidal to a stable, but more complicated waveform.

As the wave is reflected back and forth between the opening of the instrument and the lips, it interacts with the both the instrument and the lips. The vibrating frequency of the lips is adjusted so it corresponds with the resonances of the air column, so during the first cycles the instantaneous fundamental frequency can vary quite a lot (figure 3.17). The transients are a very important part of the characteristics of the instrument, without them, the wind instruments are very much more difficult to distinguish from eachother [51], [52]. Both oscillations around and descents/ascents towards the desired frequency are possible. The fundamental isn't necesseraly the first to be excited.

3.5 Some comments on different playing techniques

Many playing techniques require that the instrument is sounded on frequencies that are not part of the instruments resonances. By changing the tension of the lips, the musician can change the acoustical input impedance so that the frequency of the standing wave changes smoothly instead of jumping from one resonance to the other.

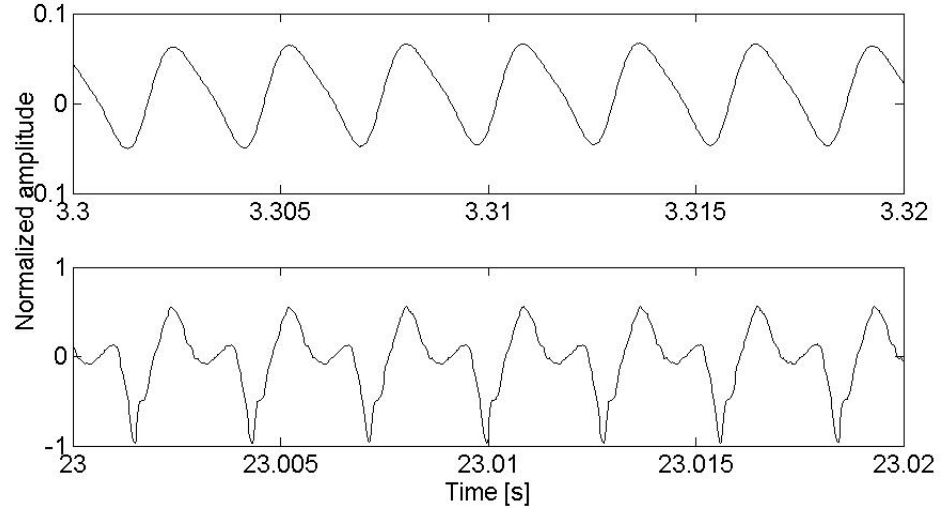

(a) Wave forms

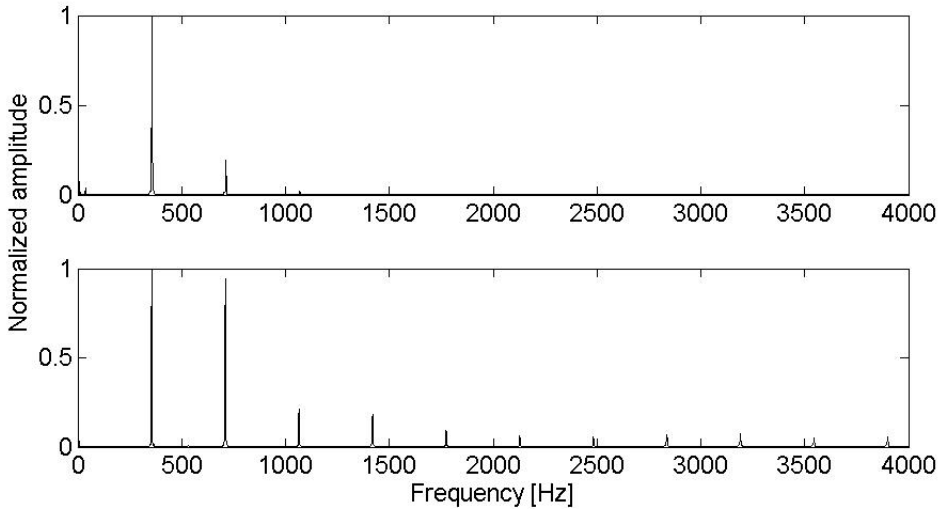

(b) Spektrum

Figure 3.16 *The upper figure shows the wave forms of a F played on a French horn (Alexander) medium loud and very loud. The medium loud tone has a nearly sinusoidal wave form since the lips don't close totally. When playing very loudly, they do, giving the note more higher harmonics, as can seen in the lower figure which shows the FFT of the two waveforms.*

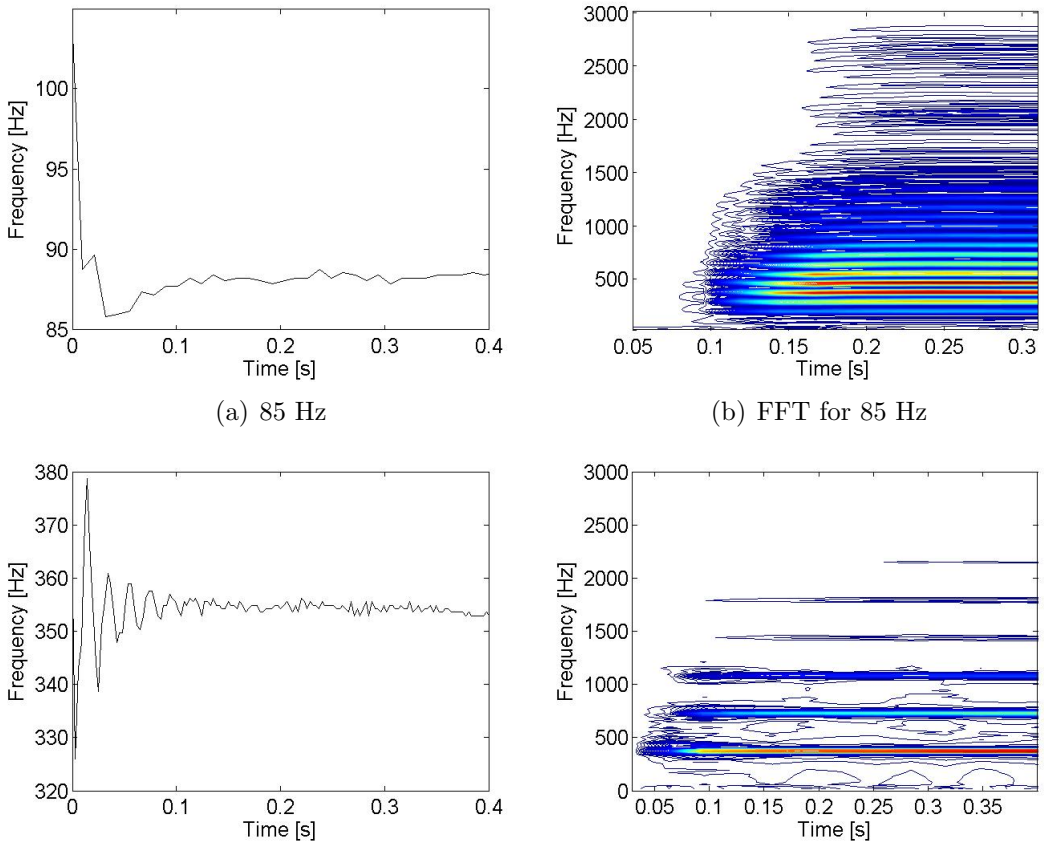

(a) 85 Hz

(b) FFT for 85 Hz

(c) 350 Hz

(d) FFT for 350 Hz

Figure 3.17 *Instantaneous fundamental frequency and frequency spectrum of the transients of 2 different notes played on a French horn (Lawson).*

3.5.1 Slurs

Slurs can be used in music (when notes are played without separation) or as exercises to strengthen the flexibility of the ambouchure and make lipping upwards or downwards easier, which helps maintain a good intonation. On brass instruments, slurs are made with the help of the lip muscles only. The musician changes the lip tension so that the impedance of the closed end changes, this means that the frequency of the standing wave can be gradually changed. Figure 3.18 shows the instantaneous fundamental frequency and the frequency of the 3 first harmonics for 2 exercise slurs, where the musicians lips the note as much down as possible, and then as much up as possible. The frequency changes gradually without jumps, for the lower slur the note is changed about 30 Hz, from a D to an F.

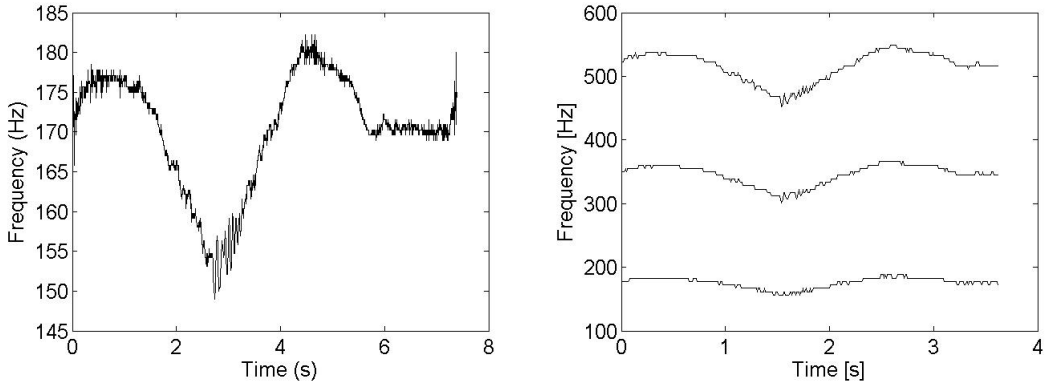

(a) Instantaneous fundamental frequency (b) Frequency of 3 first harmonics

Figure 3.18 *The left figure shows the instantaneous fundamental frequency of a slur starting on a small F played on a Alexander tripple horn, the right figure shows the frequencies of the 3 first harmonics of a slur starting on an f.*

3.5.2 Lip trills

Trills are musical ornaments made by changing rapidly between two adjecent notes. On valveless instruments lip trills can be made by slurring on adjacent tones, before valves were introduced this was normal on f.ex. natural trumpets and Baroque era horns. On modern horns lip trills are used primarily from the second-line G up approximately an octave. For lower frequencies, lip trills are difficult because the harmonics are too far apart and for higher frequencies they are too close. The most commonly used interval for lip trills is a whole tone, although trills of minor or major thirds can be found. The main requisites for a proper lip trill are two tones that are one tone apart and can be played with the same fingering. For some combinations this means that the player will have to resort to optional or false fingerings.

Figure 3.19 show the instantaneous fundamental frequency and the frequency (found with

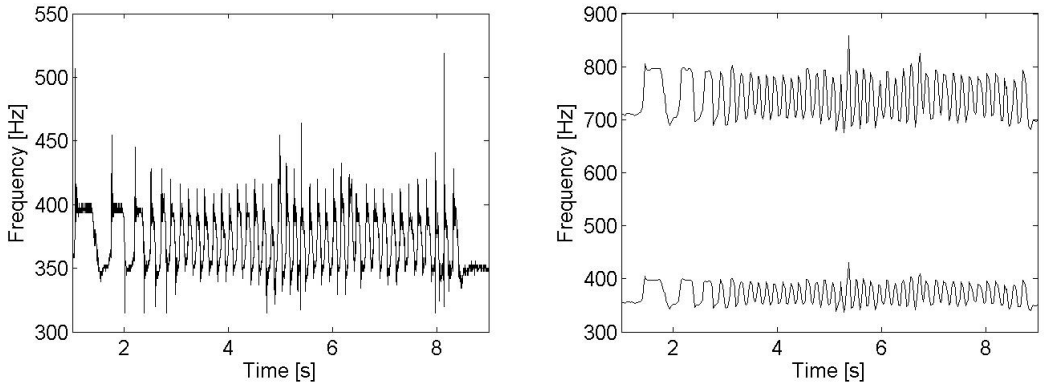

(a) Instantaneous fundamental frequency (b) Frequency of 2 first harmonics

Figure 3.19 *The left figure shows the instantaneous fundamental frequency for a lip-trill (played on a tripple Alexander horn), the right figure the two first harmonics of the same lip-trills.*

FFT) of the 2 first harmonics of a lip-trill. The peaks in the instantaneous fundamental frequency is not visible in the FFT transform. The higher peaks upwards than downwards suggest that the musician presses harder to get up, as it is more difficult to press notes upwards than downwards.

3.5.3 Stopped horn

On natural horns, the hand is inserted in the bell to produce diatonic and chromatic notes. By inserting the hand in the bell the pitch can be lowered up to a whole step. The invention of the technique is normally credited to the Czech horn player Anton Joseph Hampel (1710-1771) [2] and also works on modern horns, but because of the valves the hand normally only serves the purpose of giving the horn it's proper tonal colour and adjusting the frequencies of the resonances. The correct hand position in a modern horn is quite similar to that of a natural horn. The hand is cupped slightly, and placed inside the bell so that the back of the fingers touch the bell throat. The position can vary a bit from player to player, but it should not be necessary to move the hand to obtain the closed position used for stopp horn. The player should not shove the hand in the bell, but close it with the heel of the hand and the thumb [9].

3.5.4 Mutes

There are mutes for various purposes. They modify the radiation characteristics of the bell, normally reducing the low-frequency radiation much more than the high-frequency radiation. The playing mute dampens the sound radiated from the instrument, allowing the musician to practice late at night without angering the neighbours. A good practicing

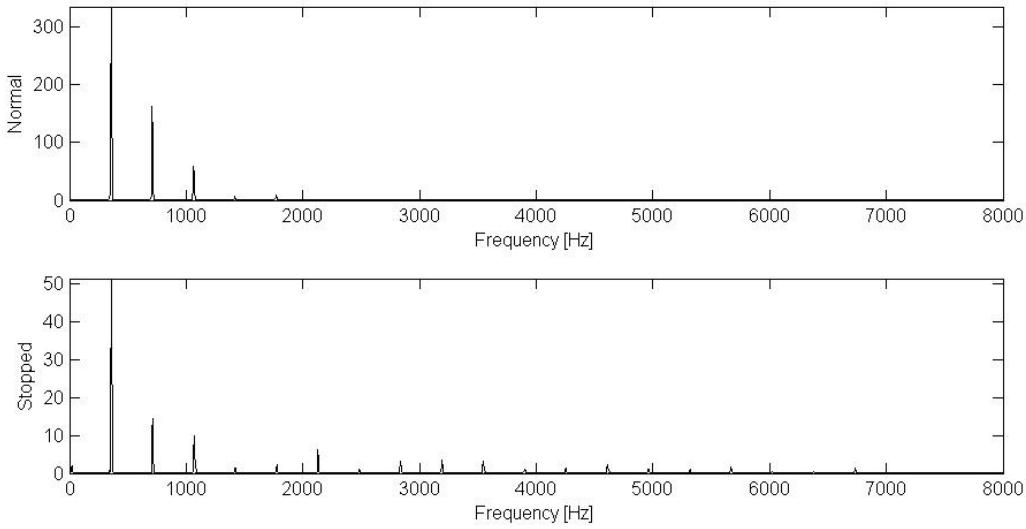

Figure 3.20 *Frequency specter of an f played with the hand held in the normal position in the bell and with the bell stopped with the hand.*

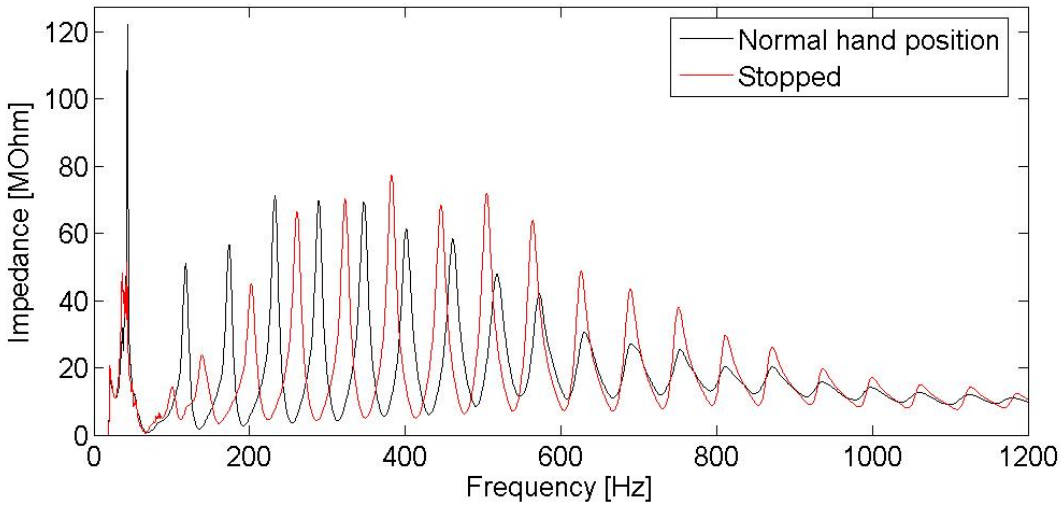

Figure 3.21 *Impdance (measured with BIAS) of a horn in F with no valves compressed with the hand in a normal position inside the bell (black line) and in the stopped position (red line)*

(a) Playing mute (b) Stop mute (c) Silent brass mute

Figure 3.22 *A playing mute (), a stop mute (Denis Wick) and a silent brass mute (Yamaha) for horn.*

mute should decrease the sound levels but change the impedance as little as possible so that it feels like the same instrument when played.

Figure 3.23 shows the impedance of a horn with the hand in the playing position and with a Yamaha silent brass mute. The silent brass mute is made of lightweigth plastic and has a rubber sealer to hold it in the bell. A microphone inside the mute sends the sound to the Personal Studio, a unit with headphones that lets the musician hear what it would have sounded like without the mute. As can be seen from the shift in the impedance peaks (tabel 3.2, the lowest resonances are too high, the mid-register resonances bit too low and the high-register resonances are shifted upwards due to the change in impedance induced by the mute. In the lowest register the mute makes the bore of the horn seem shorter since the flare is reduced. For the higher frequencies, the bore also seems shorter as the waves are reflected earlier than for the open bore. The mid register is changed the least, and also amplified by the mutes Helmholtz resonance.

Stopping the horn effectively can be difficult, especially in the lower register. Stop mutes are made to replace the hand for the hand-stopping effect, and most of them are supposed to give an exact semitone transposition or no transposition over the whole register. The stop mute closes the bell but has a funnel-like ending with an opening of about 0.5 cm.

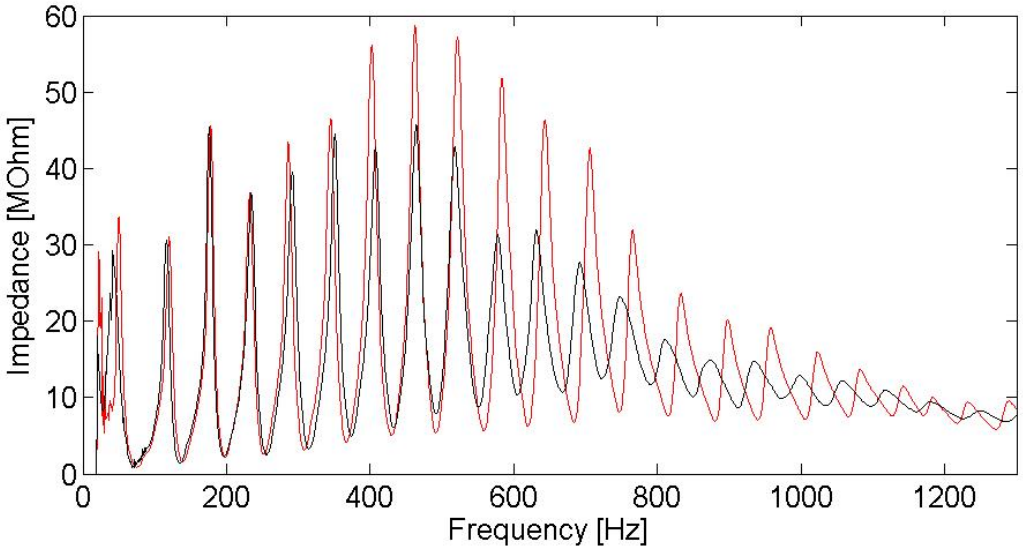

Figure 3.23 *Impedance measured with BIAS of a horn with the hand held normally in the bell (black) and with a Silent Brass mute (red)*

Table 3.2 *Impedance peaks of a horn with the hand in the bell and with a silent brass mute*

Harmonic	Hand in bell	Silent brass
1	42.0	50.0
2	116.0	120.0
3	176.0	178.0
4	232.0	234.0
5	292.0	286.0
6	350.0	345.0
7	407.0	402.0
8	464.0	462.5
9	518.0	521.0
10	578.0	583.0
11	631.0	643.0
12	691.5	706.0
13	747.5	765.0

Chapter 4

Wall vibrations

4.1 Introduction

Most musicians and instrument manufacturers mean that different materials and wall thicknesses influence the quality of the tone and the response of brass instruments, wood instruments, organ pipes etc. Flutes made of platinum or gold, silver trumpets and horns with special coatings are said to have better sound than instruments made of other, often cheaper, alloys. Lurmakers say that lurs made of driftwood are easier to play than f.ex. lurs made of spruce. Brass instrument makers find that instruments made of gold brass (85 percent copper and 15 percent zinc) give a mellower tone than those of silver/nickel alloys (nickel silver consists of 65 percent copper, 18 percent nickel and 17 percent zinc), the former also tends to give a brassy sound at lower excitation levels. Among scientists, the opinions are divided despite (or maybe because) of the large number of studies done since they tend to give different answers. As there are many parameters and boundary conditions to control (excitation, instrument support, temperature etc.), measurements can be difficult and numerical simulations tend to get very memory demanding.

This chapter starts with an introduction to wall vibrations, a short summary of the latest studies on the subject and how the FEM simulations with COMSOL multiphysics where done. Then the results of FEM simulations of the wall vibrations of cylinders are discussed, first in an two dimensional, axi-symmetrical approach of the simplest geometry possible, a cylinder. This to see how different metals and geometry parameters influence the acoustically induced movement of the walls and how the wall vibrations can influence the acoustical input impedance and the sound radiated from cylindrical tubes. The sound from the vibrating cylinders are first compared to the sound radiated from a rigid cylinder, and then the difference between the sound field radiated from vibrating cylinders of different alloys is discussed. The 2 dimensional cases are compared to 3 dimensional simulations, with both acoustical and mechanical excitation to study the directivity of the sound radiated from the walls and how dents and other irregularities in geometry can influence the wall vibrations and thus the radiated sound. The simulations done on

cylinders are then repeated on some more complicated geometries that are closer to the geometries of real brass instruments.

4.2 Theory

When a tube of any shape is excited, vibrations occur. The form and magnitude of the vibrations are decided by the structural eigenmodes of the tube, the frequency with which it is excited and the amplitude and form of the excitation, whether it is by a vibrating air column or by a shaker. Structural waves can propagate in three directions in the tube, axial, circumferential and radial. For brass instruments (which have thin walls) the radial propagation is negligible in the frequency range the instruments are played. That does not mean that the walls don't move in the radial direction, but the frequencies by which radial waves propagate inside the walls are far higher than the ones used for playing. For circumferential waves, the waves travel around the tube across a continuous surface, so there must be an integer number of wavelengths. For the axial waves, the boundary conditions depends on the excitation. For excitation by the vibrating air column inside the instrument, the end where the excitation occurs can be set to fixed and the axial waves have a antinode at that point. The open end is free, as this is the case for most brass instruments when played without mutes.

Various characteristics of the instrument can influence the vibrations of the walls.

- Wall thickness
- Material
- Clamping
- Rim size
- Coatings (lacquer, silver-plating etc.)
- Shape of the bell

The vibrations of the walls can influence the output of the instrument in different ways, although one does not exclude the others.

- If the vibrations are transmitted through the mouthpiece they can cause the player to adjust the lip tension. This difference would noticed mainly by the player and it would prove very difficult to find such effects by numerical simulations.
- The wall vibrations will radiate sound out into the surroundings, the directivity of which will depend on where the instrument's walls move. The sound radiated from

the vibrating walls tend to decrease more rapidly than the sound radiated from the opening of the instrument, so the effect would be larger for the musician and those in the vicinity of the musician than an audience some meters away. This effect should be possible to find if the sound pressures radiated from identical instruments with vibrating and rigid walls are compared.

- The vibrating walls can also interact with the vibrating air column and change the impedance of the bore. This effect would change the sound of the instrument so it should be possible for everyone to notice it, and can be found numerically by comparing the calculated impedances for vibrating and rigid walls.

4.3 Literature review

Pyle [23] used French horns with lacquered, silver plated and uncoated bell flares and recorded a slight reduction in relative sound pressure levels at the high frequencies for the lacquered bell. Using a trombone with interchangeable bells Pyle [25] found noticeable different spectra for the lower frequencies. Lawson and Lawson [24] found that the sound levels of annealed brass flares at 1-3 kHz were higher than for the not annealed brass flares, whereas for nickel-silver flares the annealed flares radiated less sound. The differences found were up to 3 dB, and recognizable even for an untrained ear. It is assumed that the differences are caused by variations in the modes of the bell caused by different Young's moduli for different coatings.

Kob [26] recorded the sound of a blown free and damped pipe, and found differences up to 10 dB for the spectral components in the transient and smaller differences in the stationary parts. The eigenmodes of the pipe body were determined from laser velocimetry and compared to FE calculations. The changes in the spectrograms coincided with eigenfrequencies of both air modes and structural modes, supporting the assumption that mode coupling are responsible for the sound changes. Widholm at al [27] tested seven flutes of different materials and wide price range with double blind tests and statistical analysis. Big differences in sound level and sound colour due to the player were found, but no perceivable differences in sound colour caused by the material could be measured.

Moore [28] found that damping the bell of a trumpet with sand increases the relative power in the fundamental and a decrease in the power of one or more the higher harmonics. He suggests to possible explanations, either the vibrating walls increases the magnitude of the viscous boundary layer thus changing the acoustical input impedance, or they give a mechanical feedback from the bell through the mouthpiece to the lips. The later would explain that more differences have been found for brass instruments with small mouthpieces like French horns and trumpets than for f.ex. trombones. Whitehouse [29] did measurements on a simplified brass instrument consisting of a brass pipe with a trombone mouthpiece pipes of 5 different materials and 3 pipes of the same metal with different thicknesses. He found differences in sound pressure but not enough to say for sure that it would influence the sound radiated from the instrument. By decoupling the

mouthpiece and the air column from the pipe he also found that the main cause of the vibration seemed to be the vibration of the lips.

Nederveen and Dalmont [31] analyzed recordings of a thin walled metal organ pipe blown with compressed air. The boundary conditions for the air column and the walls were changed by grasping the pipe, holding a hand over the opening and changing the temperature. A laser vibrometer was used to measure the wall vibrations. For some notes, beats were recorded, and an oscillation like the wolf-note in string instruments was found. They also describe a phenomenological model that explains the findings, taking into account that the pipe didn't have a prefectly circular cross-section. The biggest deviations compared to a pipe with rigid walls occurred when a wall resonance was close to one of the air resonances. The sound levels differed with up to 6 db and the max frequency shift found was 20 cents. Although the measurments were made on an organ pipe, it is likely that similar effects might occur for f.ex. bassoons and trumpets.

Klausel, Mayer and Nachtmann [35] recorded a French horn both undamped and damped with sand blown with water-filled rubber lips , and found significant differences in the harmonic levels of both the near field and the far field. By decoupling the mouthpiece with a elastic rubber tube the vibrations of the artificial lips did not influence the measurements, and the results suggest that a change in the radiation impedance caused by the vibrating walls is responsible for the differences. Nief et al [34] did measurements on two cylindrical tubes, one made of very thin plastic, the other made of brass. A rigid slide was fitted to the cylinders so that the air column resonances could be fitted to match the mechanical ones. The vibrating tubes were slightly distorted to break their circular symmetry. They found slight spectral modifications for the brass pipe, and a wolf note produced by the vibroacoustic coupling for the plastic pipe.

The findings of Nief et al [34] are confirmed by Pico et al [32], [33] who made an analytical approach to the input impedance of vibrating cylinders, using and integro-modal method based on axisymmetric shell vibration. The influence of the vibrating walls can be seen as a small correction in the acoustic input impedance of the cylinder. By finding a expression for the correction factor for the wall vibration influence on the acoustic input impedance the deviations from the impedance of the rigid cylinder are found to be biggest when the structural resonance, the spatial coincidence and the acoustic resonances coincides. Using different material parameters, it is shown that the structural modes of a cylinder can stimulate the air column and that the coupling can produce a wolf-tone. Nief et al [37] used a model of equivalent monopoles representing each mode of the bell that each bell has a cut-off frequency above which the bell radiates effectively.

4.4 Finite element simulations

The finite element simulations were made with COMSOL multiphysics in a two dimensional axi-symmetric geometry and a three dimensional geometry. If not mentioned oth-

erwise, the fluid density of air was set to 1.25 kg/m^3 and the speed of sound in air to 343 m/s.

4.4.1 2-D simulations

In the 2 dimensional simulations the geometry is divided into 2 sub-domains. The air inside and around the instrument is one sub-domain, modelled with the Acoustics module, pressure acoustics, time-harmonic analysis and the walls are the other sub-domain, modelled using the Plane strain part of the Acoustics Module. The instrument and the air are coupled through the forces they exert on each other. The force F from the vibrating air on the walls equals the normal component of the acoustical pressure, the force from the walls on the air the normal component of the acceleration of the wall.

$$F_r = -p * n_r \tag{4.1}$$

$$F_z = -p * n_z \tag{4.2}$$

$$a_n = u_{tt} * n_r + w_{tt} * n_z \tag{4.3}$$

with F_r and F_z being the r- and z-components of the force F on the walls and n_r and n_z vectors normal to the wall [1]. a_n is the inward, normal accelration of the air and u_{tt} and w_{tt} the accelration of the wall in r and z-direction [2]. Figure 4.1 shows the geometry of the 2 dimensional axi-symmetric cylinder, with a close-up of the cylinder showing the sub-domains and exitation. The size of the sub-domain surrounding the cylinder necessary to avoid reflections and interference depends on the frequency of the excitation, but as the radiated sound hits the outer boundary more or less perpendicular, the impedance boundary conditon worked fine also without a PML.

The excitation is an incoming plane wave, $p_0 e^{-i\mathbf{kr}}$, made by the pressure source option in the boundary condition *radiation condition*. The sound pressure levels for the air sub-domain and the shape and amplitude of the displacement (figure 4.2) and various other parameters were calculated for frequencies that could be used on an instrument of similar size. To find at which frequencies the wall vibrations had the largest amplitudes, the maximum total displacement was plotted as a function of frequency as can be seen in figure 4.3. As the Q values of the major peak are large, the maximum total displacement is normally plotted in log-plots to make the smaller maxima and minima easier to distinguish.

[1] *nr_acaxi* and *nz_acaxi* in COMSOL
[2] *uaxi_tt_acaxi* and *w_tt_acaxi* in COMSOL

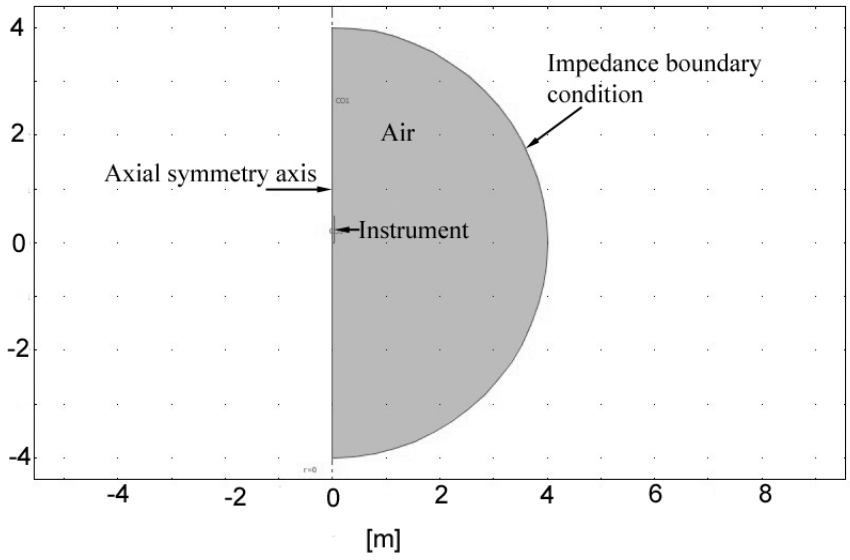

(a) The whole geometry

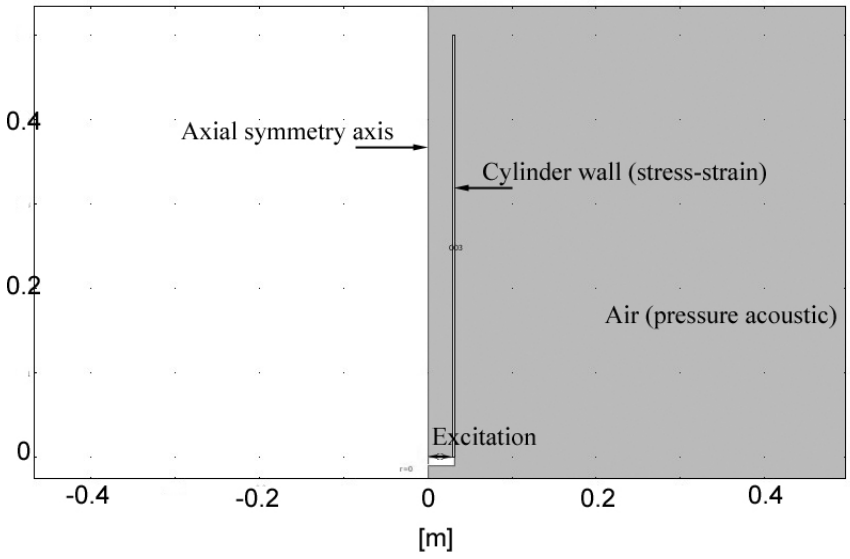

(b) Close-up of instrument

Figure 4.1 *Geometry for the two dimensional axi-symmetrical simulations. The upper figure shows the whole geometry and the lower figure a close up of the cylinder. Both axis in meters.*

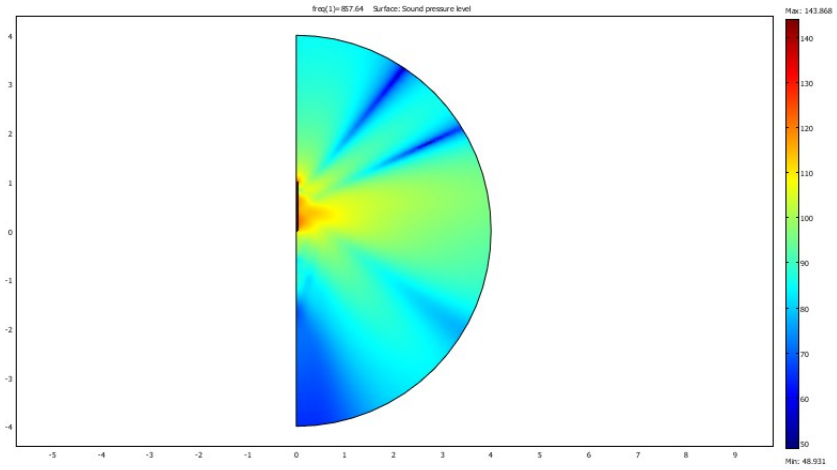

(a) Sound pressure

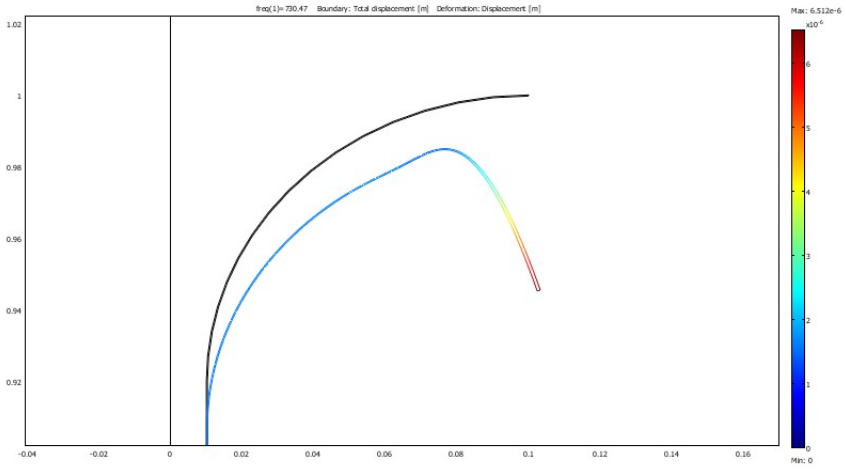

(b) Total displacement

Figure 4.2 *Example of 2D axial symmetric simulation. Figure 4.2(a) shows the sound pressure radiated from a 1 m long brass pipe with radius = 2 cm, wall thickness = 0.3 mm, excitation frequency = 857.64 Hz and excitation amplitude = 250 Pa. Figure 4.2(b) shows the amplitude and shape of the total displacement for the bell of a simplified brass instrument, excited with f=730.47 Hz. Both axis are in meters; the upper colour bar shows sound pressure in dB; the lower total displacement in meters.*

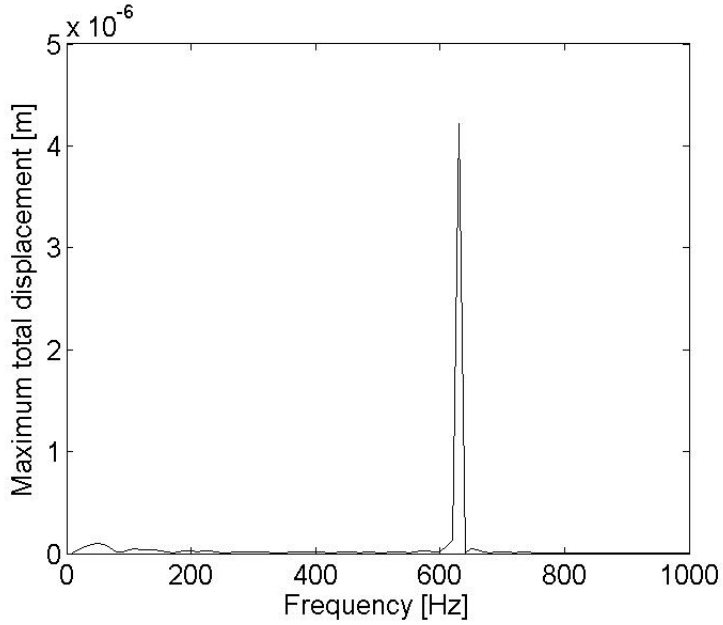

(a) Total displacement

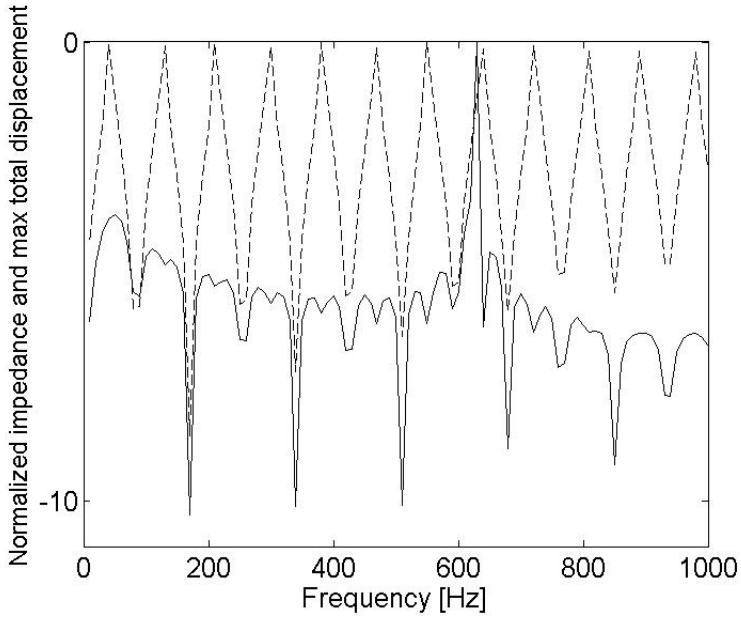

(b) Log of the normalized total displacement and acoustical input impedance

Figure 4.3 *By calculating the sound pressure and the displacement of the walls for different frequencies the maximum total displacement can be plotted as function of frequency. The top figure shows this for a 2 meter and 0.3 mm thick brass cylinder. Since the peaks tend to have high Q-values, it is usually better to use a logarithmic scale. The bottom figure shows the normalized log of data in the upper figure (solid line), and also the same of acoustical input impedance of the cylinder (dotted line).*

4.4.2 3-D simulations

Two approaches were used to model the instrument, one with and one without surrounding air.

- Since the sound pressure outside the instrument is much lower than inside, a model consisting only of the instrument, the air inside the instrument and a PLM at the bell was made, as shown in figure 4.5. One pressure air acoustic mode was used for the air and a structural mechanics shell for the instrument. This model was useful for finding how the displacement varied with the frequency, although it of course didn't say anything about the acoustical pressure outside the instrument.
- To model the air both inside and outside the instrument a sphere was split in two pressure acoustics modules, one for the upper half, into which the sound from the instrument was radiated, and the instrument and one for the lower part, or half a sphere was used for an acoustic pressure mode for the air outside the instrument as in figure 4.4. A structural mechanics shell mode was used for the instrument here too, as the walls are too thin for shear forces and radial waves to contribute to the vibrations.

The force in the x-direction F_x is given as

$$F_x = p * n_x + p2 * n_{x2} \tag{4.4}$$

where n_x and n_{x2} are the inward normal vector for the acoustical domains [3] and a normal accelration a_n at the walls as

$$a_n = -(u_{tt} * n_x + v_{tt} * n_y + w_{tt} * n_z) \tag{4.5}$$

where u_{tt}, v_{tt} and w_{tt} (u_tt_smsh etc in COMSOL) are the accelration of the wall in x, y and z-direction. Similar equations apply for the forces F_y and F_z in the y and z-direction.

To find what difference the vibrating walls made for the sound radiated from the instrument and the instruments' acoustical input impedance, the sound pressure was calculated both for vibrating and rigid walls, and for vibrating walls of different materials and with different boundary conditions. The effect of small changes in the geometry was also analyzed.

[3] nx_acpr and nx_acpr2 in COMSOL multiphysics

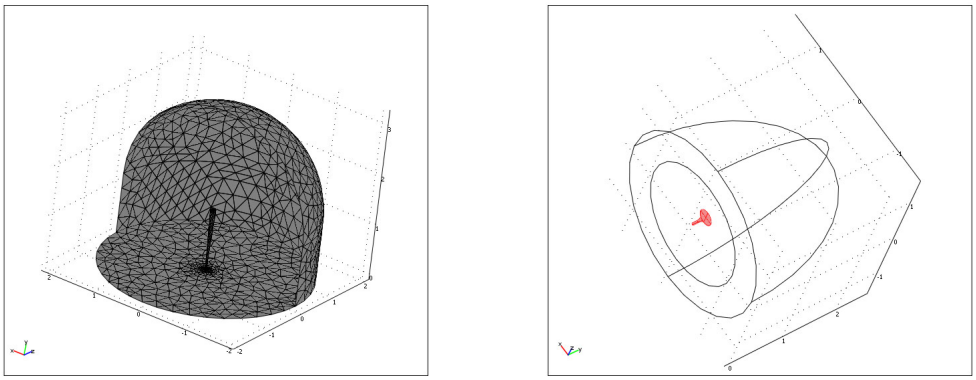

(a) Mesh (b) Subdomains

Figure 4.4 *Example of 3D-mesh and geometry. The left figure shows the mesh, the right figure the air pressure acoustics module that represents the instrument (pink) and the other one that represents the air (transparent). For most of the simulations including the surrounding air, the sub-domain outside the instrument had the shape of an ellipsoid.*

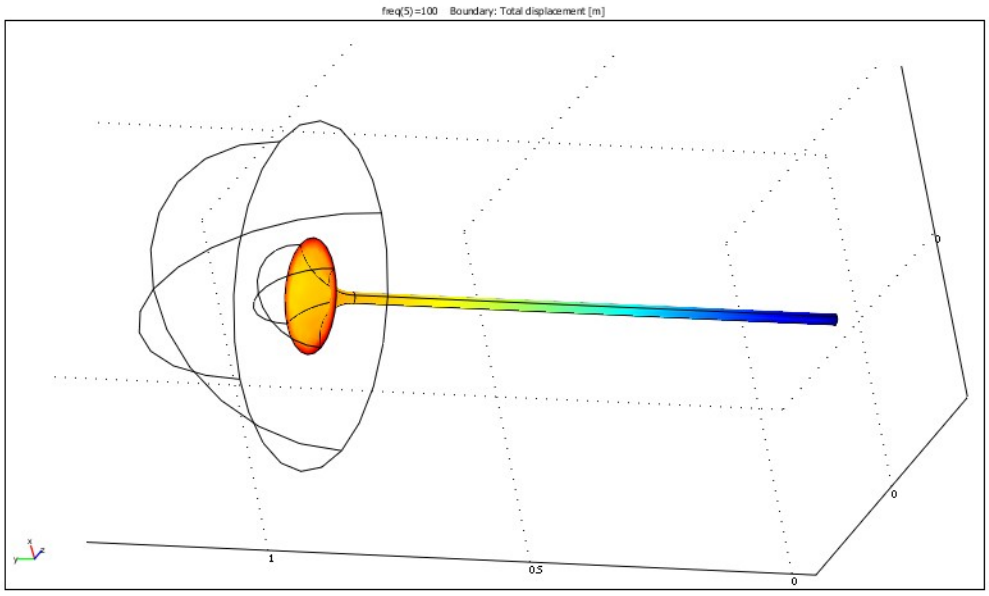

Figure 4.5 *Example of 3D simulation without the surrounding the air. The instrument ends in a half sphere, all of which is a PLM .Axis are in meters.*

4.4.3 Materials

The materials used in the numerical simulations (material parameters shown in Appendix B) were chosen because they have all been used to make brass instruments, except lead, which can be found in organ pipes. Lead came in handy since it is soft and not so heavy as gold and therefore has a higher density of eigenfrequencies. Since especially the 3 dimensional simulations became very big, computer capacity limited the total number of elements and thus the size of the maximum element size downwards. As a total of 5 elements per wavelength (2nd-order elements) is necessary for accurate solutions in 2 dimensions, the maximum frequency for some of the simulations only excited one, or possibly none, of the structural eigenmodes for the stiffer materials. For the material parameters, see Appendix B.

4.5 Results

4.5.1 Cylindrical tubes

Cylindrical tubes don't make very good brass instruments if the goal is an harmonic series, as their resonances don't form an harmonic series. In addition, their radiation efficiency isn't very good, but because of the rather simple geometries, they are easy to model and require fefwer elements and thus use less computer capacity than more realistic forms. More or less cylindrical tubes are found in for example organs and flutes. For 2-dimensional, axi-symmetrical simulations, perfectly cylindrical tubes with no indentations or bends are assumed, although for real instruments the thickness of wall will often vary, depending on the way they are made and on whether they are clamped or coated.

When the air column inside the cylinder is excited (in the simulations, a plane wave is used), the air will vibrate and set the walls in motion. The shape and total displacement of the walls are dependent on the frequency of the air column, figure 4.6 shows the displacement of the wall of a 1 meter long iron cylinder for 4 different frequencies. Since the simulations are linear, the shape of the wall vibrations does not change when the excitation increases, only the total displacement increases.

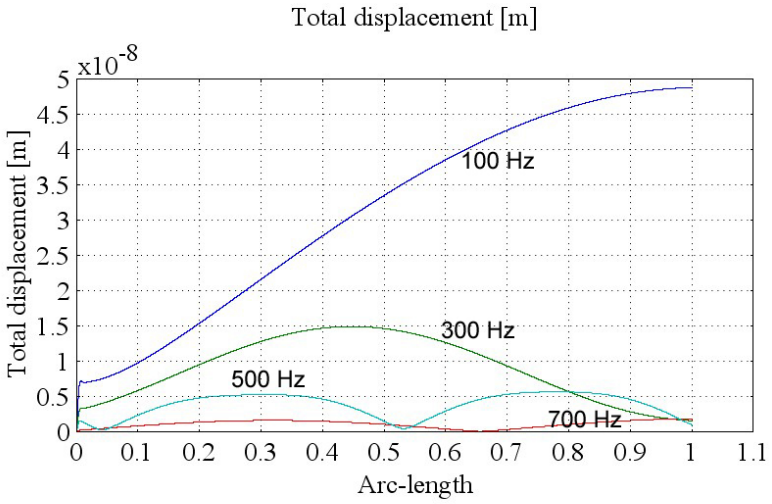

Figure 4.6 *Total displacement along the wall of a 1 meter long and 0.3 mm thick cylindrical iron tube with radius = 3 cm excitated with a plane wave with frequency = 100, 300, 500 and 700 Hz and amplitude 250 Pa at the radiation source.*

To find the sound radiated from the walls, the sound field from two identical cylinders, one with vibrating and one with rigid walls, was found and the difference calculated. The cylinders are 2 meters long and have 0.5 mm thick walls made of iron. The directivity is different to that of the sound radiated from the pipe opening, the main part of the sound

radiated from cylinders due to wall vibrations tend to go straight out from the walls as seen in figure 4.7. The sound pressure decreases quite rapidly with the distance to the cylinders' walls.

The force exerted by the air column on the walls and thus the total displacement of the walls is dependent on the acoustical input impedance of the cylinder as seen in figure 4.8, showing the maximum total displacement of the walls and the acoustical input impedance as functions of frequency. The maximum total displacement of the walls is found by finding the maximum of the total displacement of the outer wall and is not always in the same place at the wall. It has minima at the acoustical input impedances minima and maxima at the resonances. The main peaks in the maximum total displacement, caused by structural resonances, are much stronger than the local maxima caused by the air columns resonances.

The directivity and strength of the sound radiated from the walls are dependent on the shape of the displacement as can be seen in figure 4.9, where the structural resonance at 630.19 Hz gives a different displacement shape and therefore different radiation patterns for the sound radiated from the walls for frequencies around 630 Hz. At the maximum total displacement of the tube (630.19 Hz), the difference between the sound radiated from the rigid cylinder and the sound radiated from the cylinder with vibrating walls has maximum values at around 25 dB. For 630.1 Hz, 0.09 Hz lower, the maximum difference is less than 1 dB, so the shift in frequency needed to reduce the radiation from the wall vibrations dramatically is quite small, and in this case it would probably not be audible but for the contribution from the walls.

As some materials bend easier than others, the total displacement of the cylinders wall depends on the material. Figures 4.10 show how the maxima and minima due to the air columns impedance remain the same for different materials, although they have different amplitudes, but the main peaks change. Lead, being softer than iron and lighter than gold, has a higher eigenfrequency density, so it has more eigenfrequencies below 1500 Hz than the other two metals. The main peaks in the 2D axisymmetric simulations coincide with the breathing modes from the 3D eigenmode simulation, the shape of the walls displacement for both the 2D simulations can be seen in figure 4.11(a). The breathing modes are axisymmetric. The vibration patter for 290 Hz for lead, 480 for gold and 900 Hz for iron all fit with the 1. breathing mode. Since the directivity and strength of the radiated sound depend on the the vibration pattern of the walls, the maximum difference in dB between the rigid pipe and the vibrating pipe will occur at different frequencies. When comparing the 2D results with the eigenmodes found in 3D, many eigenmodes show up that don't contribute to the vibration of the walls as they are not axi-symmetric. A 1 meter long lead cylinder (0.3 mm thick walls) have over 100 eigenmodes under 700 Hz, but only one that contributes to the axi-symmetric wall vibrations. Figures 4.11(b), 4.11(c) and 4.11(d) show the eigenmodes (the 3 first breathing modes) that contribute to the maxima for the total displacement in a 2D, axi-symmetric case.

Figure 4.12 shows the acoustical input impedance of one rigid and 3 vibrating pipes made of different materials, and how the acoustical input impedance can be influenced

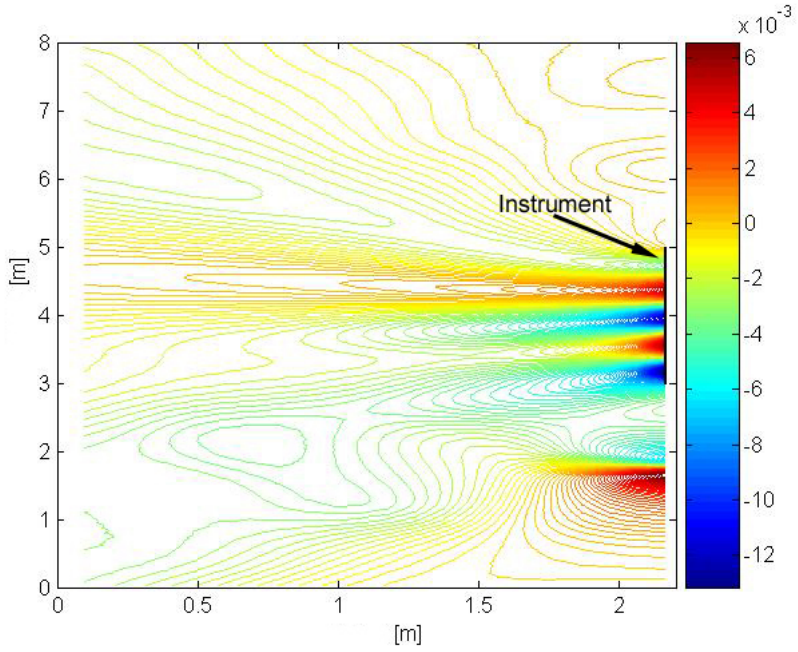

(a) 210 Hz

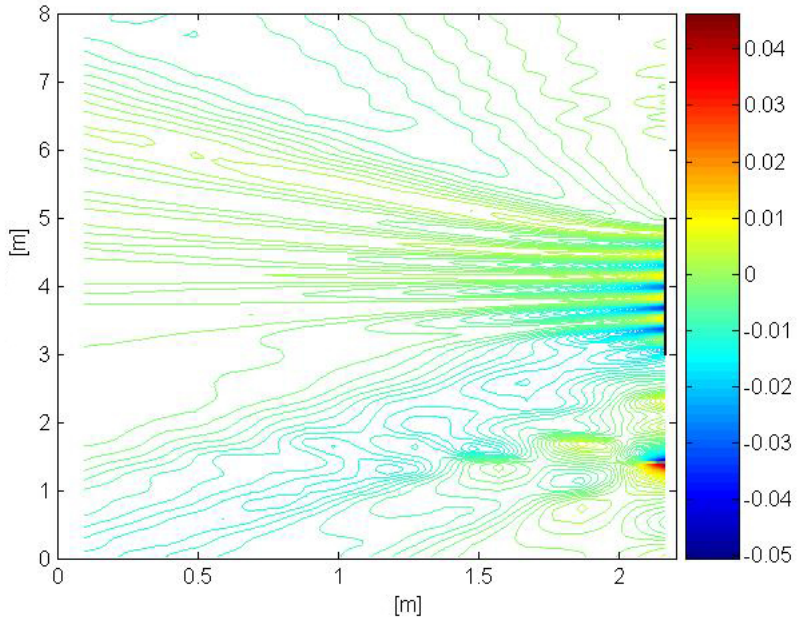

(b) 550 Hz

Figure 4.7 *Difference in dB between the sound radiated from a 2 meter long cylindrical iron tube with 0.5 mm thick vibrating walls and the same tube with rigid walls excited with a plane wave with frequency 210 and 550 Hz. The air column is excited with a plane wave going upwards, and the pressure at the origin is 250 Pa. The colour bars show the difference between the sound pressures in dB.*

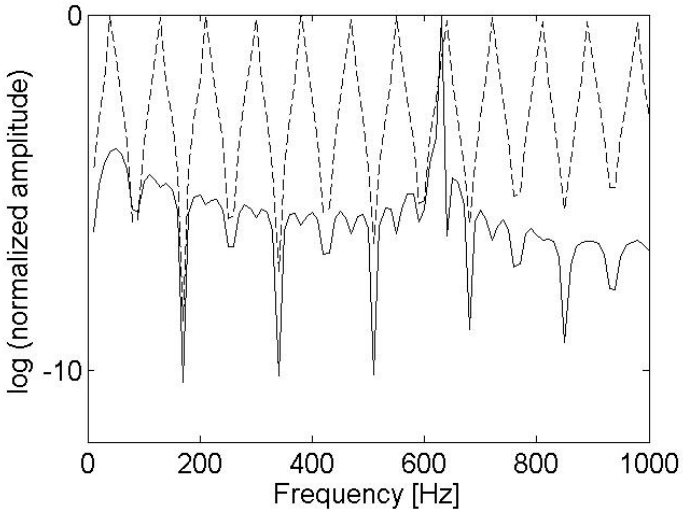

Figure 4.8 *Log of the maximum of the total displacement of a 2 meter long cylindrical iron tube and log of the tubes impedance (dashed line). The total displacement has minima at the same frequencies as the anti-resonances but local minima at most of the resonances.*

by the vibrating walls. The maxima and minima are all shifted, how much depends on the material, but for the cylinder in question (1 meter long, 0.01 m radius, 0.3 mm thick walls) the peaks are not moved more than 0.3 Hz for frequencies below 1500 Hz. Figure 4.13 shows how a structural resonance peak can change the acoustical input impedance, creating an extra peak for the lead cylinder. For the iron cylinder in figure 4.13 no such change is found. This could be due the larger amplitude of the vibrations in the lead cylinder, as the max displacement is about 100 larger for lead than for iron.

If the breathing modes have the same frequency as the minima or maxima of the acoustical input impedance of the air column of the rigid cylinder, the acoustical input impedance of the vibrating cylinder might change. By changing the different material parameters (density, Youngs modulus, Poissons ratio) the eigenfrequencies of the structural resonances changes. By changing the density of lead the second breathing mode is moved so it coincides with a impedance minima and thus creates an extra peak, albeit a fairly small one, where the minima is for the rigid cylinder, as can be seen in figure 4.14. These changes in the impedance are in agreement those found by Pico et al [32], [33].

Figures 4.15 and 4.16 show the sound radiated from a rigid cylinder and a cylinder with vibrating walls excited a frequency that excites a breathing mode, and the difference in radiated sound pressure between these cylinders plus the difference in sound pressure between cylinders of different materials. When the frequency doesn't correspond with a breathing mode, the different pipes show the same directivity and the difference in sound pressure is usually below 1 dB or lower, depending on how much the material vibrates. For the breathing modes, the deviations in sound pressure are much bigger and directivity changes. The maximum difference in sound pressure isn't necessarily located in the same

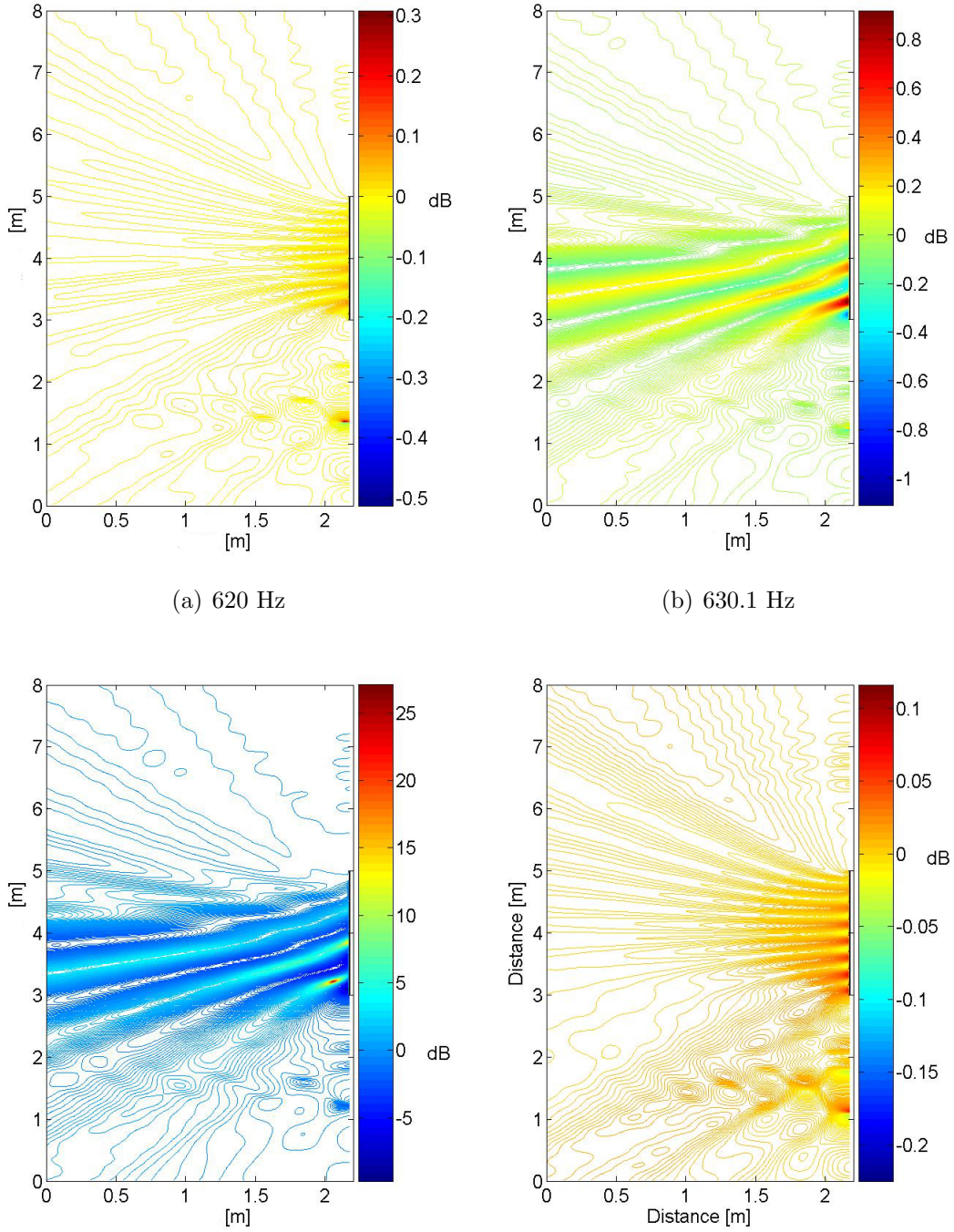

(a) 620 Hz

(b) 630.1 Hz

(c) 630.19 Hz

(d) 640 Hz

Figure 4.9 *Difference in dB between the sound radiated from a 2 meter long cylindrical iron tube with vibrating walls and the same tube with rigid walls excited with a plane wave with frequency (from top to bottom) 620 , 630.1, 630.19 and 640 Hz. The maximum total displacement of the tube is found at 630.19 Hz and corresponds with a different vibration pattern as can be seen from the difference in radiated sound.*

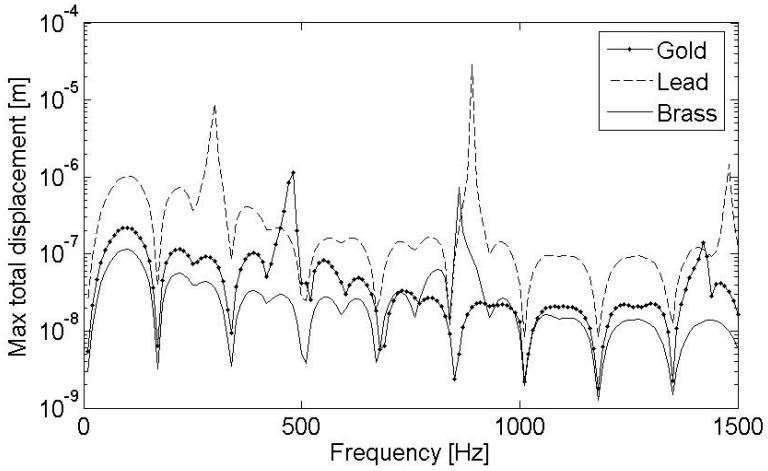

Figure 4.10 *Maximum total displacement for three 1 meter long cylindrical tubes with 0.3 mm thick walls made of gold, lead and brass. The main peaks for the different materials are at different frequencies but the smaller ones follow the impedance of the cylinder.*

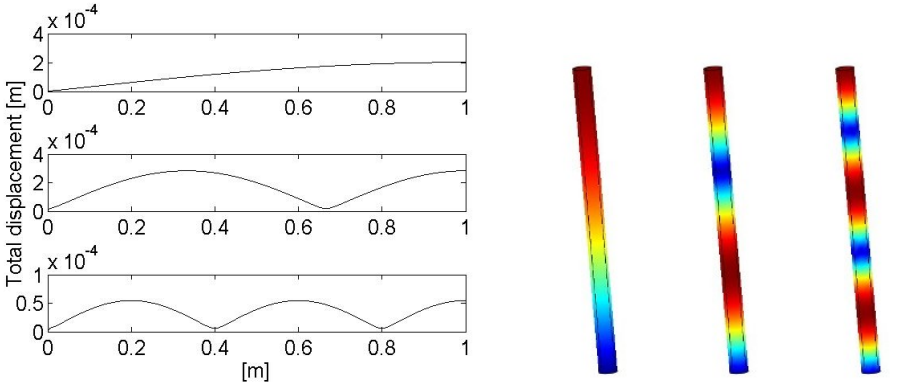

(a) 2 D (b) 297 Hz (c) 889 Hz (d) 1476 Hz

Figure 4.11 *The total displacement for the 3 resonance peaks (297 Hz, 890 Hz and 1477 Hz) of a 1 meter long lead cylinder and the total displacement of the 3 first breathing modes (297, 889 and 1476 Hz) of a 3D lead cylinder.*

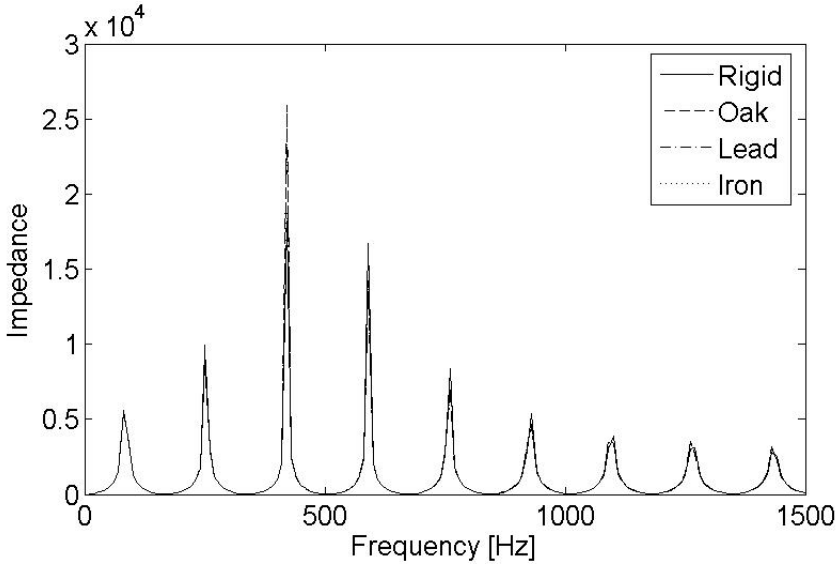

(a) Impedance

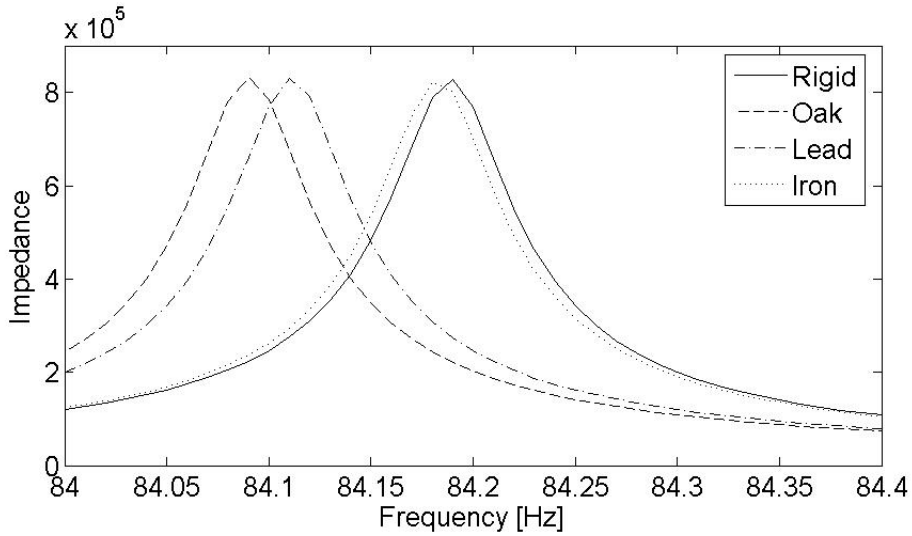

(b) Close-up of the first resonance peak.

Figure 4.12 *Acoustical input impedance of a 1 meter long rigid cylinder and cylinders made of oak, lead and iron. The top figure shows the impedance for all 4 cylinders, and the bottom figure a close-up of the first impedance peak.*

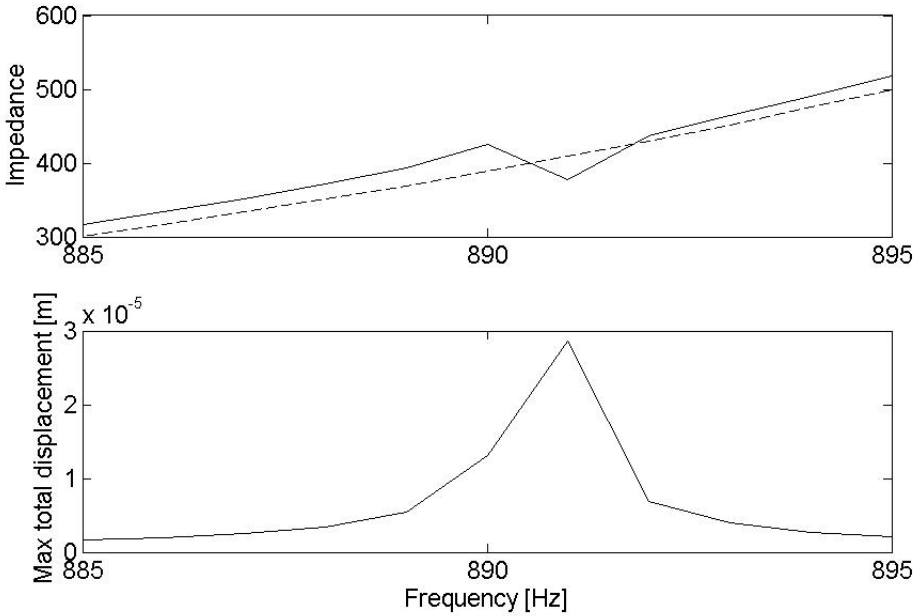

(a) Lead

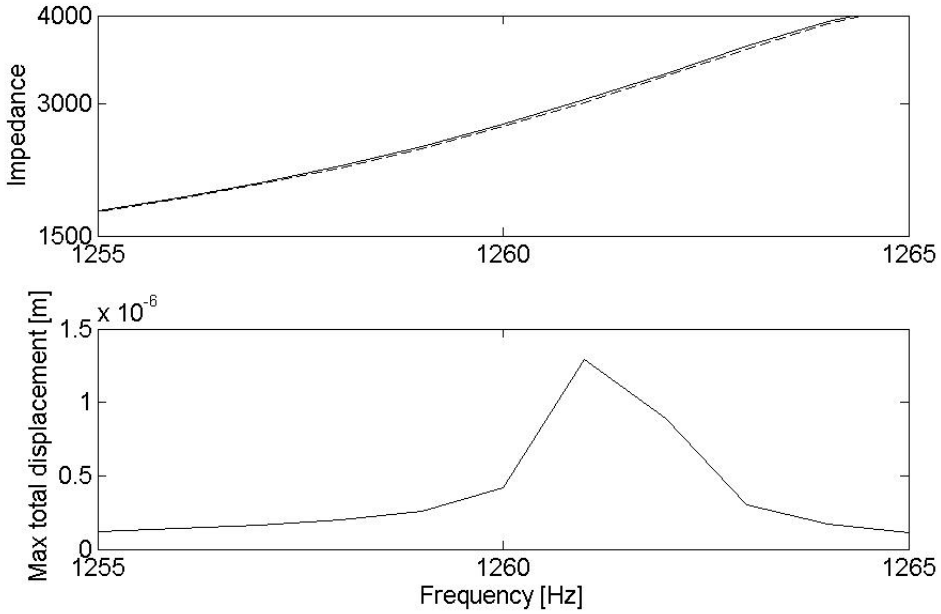

(b) Iron

Figure 4.13 *The top figure shows a close-up of the acoustical input impedance for a 1 m long lead cylinder and a rigid cylinder (dashed line) and the maximum total displacement for the lead cylinder; the bottom figure shows the same for a iron cylinder. The impedance of the lead cylinders shows an extra peak corresponding to the maximum total displacement whereas the impedance of the iron cylinder shows no such peak.*

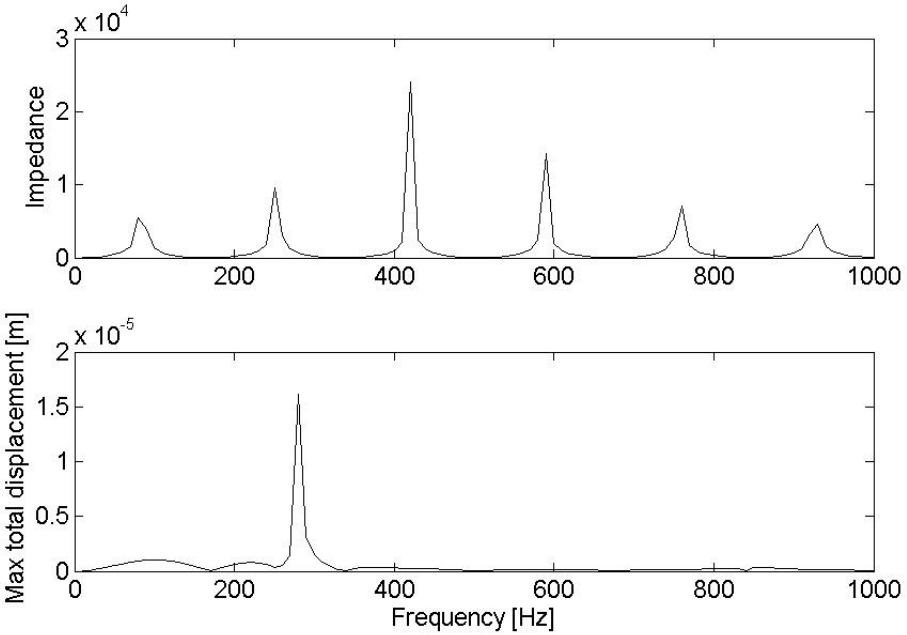

(a) Impedance and maximum total displacement

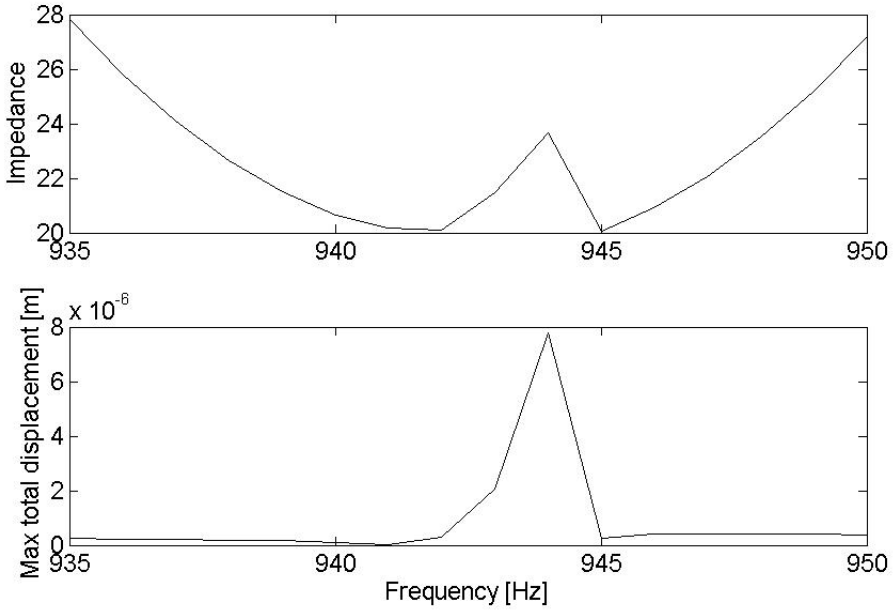

(b) Close-up of impedance and maximum total displacement

Figure 4.14 *Acoustical input impedance and maximum total displacement of a 1 meter long cylinder made of a material with the same material properties as lead but with density 10300 kg/m3. The lower figure shows a close-up of the second peak in the maximum total displacement, this peak corresponds to a minimum in the impedance and gives and extra peak where the minimum would have been for a rigid cylinder.*

place for different eigenmodes. If several harmonics of the air column are excited, one might excite a structural eigenmode and make the ratio between the harmonics dependent on where the musician/listener is located.

The frequencies of the breathing modes are dependent on the length and circumference of the cylinder but not on the thickness of the walls. Thicker walls vibrate less then thinner walls, but the resonances caused by the breathing modes are at the same frequencies. If the air column is made longer but the vibrating part of the cylinder stays the same, the local minima and maxima caused by the acoustical input impedance changes, but the structural resonances don't.

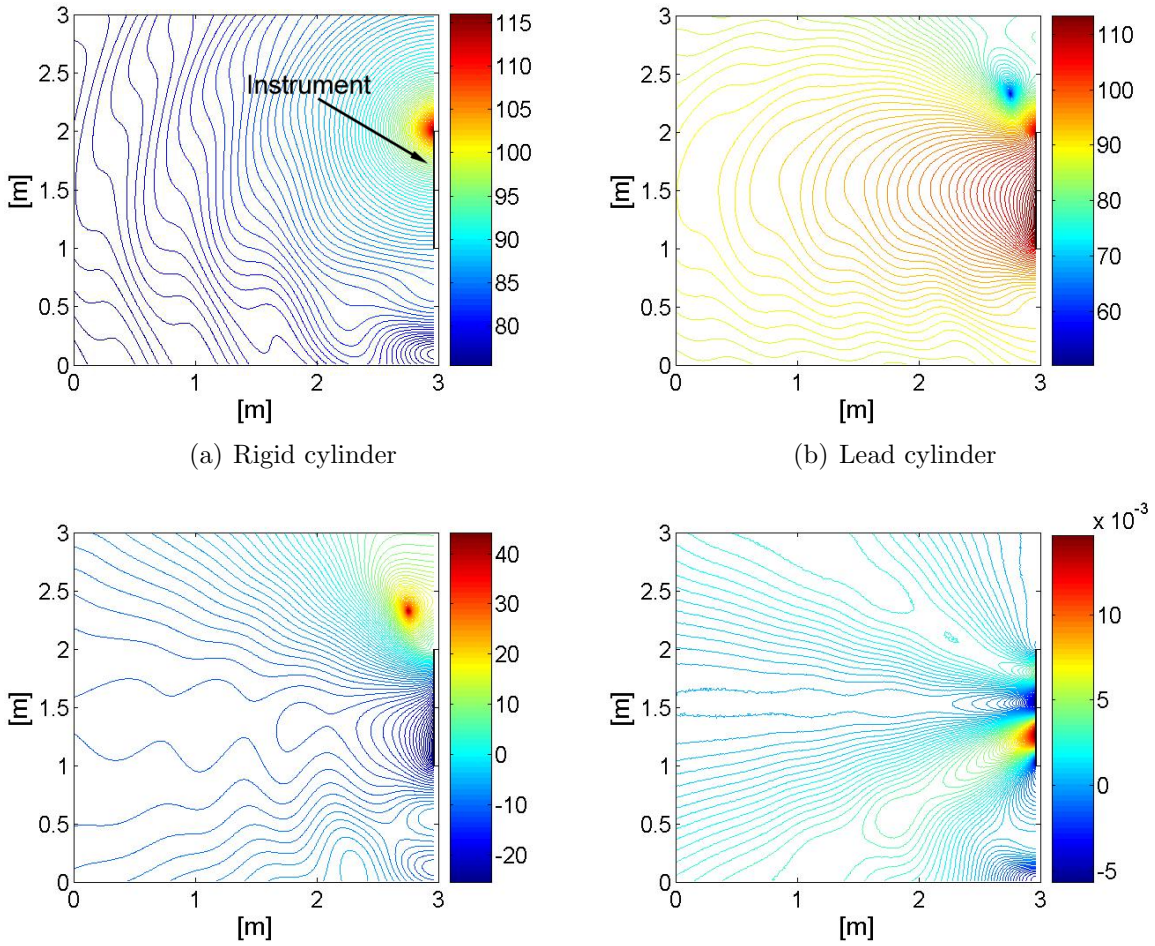

(a) Rigid cylinder

(b) Lead cylinder

(c) Difference between rigid and iron

(d) Difference between rigid and lead

Figure 4.15 *Difference in dB at 297.07 Hz between the sound radiated from a 1 meter long cylindrical tube with 0.3 mm thick vibrating walls, radius=30 mm and the same tube with no wall vibration. The upper left figure shows the sound pressure for the rigid cylinder, the upper right the sound pressure for a lead cylinder when the walls vibrate. The bottom left figure shows the difference in sound pressure between a rigid cylinder and an iron cylinder, the bottom right figure the same for a gold cylinder. The radiation pattern for lead and iron are quite different. The lead pipes' total displacement has a peak at 297.07 Hz and shows a quite different radiation pattern. The differences from the rigid cylinder are much bigger and would be audible, especially close to the pipe.*

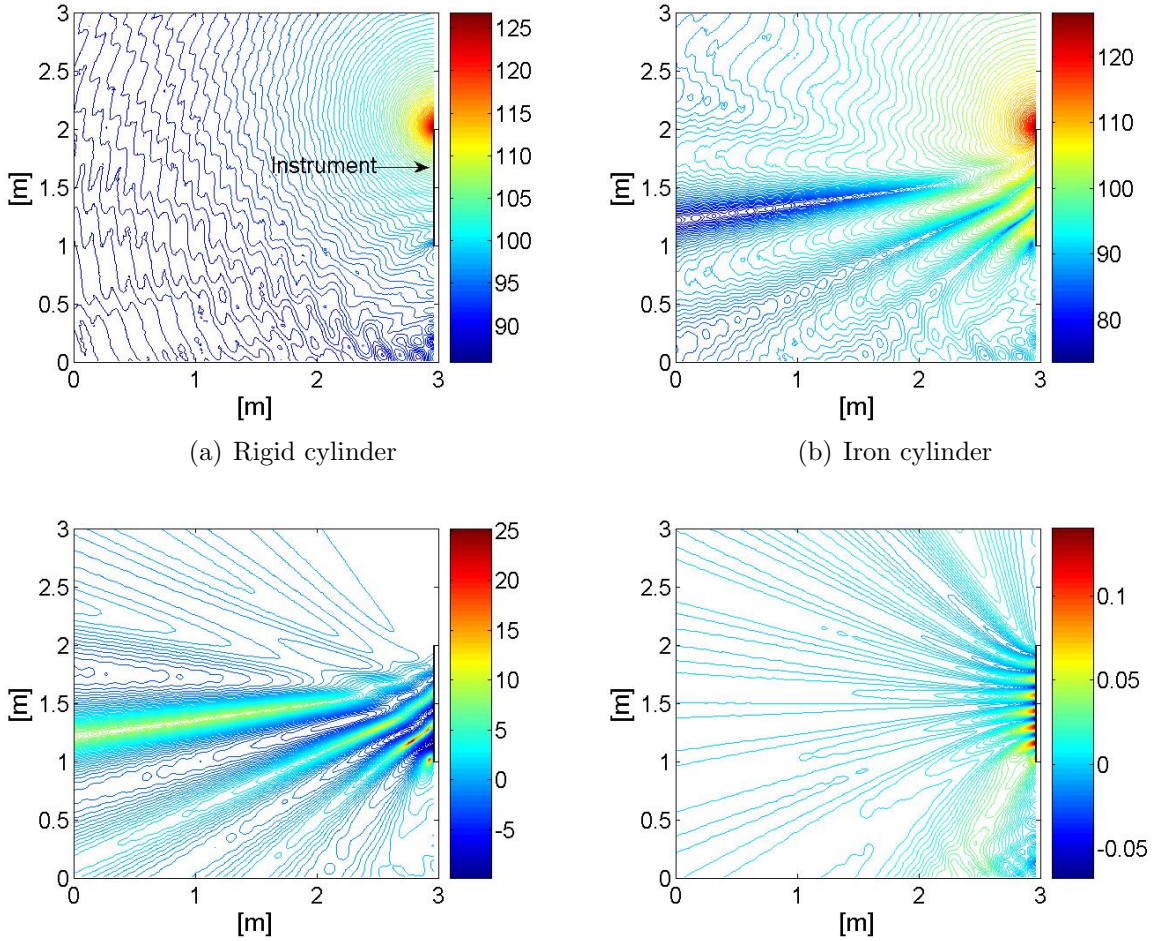

(a) Rigid cylinder

(b) Iron cylinder

(c) Difference between rigid and iron

(d) Difference between rigid and gold

Figure 4.16 *Difference in dB at 1260.43 Hz between the sound radiated from a 1 meter long cylindrical tube with 0.3 mm thick vibrating walls, radius=3 cm and the same tube with no wall vibration. The upper left figure shows the sound pressure for the rigid cylinder, the upper right the sound pressure for the iron cylinder when the walls vibrate. The bottom left figure shows the difference in sound pressure between a rigid cylinder and an iron cylinder, the bottom right figure the same for a gold cylinder. The radiation pattern for gold and iron are quite different. The iron pipes' total displacement has a peak at 1260.43 Hz and shows a quite different radiation pattern. The differences from the rigid cylinder are much bigger and would be audible, especially close to the pipe.*

4.5.2 3-D cylinders

The two dimensional axi-symmetric simulation only show which axi-symmetric eigenmodes got excited by the vibrating air column. The three dimensional cylinders as expected show more structural resonance peaks than the axisymmetric solutions, as can be seen in figure 4.17. The two dimensional cylinder only had one major peak in the maximum total displacement under 800 Hz, which corresponds to the peak at 270 Hz (the first breathing mode) in three dimensions, but the 3 D simulation show an additional 11 peaks under 800 Hz. The deviation in frequency for the first breathing mode is most likely due to difference in resolution. The local maxima and minima due to the impedance top and bottoms aren't longer as clear as for the axi-symmetric case, due to the larger number of excited eigenmodes the maximum total displacement no longer follow the curve of acoustical input impedance as closely as for two dimensions. The 12 eigenmodes excited below 800 Hz are shown in figure 4.18 and include both axi-symmetric and non-symmetric vibration patterns.

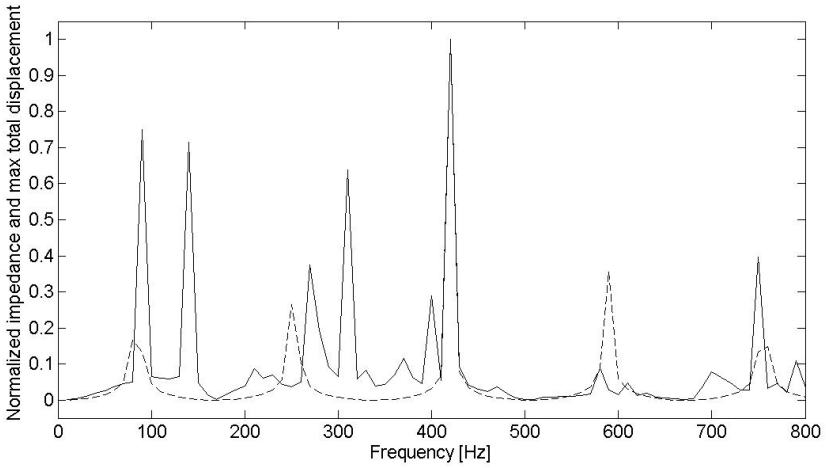

Figure 4.17 *Normalized maximum total displacement and normalized acoustical input impedance (dashed line) for a 1 meter long lead cylinder with a radius of 3 cm and 0.3 mm thick walls.*

Small indentations might not change the impedance of the cylinder significantly, but the structural response can be changed by small irregularities in f.ex. the shape of the walls or material thickness. Organ builders will dent the pipes to get rid of unwanted resonance due to structural eigenmodes. Figures 4.19 to 4.24 show the geometries and maxium total displacement for two dented cylinders, one has a indentation shaped as half a sphere with radius 0.6 cm placed 30 cm up from the excitation, the other has a ellipsoid indentation 30 cm down from the opening which is 1 cm long in the length direction of the cylinder, 5 mm broad and 3 mm deep. Apart from the dent, the cylinders have the same dimension as the cylinder in figure 4.17. Although the dents don't change the frequency of the eigenmode much, for the lower eigenfrequencies the change is normally less than 1 Hz as can be seen in figure 4.25, it changes the structural response of the pipe and makes the maximum vibration occur at different frequencies. For the bigger dent, the number of

eigenmodes below 500 Hz is reduced from 7 to 3. For the smaller dent, the number if eigenmodes excited below 500 Hz stays the same but the frequencies change.

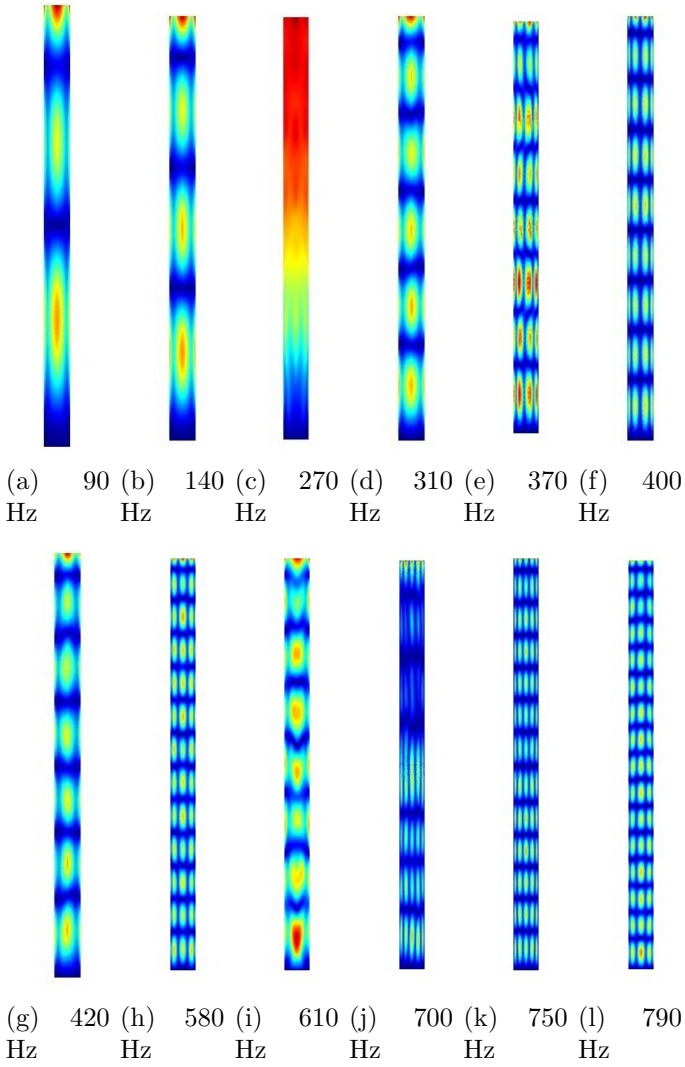

Figure 4.18 *The first 12 resonance peaks for a 1 meter long lead cylinder, with radius = 3 cm and 0.3 mm thick walls. The eigenfrequencies are between 90 and 790 Hz.*

Small changes in the overall shape of the cylinder can also change the structural response, either by shifting the frequencies of the excited eigenmodes or by exciting different eigenmodes. For a pipe with an elliptical circumference with one radius being 1 procent wider than the other the changes in impedance compared to the cylindrical pipe are quite small but the mechanical resonance pattern changes significantly (see figure 4.26) and the number of eigenmodes excited under 500 Hz is reduced from 7 to 2, both of which are under 100 Hz and shown in figure 4.27.

Bending the cylinder also changes the structural response, figure 4.28 shows the maximum total displacement of a 1 meter long lead pipe bent as a half circle. All the resonances under 1000 Hz disappears and a new one is created at 20 Hz. The vibration pattern

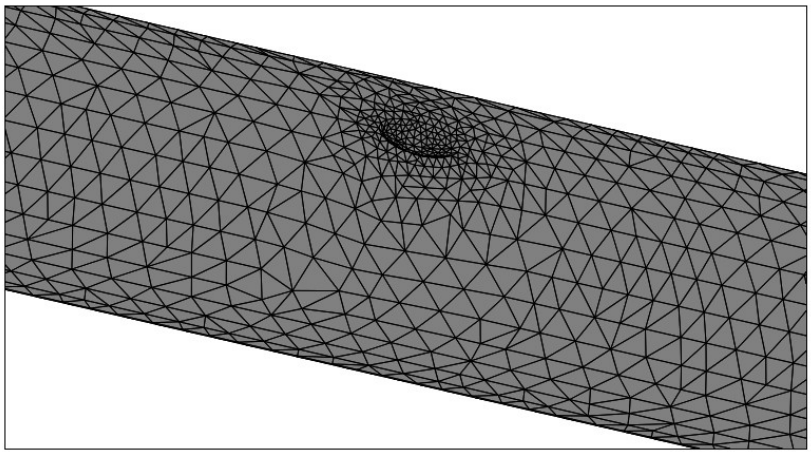

Figure 4.19 *Mesh of pipe with elliptic indentation 0.3 meter down from the opening of the cylinder. The dimensions are the same as for the perfect cylinder in figures 4.17 and 4.17.*

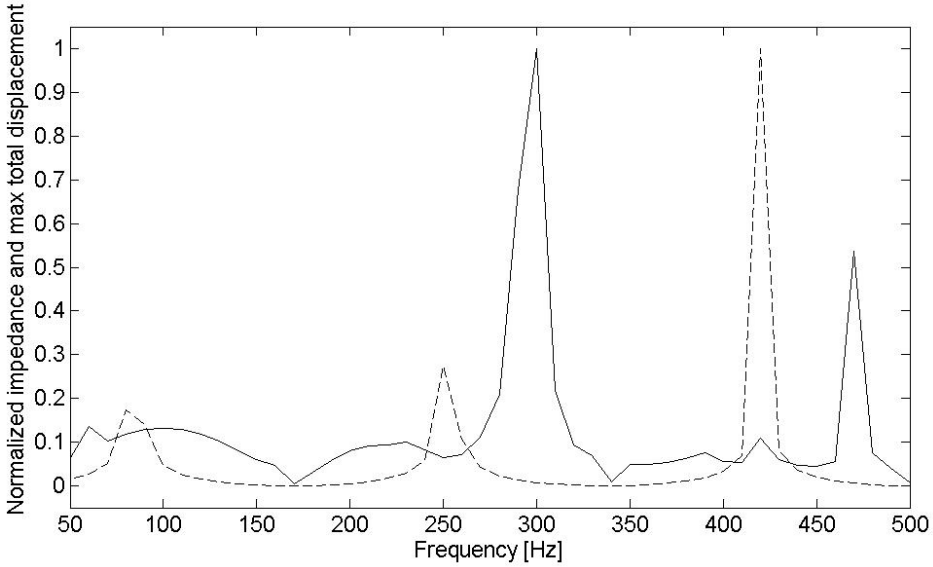

Figure 4.20 *Mechanical response and impedance (dashed line) of the pipe in figure 4.19*

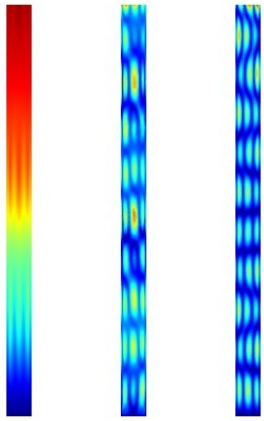

(a) 300 Hz (b) 420 Hz (c) 470 Hz

Figure 4.21 *The first 3 resonance peaks for the pipe in figure 4.19, the lead pipe without indentation has 7 peaks in the same frequency range.*

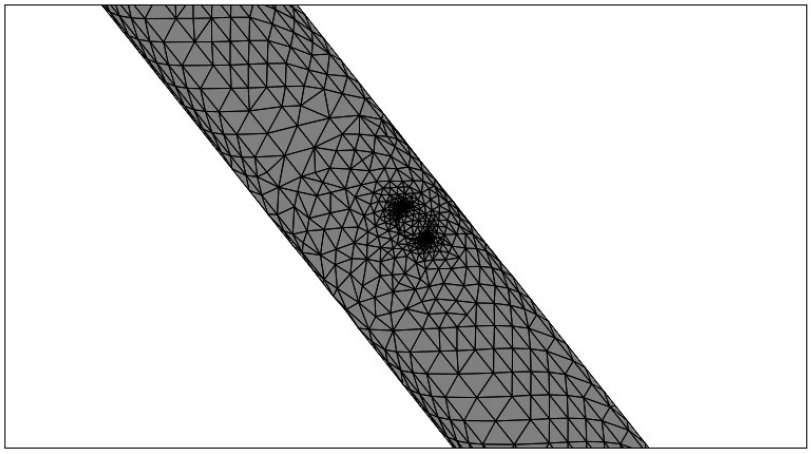

Figure 4.22 *Close-up of the mesh of 1 meter long and 3 cm wide pipe with cylindrical indenation 0.5 meter down from the opening.*

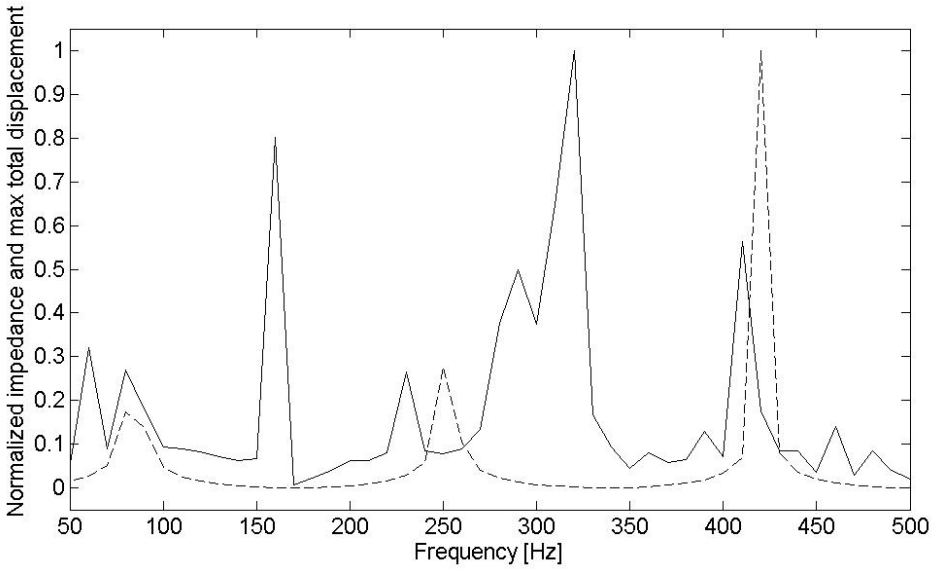

Figure 4.23 *Normalized maximum total displacement and normalized acoustical input impedance (dashed line) of the pipe in figure 4.22*

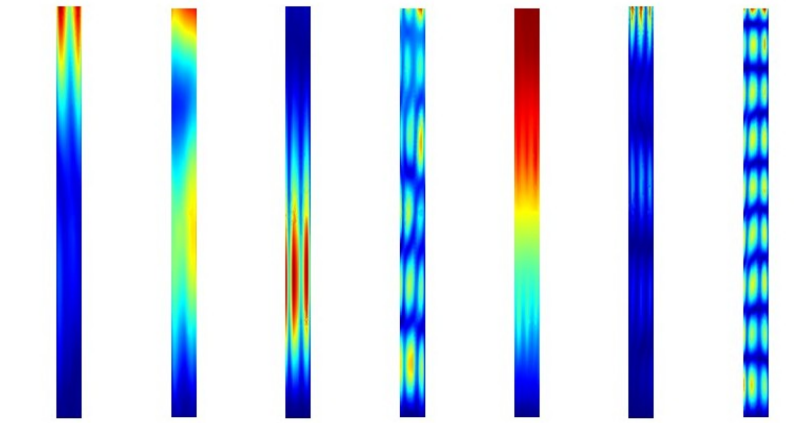

Figure 4.24 *The first 7 resonance peaks of the pipe in figure 4.22. The pipe has the same number of peaks under 500 Hz as the symmetrical lead pipe, but they don't occur at the same frequencies.*

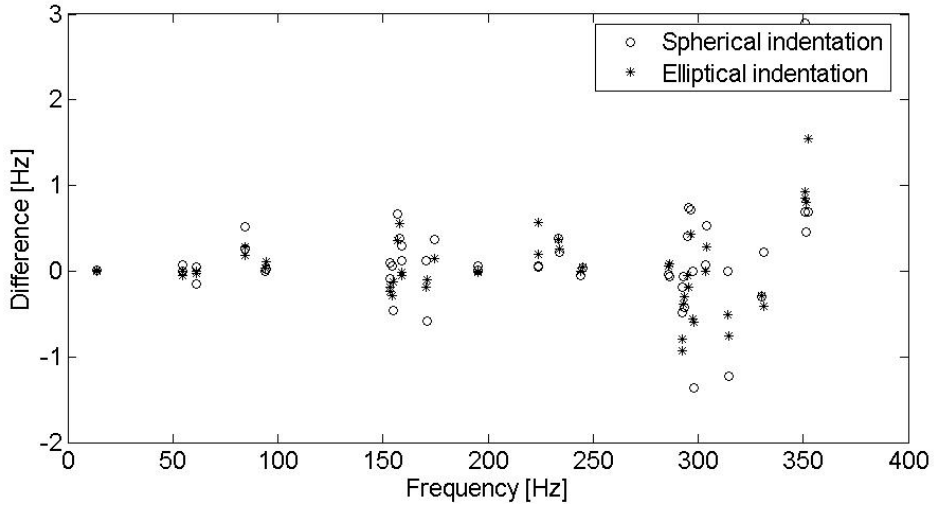

Figure 4.25 *Difference in Hertz between the 50 first eigenfrequencies of a perfectly cylindrical, 1 meter long lead pipe and two pipes with irregularities, one with a circular indentation and one with an elliptical one. The differences are well under 1 Hz for most of the eigenfrequencies.*

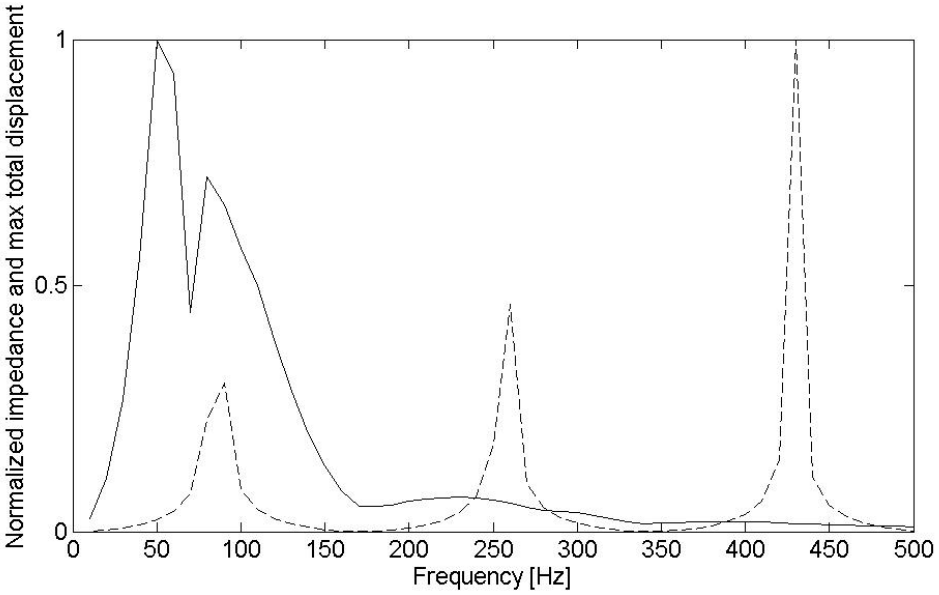

Figure 4.26 *Normalized maximum total displacement and normalized acoustical input impedance (dashed line) of a 1 meter long pipe with elliptical circumference, with one radius 3.03 cm and the other 3.00 cm.*

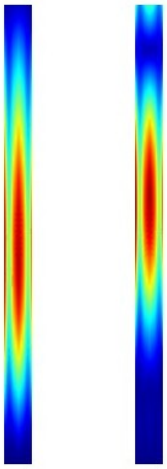

(a) 50 Hz (b) 80 Hz

Figure 4.27 *The first 2 resonance peaks for the pipe described in figure 4.26. The pipe doesn't have other clear resonance peaks under 500 Hz.*

changes between the maxima and minima of the tubes acoustical input impedance (figure 4.29).

To study the sound radiated only from the vibrating walls of the cylinder the boundary condition (fixed) of edges at the excited end of the cylinder were replaced with a given velocity to resemble a shaker, and acoustical excitation removed. The maximum total displacement when excited with the shaker did not look quite like the acoustically excited equivalent. Figure 4.30 shows the difference between a 1 meter long pipe made of pure lead and a 1 meter long pipe of lead where the upper 10 cm (furthest away from the excitation) are replaced with gold. Figures 4.30 and 4.31 show the difference in radiated sound pressure for 2 frequencies, 80 Hz and 250 Hz. The biggest differences are found in the cylinders near-field where the different metals have different radiation patterns.

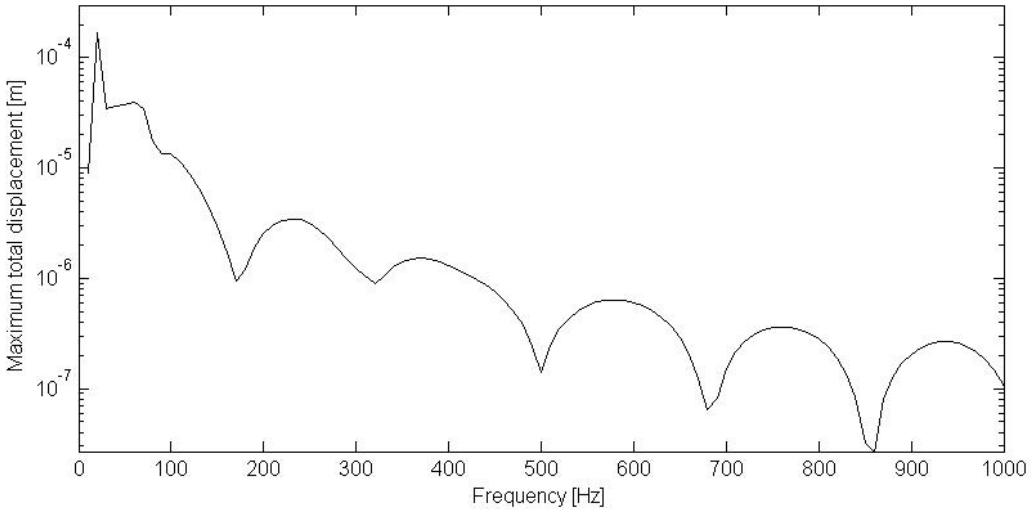

Figure 4.28 *Normalized maximum total displacement and normalized acoustical input impedance (dashed line) of a 1 meter long pipe bent in a half circle. Over 50 Hz, the maxima and minima follow the acoustical input impedance of the tube.*

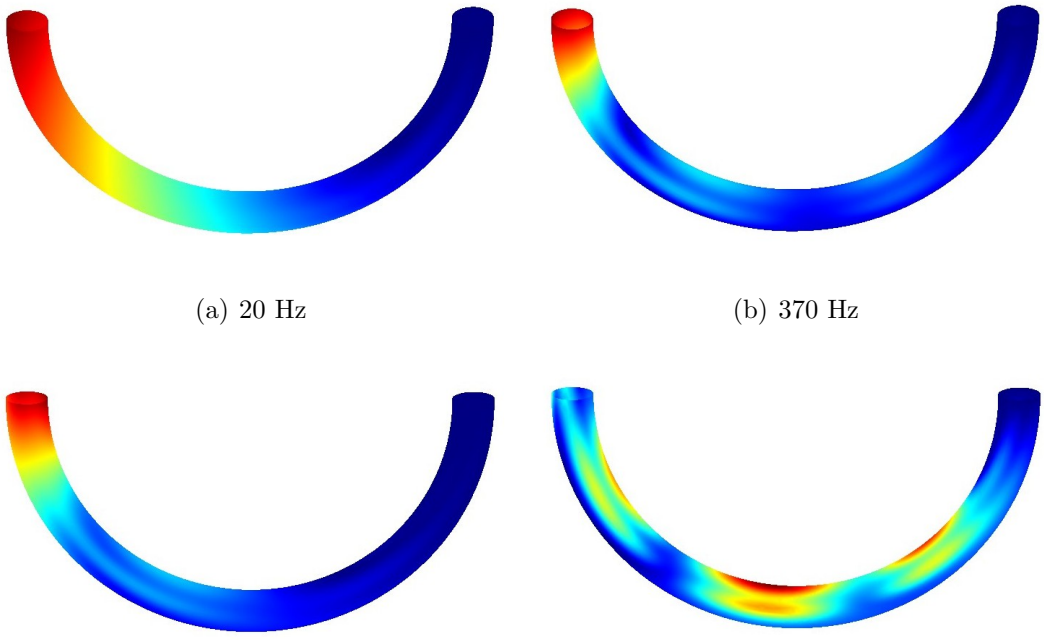

(a) 20 Hz

(b) 370 Hz

(c) 580 Hz

(d) 510 Hz

Figure 4.29 *The vibration pattern at the maxima due to the maxima in the impedance show similar patterns as the main mechanical resonance at 20 Hz, at the minima other vibration patterns, like the one for 510 Hz, can be found.*

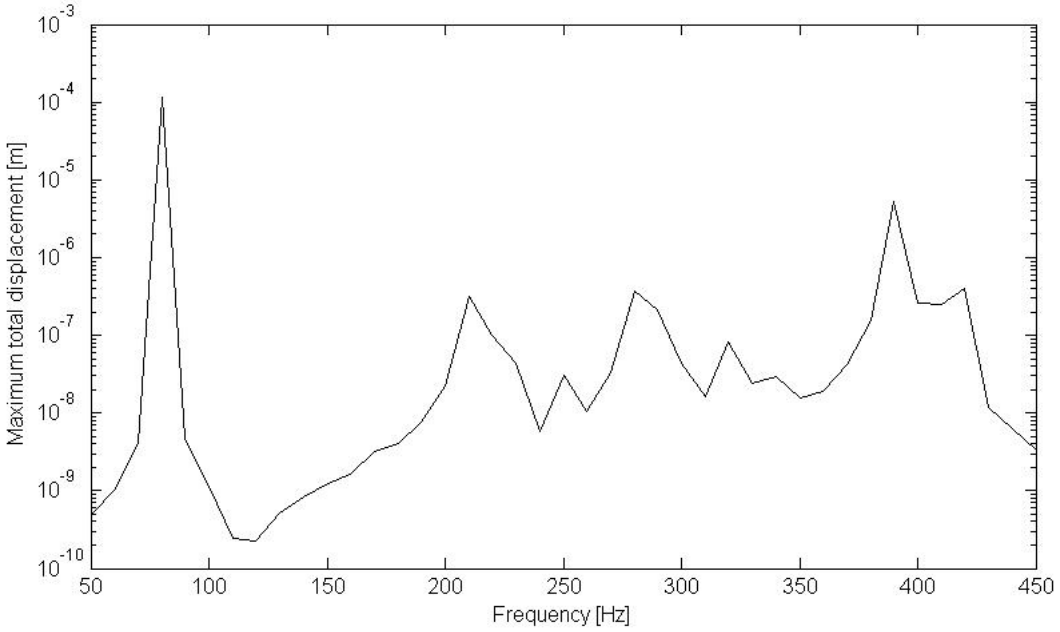

(a) Lead

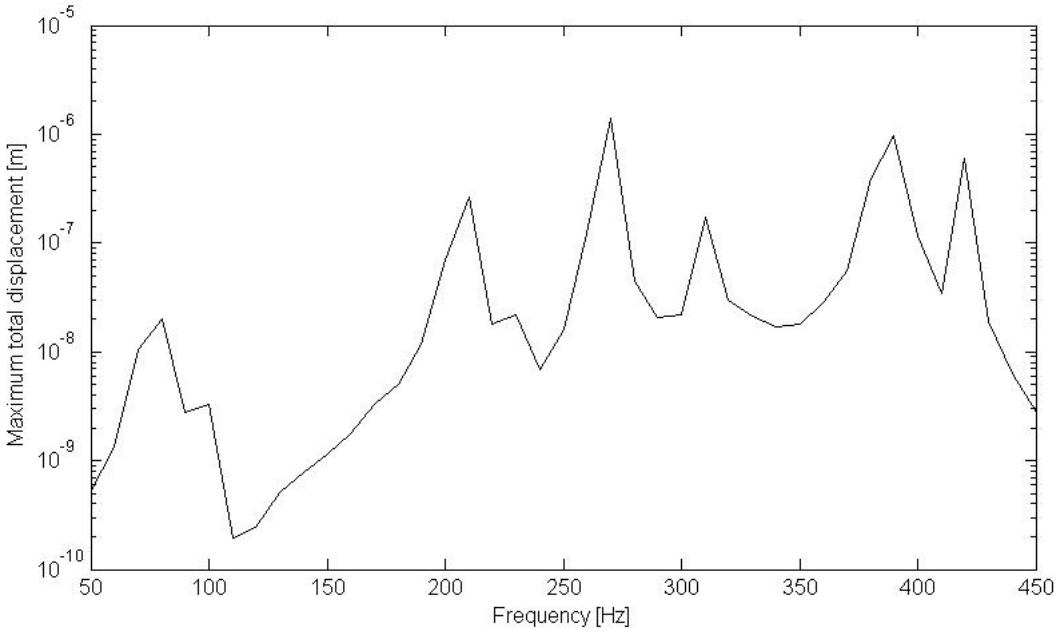

(b) Lead and gold

Figure 4.30 *Maximum total displacement for a 1 meter long lead pipe (top) and 1 meter long pipe with gold in the 10 top cm. The pipes where excited with a given velocity to resemble a shaker.*

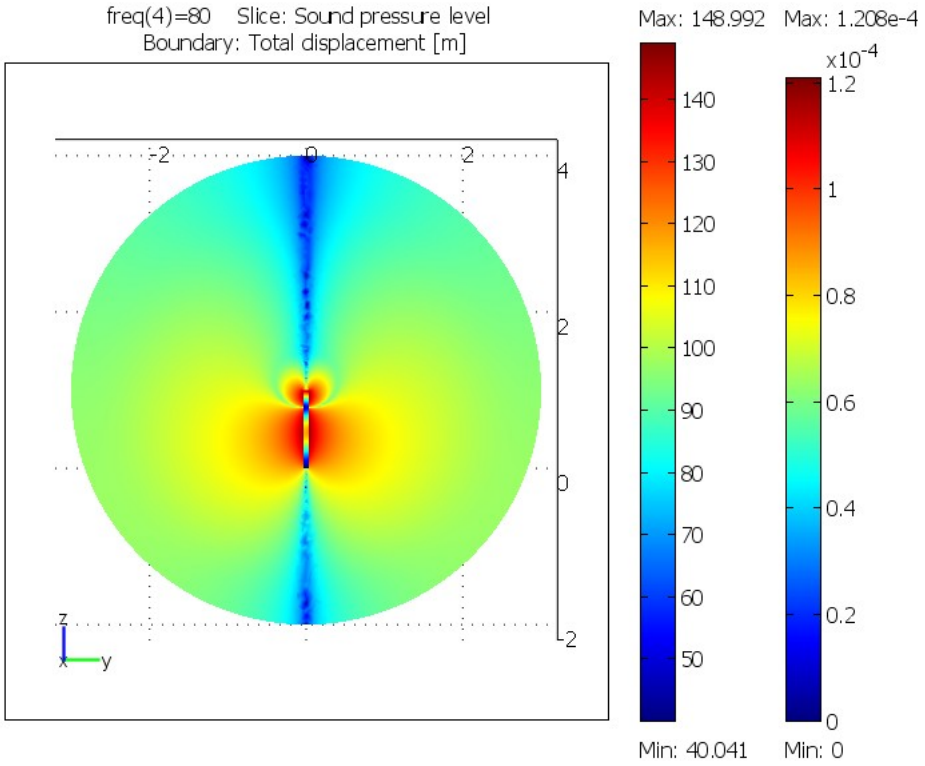

(a) Lead

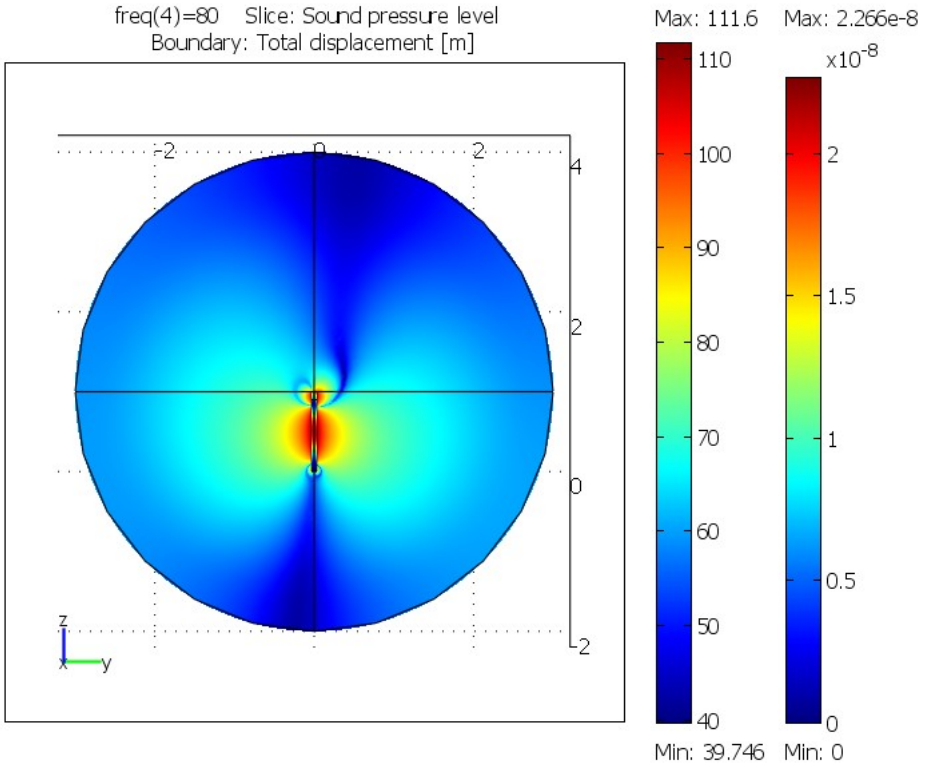

(b) Lead and gold

Figure 4.31 *Sound pressure levels for the sound radiated from the vibrating pipes for 80 Hz. The colour bars show the sound pressure in dB and the total displacement in meters.*

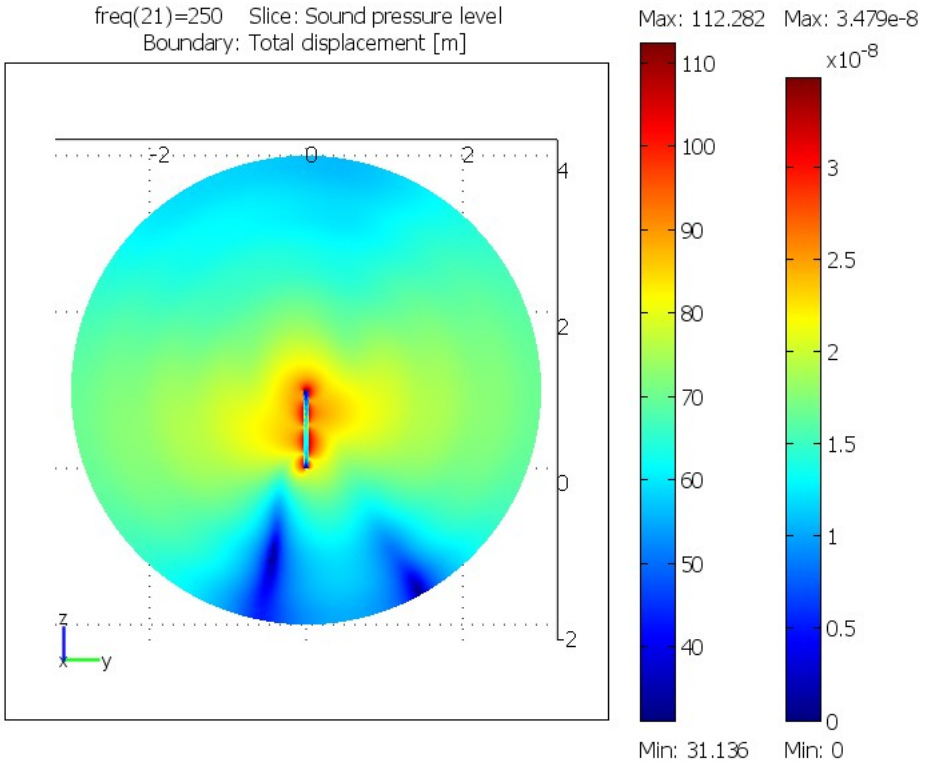

(a) Lead

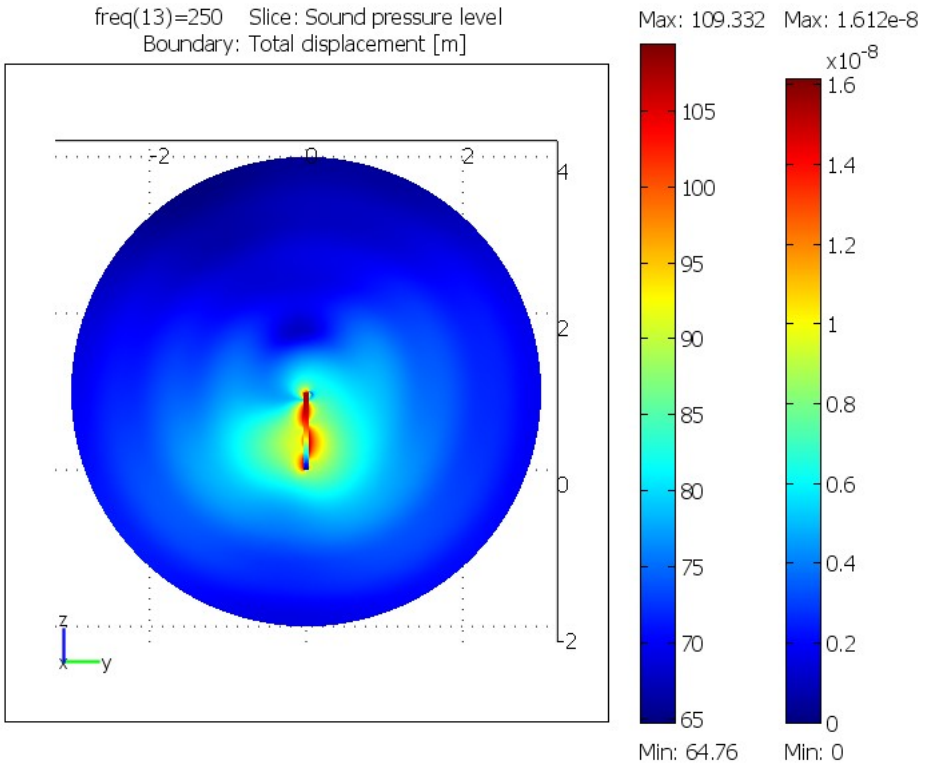

(b) Lead and gold

Figure 4.32 *Sound pressure levels for the sound radiated from the vibrating pipes for 250 Hz. The colour bars show the sound pressure in dB and the total displacement in meters.*

4.5.3 Various other forms

Small changes in the bore can influence the sound made by the instrument in different ways. Most important is the change in the acoustical input impedance of the instrument, but small changes in form might influence some frequencies more than other, either by changing the acoustical input impedance or by moving the structural resonances. A flange on a cylinder influences the acoustical input impedance by changing the end correction. The acoustical input impedance peaks found with COMSOL differ with less than 1 Hz for the 1 cm long flange on a 1 meter long cylinder, and less than 2 Hz for the a flange with diameter 2.5 cm compared to the cylinder without a flange. However, the mechanical resonance is moved 20 Hz for the shortest flange and 900 Hz for the longest flange, as can be seen in figure 4.33. For the shorter flange, the added length moves the structural resonance but it still has a similar shape, but for the longer flange, a totally different eigenmode is excited.

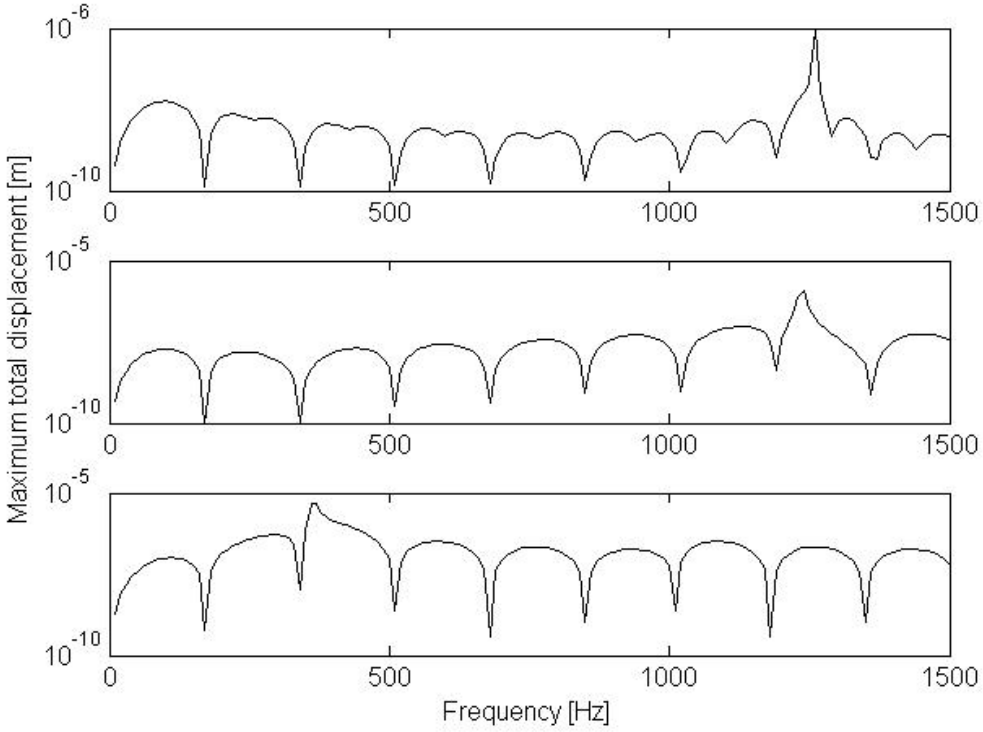

Figure 4.33 *Maximum total displacement for the wall vibrations of three 1 meter long cylinders made of iron, one without a flange, one with a 1 cm wide flange and the last with 2.5 cm wide flange*

Figure 4.34 shows the difference in the sound pressure between the rigid cylinder with 25 mm wide flange and its vibrating equivalent. At 364 Hz, the directivity is similar to that of instrument with a bell, but for 1236 Hz it is similar to the radiation patterns of a cylinder without a flange. The sound pressure levels of the radiated sound decrease rapidly with increased distance from the instrument. Adding a flange on the end of a

cylinder would increase the radiation in front the it, and could also take away or add excited structural eigenmodes that possibly could influence the sound more than the change in acoustical input impedance, as a small flange wouldn't shift the impedance more than what could be compensated by the player.

For more complicated geometries, like the simplified instrument in figure 4.35 (with a 10 cm long bell and a cylindrical, 90 cm long main part), the structural response is more complicated than for cylindrical tubes. Figure 4.36 shows the maximum total displacement for the instrument in figure 4.35, the peaks are more numerous and not as sharp as for cylinders. For higher frequencies the local minima and maxima no longer coincide with the maxima and minima of the acoustical input impedance, figure 4.37.

Figure 4.38 shows the 2 eigenmodes corresponding with the 2 main peaks in the maximum total displacement for the different materials. The main displacement is at bell, the main body of the instrument has much smaller amplitudes than the rim of the bell. Because of the 2D axi-symmetrical simulations, the eigenmodes are of course axi-symmtric. Since the main displacement is at the bell, the main difference in sound pressure between vibrating and rigid or between different materials would be expected to be consentrated around the bell, or radiate from the bell. As can be seen from figure 4.39 the sound from the vibrating walls is radiated from the rim of the bell, and the difference between the sound pressure between different materials is strongest nearly straight out from the bell.

Figure 4.40 shows the acoustical input impedance between 710 and 832 Hz for a simplified instrument as shown in figure 4.35. Figure 4.40(a) shows the acoustical input impedance for brass and iron, Figure 4.40(b) the maximum total displacement for the same two material over the same frequency range. The peaks in the maximum total displacement correspond to peaks in the acoustical input impedance for both instruments. The difference between the acoustical input impedance of the rigid cylinder and the brass cylinder is bigger than the difference between the rigid cylinder and the iron cylinder, most likely because the brass cylinders' total maximum displacement is more than twice that of the iron cylinder.

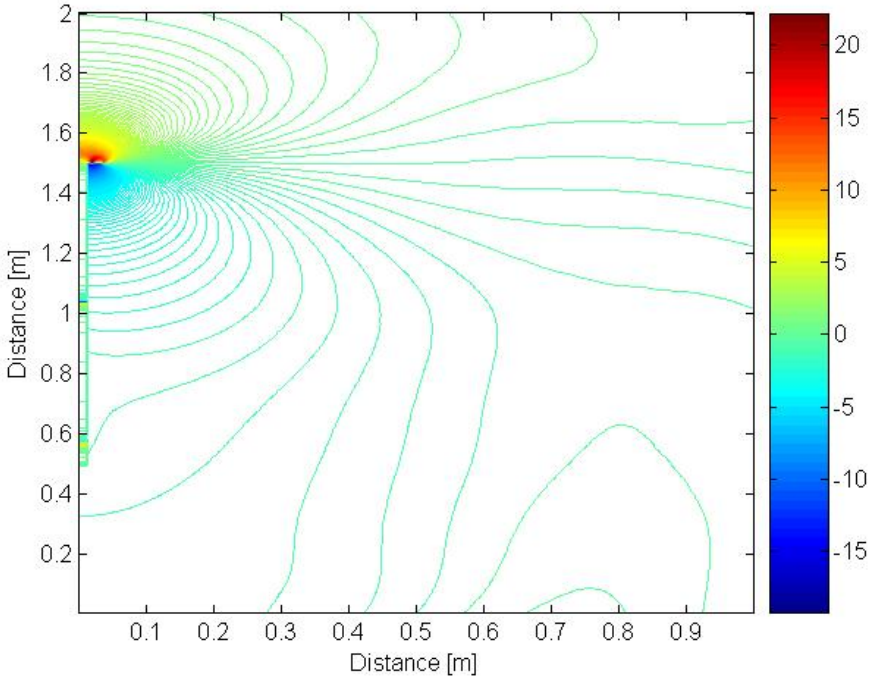

(a) 364 Hz

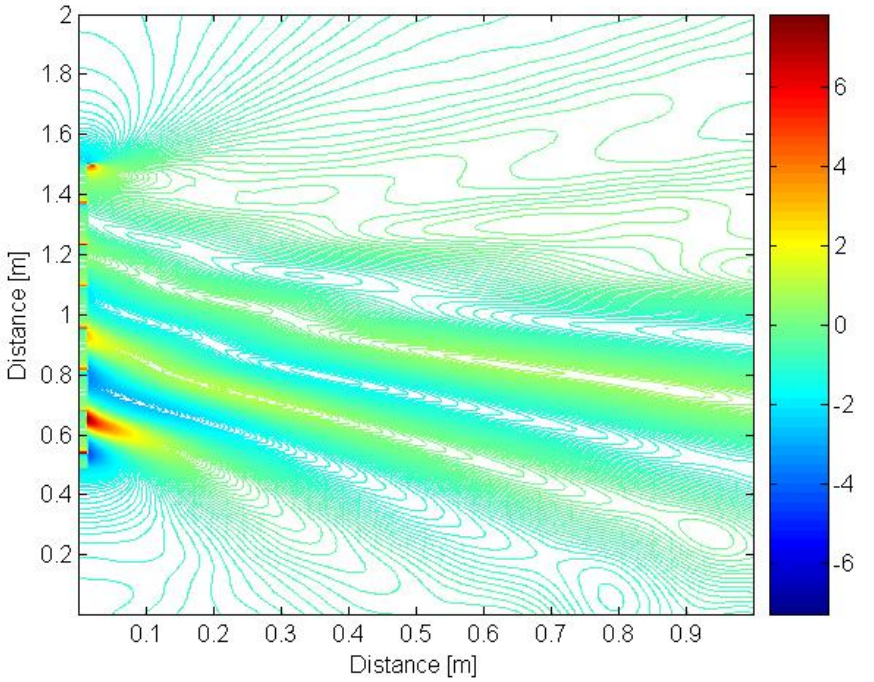

(b) 1236 Hz

Figure 4.34 *Difference in sound pressure between two 1 meter long cylinders with a 25 mm wide flange excited with a 364 Hz (upper figure) and a 1236 Hz plane wave (lower figure), one with rigid and one with vibrating walls. The colour bars show the difference in dB.*

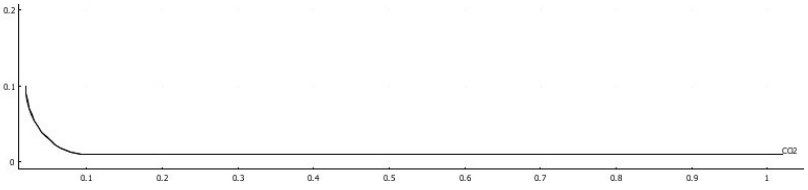

(a) Geometry

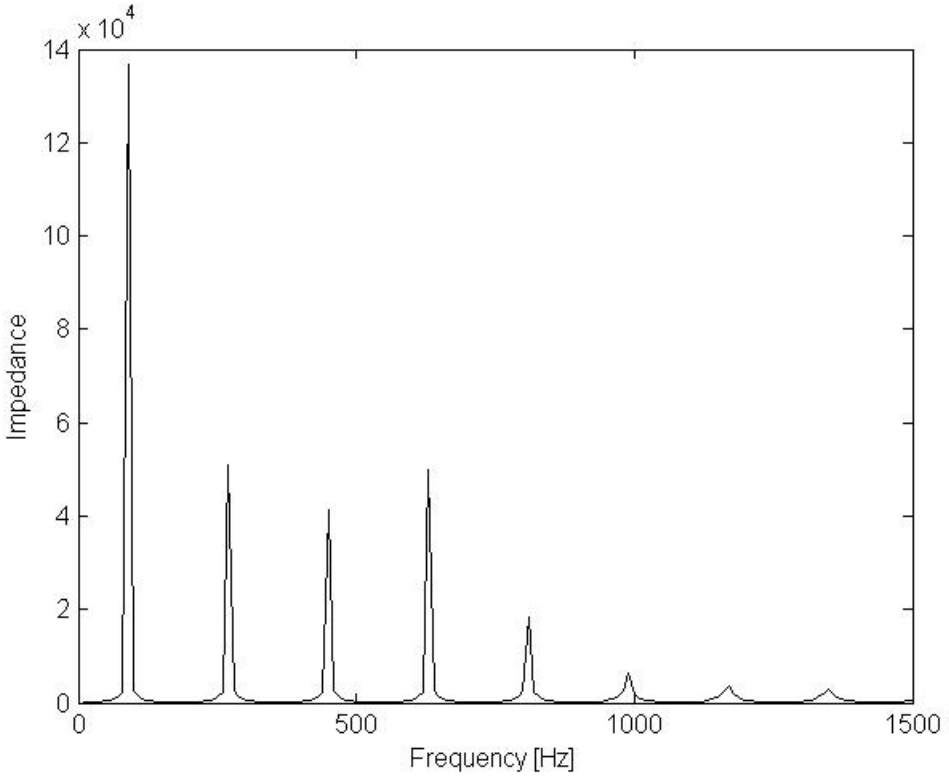

(b) Acoustical input impedance

Figure 4.35 *Geometry and acoustical input impedance of a simplified, 1 meter long instrument with a 10 cm bell and cylindrical body.*

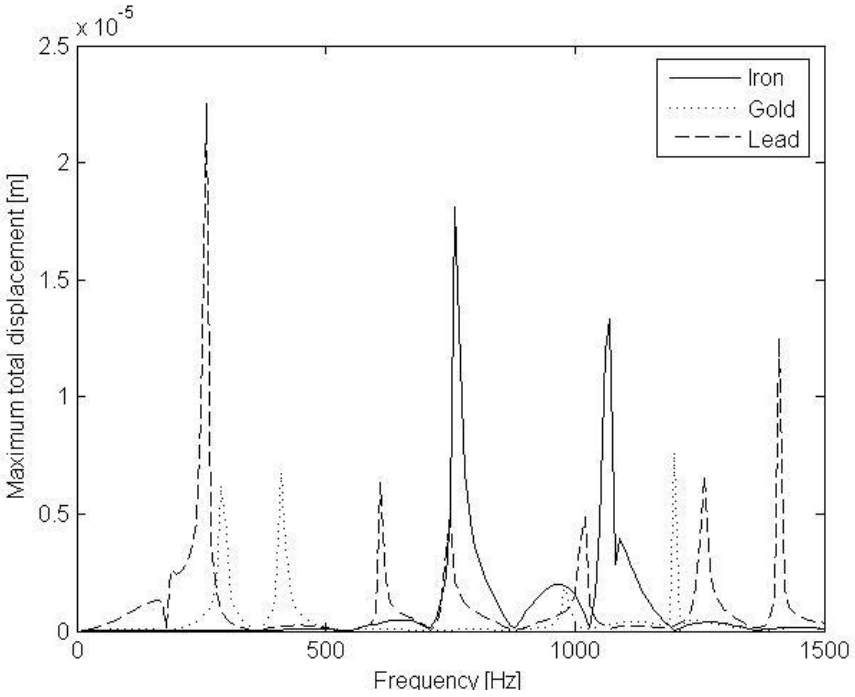

Figure 4.36 *Maximum total displacement for the instrument in figure 4.35 for 3 different materials. The peaks are more numerous and not as sharp as for the cylinders.*

Figure 4.41 shows the same graphs for a 20 cm longer instrument that has the same length of vibrating walls, thus ensuring that one of the structural resonances coincide with one of the resonances for the rigid instrument. Compared to the rigid instrument, the acoustical input impedance of the iron cylinder (that doesn't have a structural resonance at the same frequency) has about the same frequency but slightly higher amplitude, probably amplified by the vibrations of the walls. The brass instrument has a wider peak than both the rigid and the iron instrument, and the peak is split in two. This corresponds to the differences between rigid and vibrating cylinders found by Pico et al [32], [33]. One of the peaks' maxima corresponds to the air columns resonance, and the other one to the structural resonance. A change like this would be noticed when playing the instrument, for good of for bad. If the structural resonance is very close to the air columns resonance, it could mean that a wanted peak is amplified, making it easier to play but affecting the balance between the harmonics. If it is close enough to split it but different enough to make two peaks, it could mean unwanted tones, or possibly an harmonic that is difficult to intonate properly.

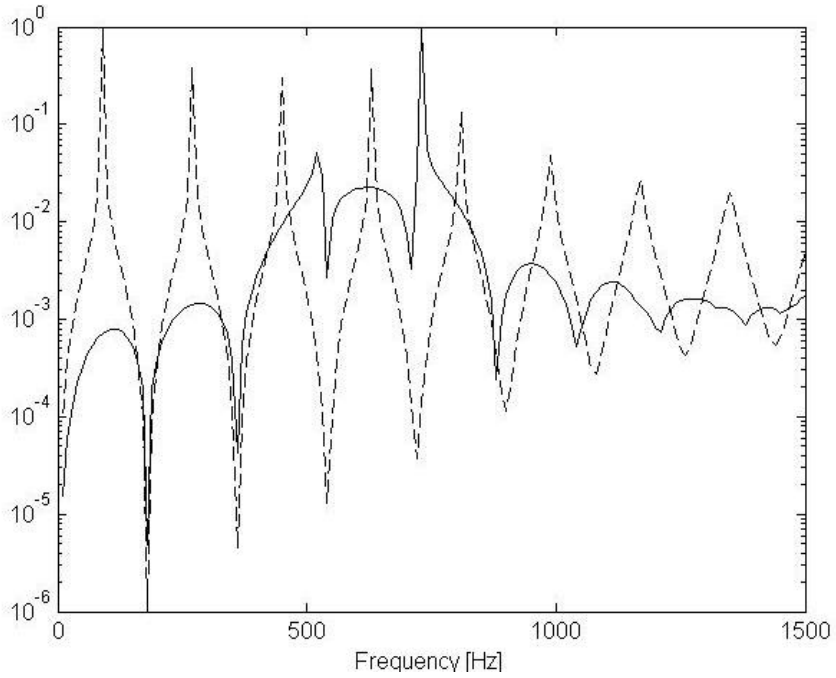

Figure 4.37 *The log of the normalized acoustical input impedance and the normalized maximum total displacement for the instrument in figure 4.35 made of brass. For frequencies above 900 Hz the maxima and minima of the acoustical input impedance and displacement no longer coincides.*

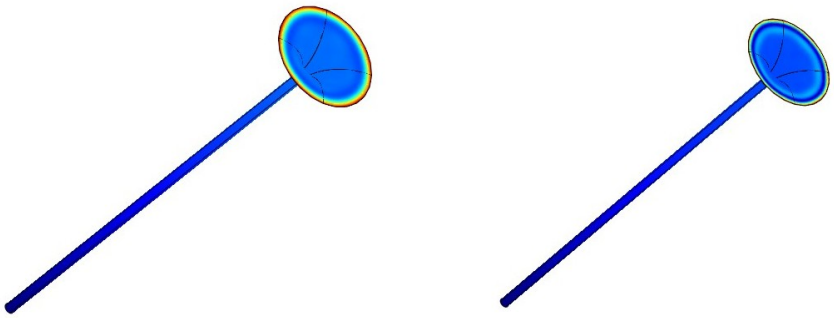

Figure 4.38 *The eigenmodes of the two main resonance peaks for the maximum total displacement of the instrument in figure 4.35. For a 0.3 mm thick iron instrument they are at 763 Hz and 1067 Hz. For both frequencies the main displacement is at the bell rim.*

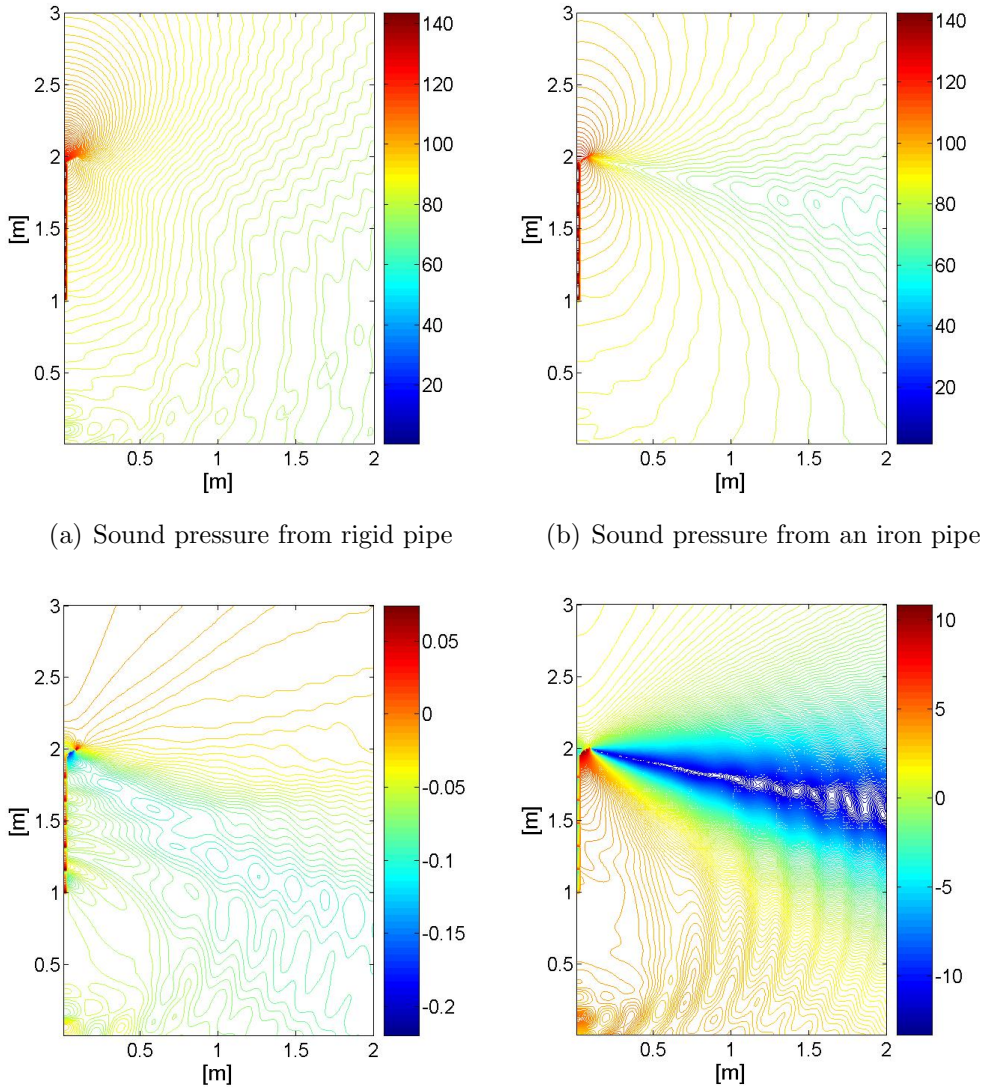

(a) Sound pressure from rigid pipe

(b) Sound pressure from an iron pipe

(c) Difference between rigid and gold

(d) Difference between gold and iron

Figure 4.39 *Figure 4.39(a) shows the sound field from a rigid instrument excited at 1066 Hz, figure 4.39(b) shows the same for an instrument of iron with vibrating walls. Figure 4.39(c) shows the difference in dB between the sound radiated from the ridig instrument and an one made of gold with vibrating walls, and figure 4.39(d) the difference between metals two instruments with vibrating walls but made of different materials (gold and iron). The colour bars show the difference between the sound pressures in dB.*

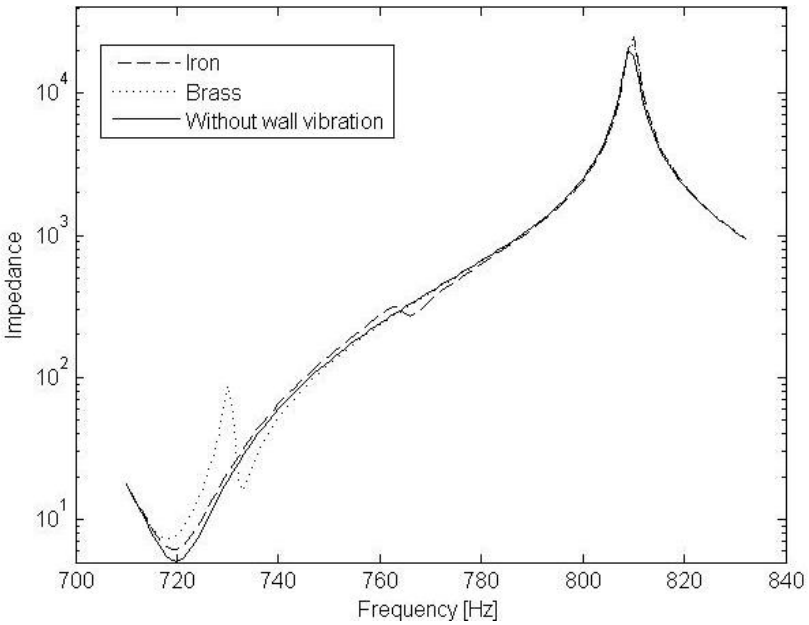

(a) Acoustical input impedance

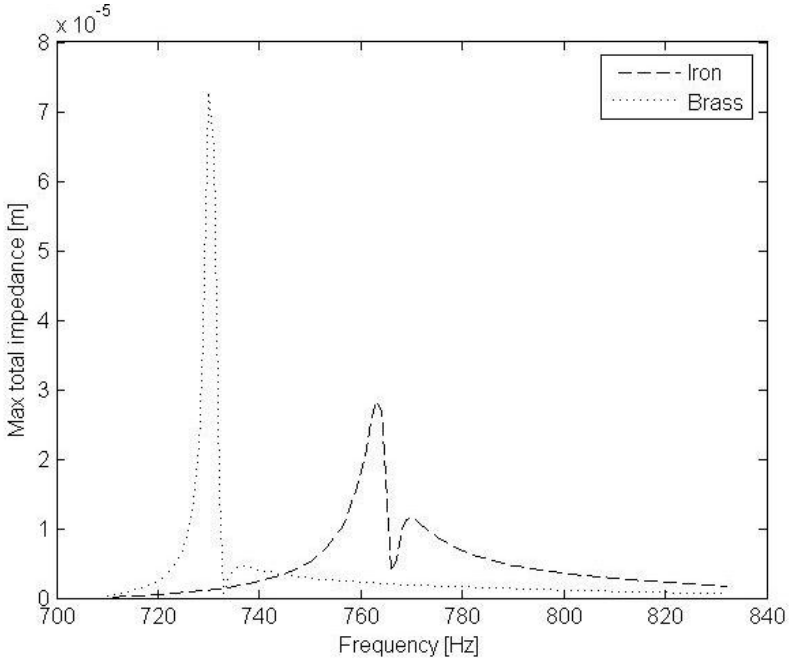

(b) Maximum total displacement

Figure 4.40 *The upper figure shows the acoustical input impedance between 710 and 832 Hz for a simplified instrument as shown in figure 4.35 . The impedance for two different materials, iron and brass, are shown. Both show small peaks corresponding to the peaks in the mechanical impedance of the walls, which is plotted in the lower figure*

.

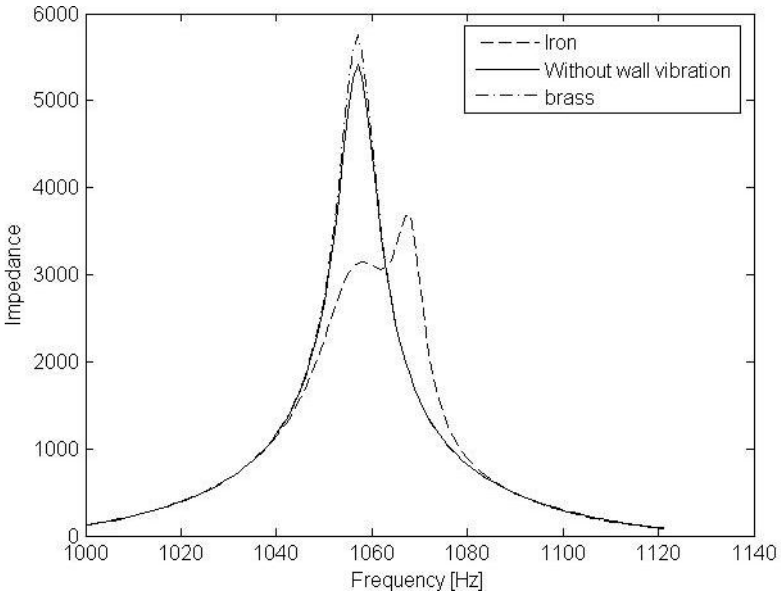

(a) Acoustical input impedance

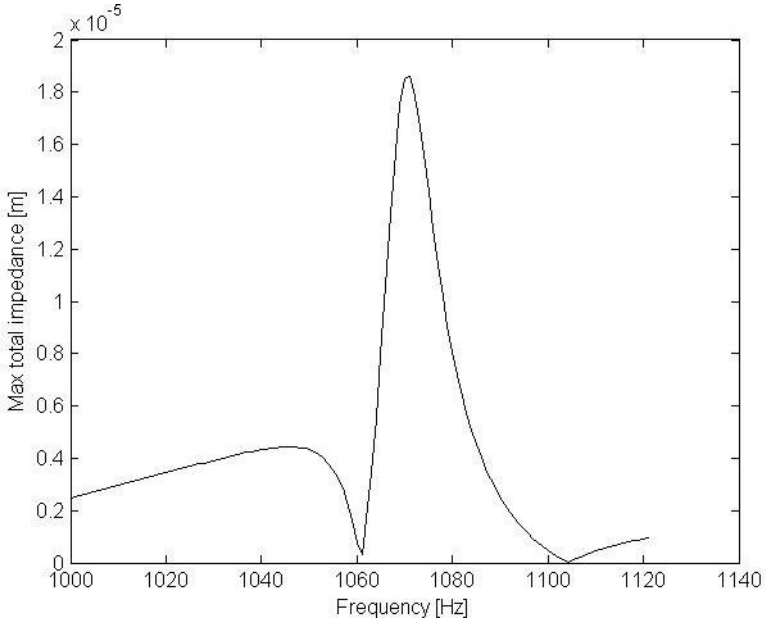

(b) Maximum total displacement

Figure 4.41 *The upper figure shows the acoustical input impedance between 1000 and 1121 Hz for a simplified instrument as shown in figure 4.35 but with an additional 20 cm added so that the peaks of the mechanical impedance for iron (in the right figure) coincide with the one of the peaks in the acoustical input impedance for the air column. The acoustical input impedance peak is wider and split compared to both the impedance for a iron tube with vibrating walls and a tube with fixed walls.*

3 D simulations

For 3 dimensional simulations of other shapes than cylindrical, the trend is similar to that of the cylindrical case : the maximum total displacement shows more peaks in 3 D than in 2 D, but the form doesn't change as much as for the cylinders, as can be seen in figure 4.42. The deviations in the frequencies of the minima between the 2D and the 3D calculations for higher frequencies are probably due to different resolutions; the 2D simulations normally had better resolution than the 3D simulations. Figure 4.43 shows that the main parts of the displacement for the major peaks are at the bell for 6 first excited eigenmodes.

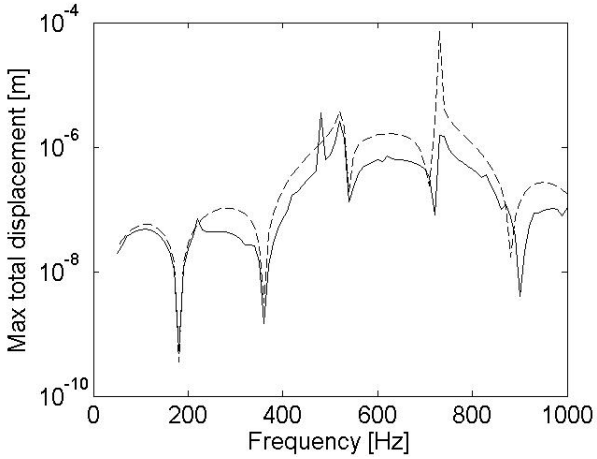

(a) Total max displacement for 2D and 3D

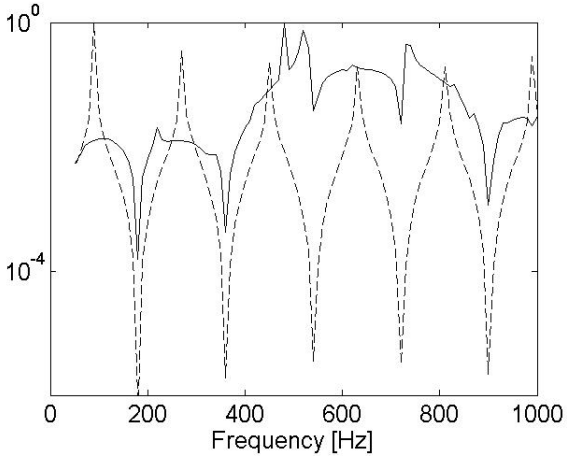

(b) Normalized total max displacement for 2D and acoustical input impedance

Figure 4.42 *Total maximum displacement for a simplified brass instrument for 2D (dotted) and 3D (solid) simulations and log of the normalized total maximum displacement and acoustical input impedance for the same simplified brass instrument.*

Figure 4.44 shows the difference in the sound radiated from two similar instruments of

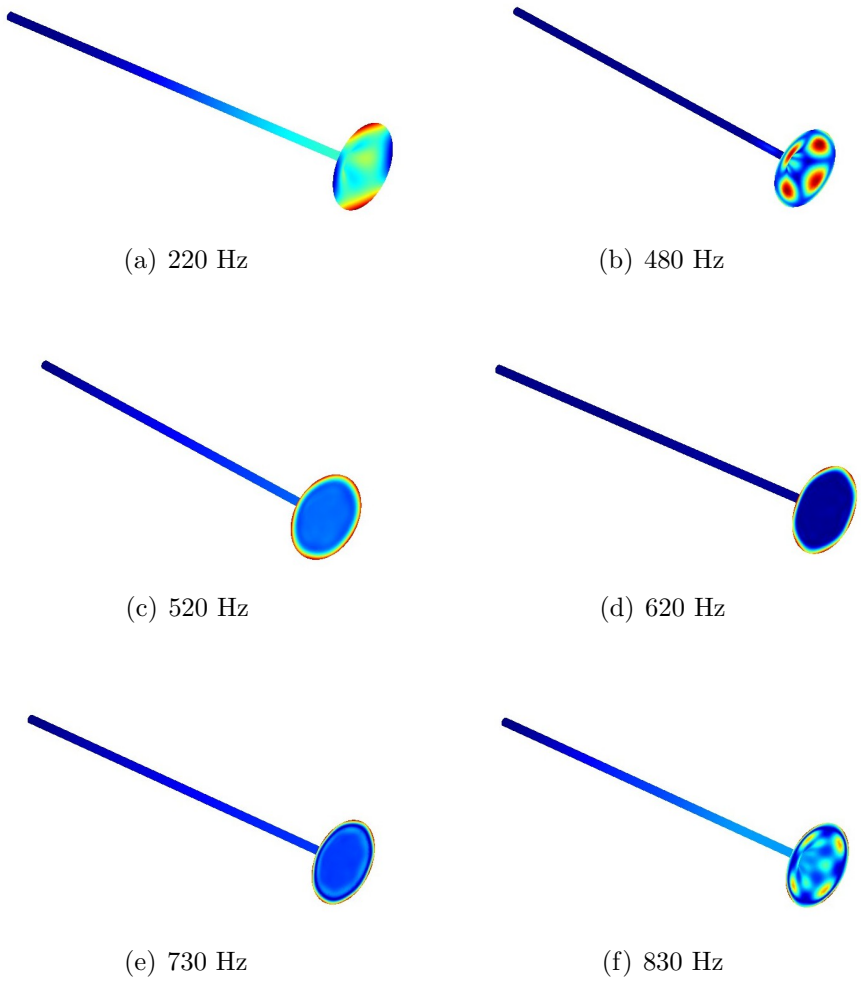

(a) 220 Hz (b) 480 Hz

(c) 520 Hz (d) 620 Hz

(e) 730 Hz (f) 830 Hz

Figure 4.43 *Vibration patterns for the mechanical resonance peaks for the instrument in figure 4.42. The frequencies are, from left to right, top to bottom, 220 Hz, 480 Hz, 520 Hz, 730 Hz and 830 Hz*

different materials (lead and brass) excited at 175 Hz with a shaker at the bottom end. The lead instrument has a structural resonance at this frequency, so the sound is radiated around and out from the bell. The brass instrument doesn't have a structural resonance, so the sound radiated from the body is as strong as the sound radiated from the bell. Figure 4.45 shows the vibration pattern and radiated sound of a lead bell excited with a shaker at 168 Hz, where it as a eigenmode as shown in figures 4.45(a) and 4.45(b). The sound radiated in a plane perpendicular to the bell is shown in figure 4.45(c), the sound is strongest close to the bell. Figure 4.46 shows how the directivity of a radiated sound changes when parts of the bell is pinned. In figure 4.46(a) the whole bell is free, in figure 4.46(b) one boundary (from the rim of the bell to excitation, where a real bell would be attached to the instrument) is pinned. In a real instrument, this could be the case if the bell had been repaired or welded for some other reason. The radiation pattern changes significantly, and the sound radiated from the free bell also has higher amplitude.

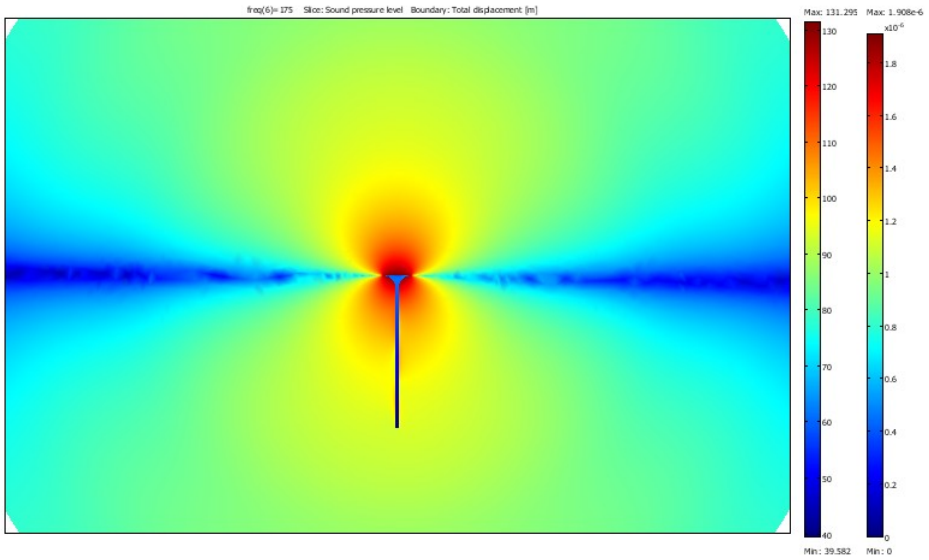

(a) Lead

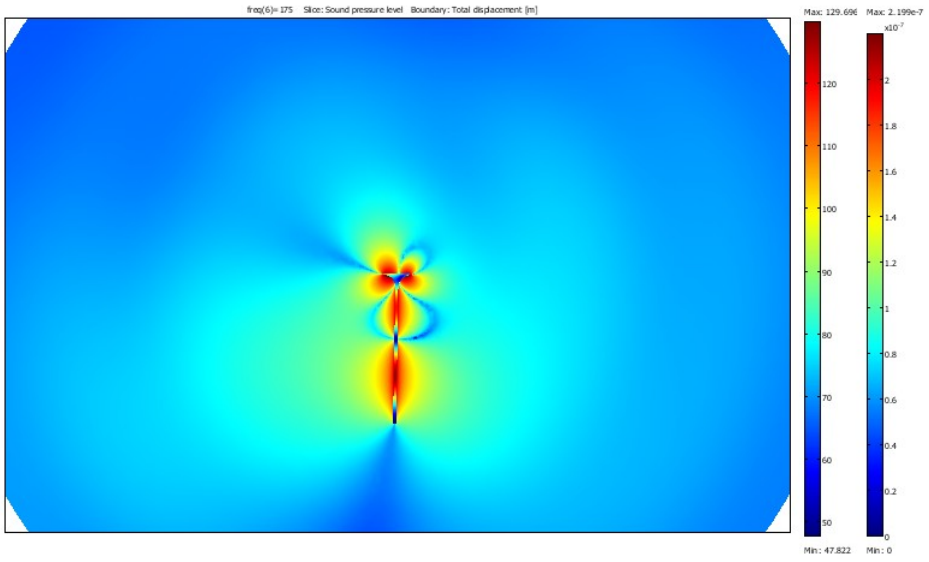

(b) Brass

Figure 4.44 *Sound radiated from the instrument in figure 4.42 made of lead (top) and brass (bottom) when excited with a shaker at 175 Hz*

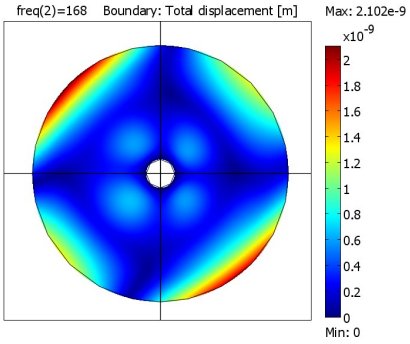

(a) Eigenmode, view from top

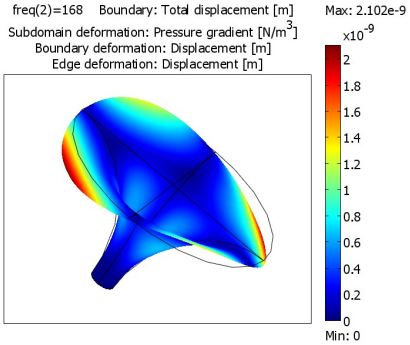

(b) Eigenmode, side view

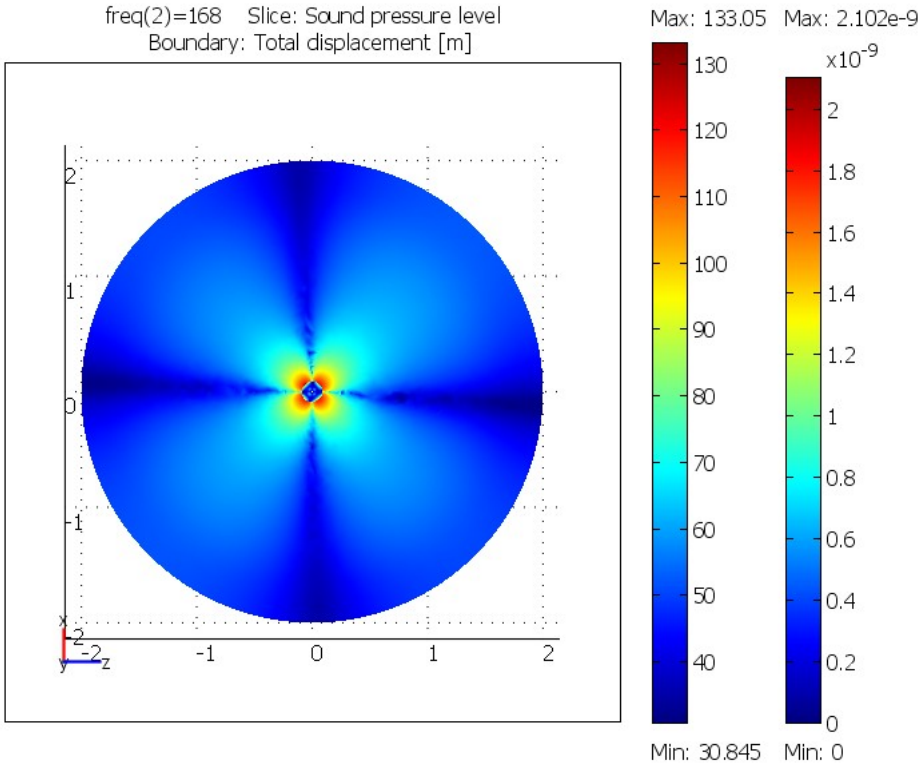

(c) Sound radiated perpendicular to the instrument.

Figure 4.45 *The vibration pattern and radiated sound of a lead bell excited with a shaker at 168 Hz.*

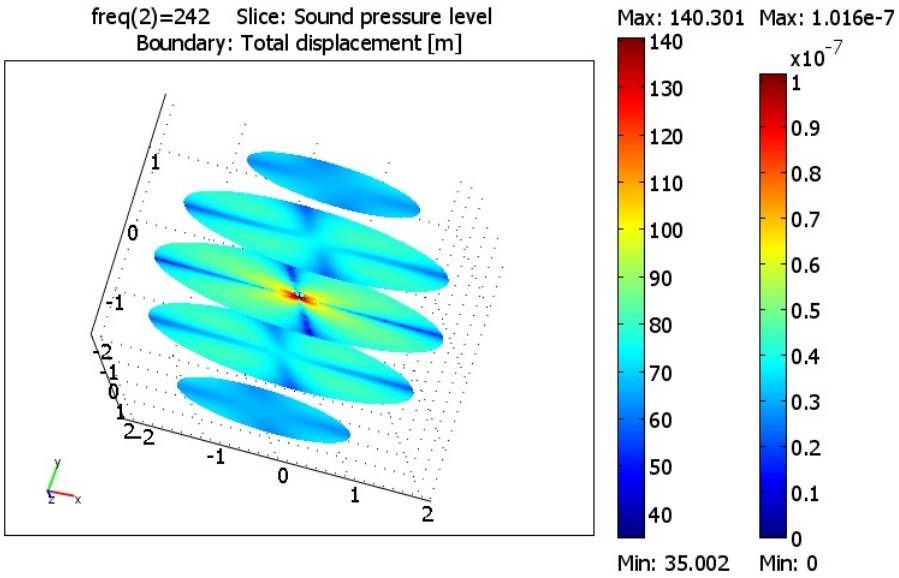

(a) Free bell

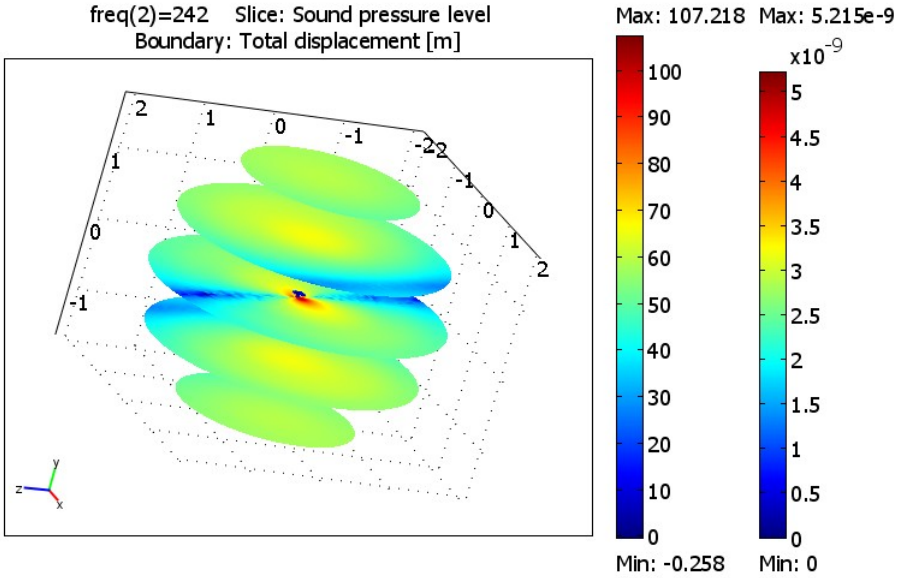

(b) Bell with one pinned boundary

Figure 4.46 *The radiated sound of a lead bell excited with a shaker at 242 Hz. The scale on the x,y and z-axis are in meters.*

4.6 Discussion and conclusion

Despite the general agreement among musicians and instrument makers, scientists don't agree on whether the material of an instrument changes it acoustical characteristics. If it does, there are several ways in which the wall vibrations can influence the instrument. They could change the acoustical input impedance of the instrument, or by radiating sound directly from the walls. It is also possible that the wall vibrations could be transferred to the mouthpiece, thus affecting the players to change the lip tension. The goal of this thesis was to test the two former possibilities, as the later is difficult to test with numerical simulations.

According to the FEM simulations, the wall vibrations can change the acoustical input impedance of a instrument . How much the impedance differs from that of a rigid instrument depends on where the frequencies of the structural eigenmodes are compared to the resonances of the instrument. When the structural eigenmodes and acoustical resonances don't coincide, the acoustical input impedances of instruments with different materials still differ. However, the differences found for the materials used in the FEM simulations are not so big that it would be easy for player or audience to distinguish between different materials (figure 4.12). For cases when the maxima or minima of the acoustical input impedance coincide with a structural resonance, the change is big enough so that it would be likely to be noticed when compared to an instrument of another material. In some cases, resonance peaks split in two or new peaks are created, which would make it possible to distinguish different materials from each other. These results are in good agreement with the results of Nief et al [34] (figure 4.41).

Both the amplitude and the directivity of the sound changes when a structural resonance is excited (figure 4.9). The differences in sound pressure levels between instruments of different materials are big enough to make it likely that the difference in total radiated sound could be audible, assuming that the excitation frequencies coincides with a structural resonance for at least one of the materials (figures [**?**], [**?**]). The differences are bigger close to the instrument. The sound radiated from the walls decreases more rapidly than the sound radiated from the opening/bell, making it likely that differences could be audible to the musician and other people close to the instrument, but not to an audience sitting several meters or more away.

The high Q-values of the maxima in the total displacement caused by structural resonances mean that a small frequency shift would decrease the wall vibrations considerably (figure 4.9). This could mean that excited eigenmodes are a bigger problem for instruments where the excitation is difficult to change while playing, like organs, than for instruments were the musician more easily can adjust the excitation, as brass and wood wind.

Small changes in geometry (for example small irregularities, figures [**?**], [**?**]) of the instrument can shift the frequencies of the excited eigenmodes without changing the acoustical input impedance of the instrument. Avoiding corresponding structural eigenmodes and

acoustical resonances would in most cases not be a problem for an experienced instrument maker, as it could be accomplished by changing the clamping or adding extra weight without changing the bore.

For a brass instrument played at loud levels, the energy in the higher harmonics increases rapidly. It is generally accepted that the main reason for this is a non-linear steepening of the wave-front and creation of shock-waves inside the instrument [46] [45] [47]. As the simulations are linear, any non-linear contributions are not accounted for. In addition to the possibility that the non-linear excitation of the air column could influence the vibrations of the walls, it is also possible that the walls show non-linear behaviour at loud levels, also when the air-column vibrates linearly.

Unlike real instruments, the simulations have mono-frequency excitation so the vibrating air column has only one frequency. For real instruments, there is normally more than one excited air column resonance. This will also influence the wall vibrations. The number of resonances excited normally increases with the sound levels. Some alloys are said to give a brassy sound earlier. As some materials are easier excited than others, it is possible that this is caused by the upper harmonics exciting structural eigenmodes. The difference could then be negligible for low sound levels but significant when playing loudly. It is also possible that certain alloys show more non-linear vibrations than others.

The amplitudes of the wall vibrations for different materials at the same excitation level are quite different. If the musician is influenced by vibrations being transferred through the mouthpiece, there might well be a difference big enough to be noticed by the player even if no one else notices. As the simulations are of stable solutions they don't include transients. The transients are a very important characteristic of the instrument, without them it gets much more difficult to distinguish between different instruments. There could be differences due to the wall vibrations that play a more significant role in the transients than in the stable part of the notes, higher modes that get excited or differences of when the vibrations are noticed by the musician.

Testing the effect of wall vibrations with real instrument is not only expensive, but would also pose other difficulties. Good instrument often have many handmade parts, and so it would be difficult to make sure that they are totally similar (with the exception of the material). Finding a consistent group of testers could also prove difficult. Differences noticed by musicians in allegedly identical instrument of different materials could be caused by small differences of the bore or in the valve mechanisms.

Bibliography

[1] W. Kausel A Musical Acoustician's Guide to Computational Physics Shriftenrehe des Instituts fur Wiener Klangstil - Musikalische Akustik, Universitat fur Musik and darstellende Kunst, Wien - Band 7, 2003

[2] A. Baines Brass Instruments, Their History and Development Dover Publications, 1993

[3] L. E. Kinsler,A. R. Frey, A. B. Coppens, J. V. Sanders Fundamentals of Acoustics, Fourth Edition, John Wiley & sons, 2000

[4] A. H. Benade Horns, Strings, and Harmony Dover Publications, 1992

[5] M. Campbell, C. Greated, A. Myers Musical Instruments Oxford University Press, 2004

[6] D. Noreland Numerical techniques for acoustic modelling and design of brass wind instruments Comprehensive Summaries of the Uppsala Dissertations from the Faculty of Science and Technology 862

[7] J. Backus Input impedance curves for the brass instruments JASA, Vol. 60, No. 2, 470-480

[8] D. Bolger, N. Griffith Multidimensional timbre analysis of shakuhachi honkyoku Conference proceedings, Conference on Interdisciplinary Musicology 10-12/03/2005

[9] P. Farkas The Art of French Horn Playing Summy-Birchland Music 1956

[10] Y. Kagawa, T. Tsuchiya, B. Fujii, K. Fujioka Discrete Huygens' model approach to sound wave propagation Journal of Sound and Vibration, Volume 218, Issue 3, Pages 419-444

[11] T. Tsuji, T. Tsuchiya, Y. Kagawa Finite element and boundary element modelling for the acoustic wave transmission in mean flow medium Journal of Sound and Vibration, Volume 255, Issue 5, Pages 849-866

[12] Y. Kagawa, T. Tsuchiya, K. Fujioka, M. Takeuchi Discrete Huygens approach to sound wave propagation - reverberation in a room, sound source identification and tomography in time reversal Journal of Sound and Vibration, Volume 225, Issue 1, Pages 61-78

[13] Y. Kagawa, T. Tsuchiya, T. Hara, T. Tsuji, Discrete Huygens modelling simulation of sound wave propagation in velocity varying environments Journal of Sound and Vibration, Volume 246, Issue 3, Pages 419-439

[14] U. R. Kristiansen, N. Brachet Diffraction studies using the Transmission-Line Matrix method

[15] H. F. Pollard, E. V. Jansson A Tristimulus Method for the Specification of Musical Timbre Acustica, Volume 52, Pages 162-171

[16] U. R. Kristiansen, M. Dhainaut, T. F. Johansen Finite Difference and Finite Element Methods Fluid-Strucutre Interactions in Acoustics, SpringerWienNewYork, pages 180-219

[17] R. Pyle Audiopyle: Factitious Tones and Hand-Stopping The Horn Call,Vol XXI, No. 1

[18] R. Pyle Audiopyle: Why does my horn feel that way The Horn Call,Vol XX, No. 1

[19] R. Pyle Audiopyle: Why does my horn feel that way The Horn Call,Vol XX, No. 1

[20] C. Lund The archeomusicology of Scandinavia World Archaeology, Volume 12 No. 3

[21] M. Campbell Brass Instruments As We Know Them Today Acta Acustica united with Acustica, Vol. 90 (2004) 600-610

[22] N. H. Fletcher Recent progress in the acoustics of wind instruments Acoust. Sci. & Tech., 22, 3(2001), 169-176

[23] R. W. Pyle The effect of lacquer and silver plating on horn tone Horn Call 11 (1981) 26-29

[24] B. Lawson,W. Lawson Acoustical characteristics of annealed french horn bell flares J. Acoust. Soc. Am 77 (1985) 1913-1916

[25] R. W. Pyle The effect of Wall Materials on the Timbre of Brass Instruments J. Acoust. Soc. Am 103 (1988) 753-754

[26] M. Kob Can wall vibrations alter the sound of a flue organ pipe?

[27] G. Widholm, R. Linortner, W. Kausel, M. Bertsch Silver, Gold, Platinum - and the sound of the flute.

[28] T. R. Moore, E. T. Shirley, I. E. W. Codrey, A.E.Daniels The effects of Bell Vibrations on the Sound of the Modern Trumpet Acta Acustice Vol. 91 (2005) 578-589

[29] J. W. Whitehouse Wall vibrations in musical wind instruments PhD thesis, Open university, 2003

[30] J. W. Whitehouse, D.B. Sharp, N.D. Harrop An investigation into wall vibration induced in wind instruments constructed from different metals

[31] C. J. Nederveen, J. P. Dalmont Pitch and level changes in organ pipes due to wall resonances. Journal of Sound and Vibration, 271 (2004), 227-239

[32] R Pico, F. Gautier, J. Gilbert The wall vibration effect in wind instruments: effect induced by defaults of circularity Conference paper, ISMA 2007

[33] R Pico, F. Gautier, J. Redondo Acoustic input impedance of a vibrating cylindrical tube Journal of Sound and Vibration 301 (2007) 649-664

[34] G. Nief, F. Gautier, J-P Dalmont, J. Gilbert Influence of wall vibrations of cylindrical musical pipes on acoustic input impedances and on sound produced. Conference paper, ISMA 2007

[35] W. Klausel,A. Mayer,G. Nachtmann Experimental demonstration of the effect of wall vibrations on the radiated sound of the horn and a search for possible explanations. Conference paper, ISMA 2007

[36] J. Backus Effect of Wall Material on the Steady-State Tone Quality of Woodwind Instruments J. Acoust. Soc. Am 36 (1964) 1881-1887

[37] G. Nief, F. Gautier, J.-P. Dalmont, J. Gilbert External sound radiation of vibrating trombone bells Conference paper, Acoustics 08

[38] J.-P. Dalmont ACOUSTIC IMPEDANCE MEASUREMENT, PART I: A REVIEW Journal of Sound and Vibration, Volume 243, Issue 3, 7 June 2001, Pages 427-439

[39] J.-P. Dalmont ACOUSTIC IMPEDANCE MEASUREMENT, PART II: A NEW CALIBRATION METHOD Journal of Sound and Vibration, Volume 243, Issue 3, 7 June 2001, Pages 441-459

[40] O. K. Ledang Musikk som skapte historie Studia Musicologica Norvegica, Issue 25, 1999, Pages 236-242

[41] J. Ilkjær Blæsehorn Skalk, Issue 4, 2002

[42] W. Tucker, R. Bates A pitch estimation algorithm for speech and music IEEE Transactions on Acoustics, Speech and Signal Processing, Volume 26, Issue 6, pages 597- 604

[43] D. A. Hendrie Development of Bore Reconstruction Techniques Applied to the Study of Brass Wind Instruments, PhD Thesis http://hdl.handle.net/1842/2582

[44] E. M. Hornbostel, C. Sachs Systematik der Musikinstrumente Zeitschrift fr Ethnologie 46, 1914 (4-5), pages 553-590

[45] S. Stevenson, M. Campbell, S. Bromage, J. Chick, J. Gilbert Motion of the lips of brass players during extremely loud playing J. Acoust. Soc. Am 125, EL152(2009)

[46] A. Hirschberg, J. Gilbert, R. Msallam, A.P.J. Wijnands Schock waves in trombones J. Acoust. Soc. Am 99(3), March 1996, pages 1754-1758

[47] M. W. Thompson, W. J. Strong Inclusion of wave steepening in a frequency-domain model of trombone sound production J. Acoust. Soc. Am. 110 (2001), pages 556-562

[48] E. Briner Reclams Musikinstrumentenführer Philipp Reclam jun. GmbH & Co., Stuttgart, 1988, 1998

[49] COMSOL A/B Acoustics module, User's guide, Version 3.3

[50] COMSOL A/B Structural mechanics module, User's guide, Version 3.3

[51] A. Jordan Akustische Instrumentenerkennung unter Berucksichtigung des Einschwingsvorgangs, der Tonlage und der Dynamik Diplomarbeit zur Erlangung des akademischen Grades Magister artium, Institut fur Wiener Klangstil, Mai 2007

[52] I. Weingerl Klangstudie zur Erkennung von Musikinstrumenten unter Bercksichtigung des Einschwingvorganges Wissenschaftliche Hausarbeit, , Institut fur Wiener Klangstil, 1997

Appendix A

Matlab files

A.1 TLM simulation

```
clear

c1=clock;
opp=4;
N=140;
M=140;
tmax=300;
midt=round([N/2,M/2]);
nodeavstand=1/opp;
r=1;

c=340;
f=200;

tidsavstand=opp*(r*nodeavstand)/(10*c);
R=4*[10 10 10 10 10 10 10 10 10 10 ...
    10 10 10 10 10 10 10 10 10 ...
    10 10 10 10 10 10 10 10 10 10 ...
    10 10 10 10 10 10 10 10 10 ...
    20 20 20 20 20 20 20 20 20 20 20 ...
    20 20 20 20 20 20 20 20 20];% ...


P=zeros(4,N,M);                                    %initializes matrices
PR=zeros(4,N,M);                                   %East=1,North=2,West=3,South=4

S=[-1  1  1  1;
    1 -1  1  1;
    1  1 -1  1;
    1  1  1 -1];

p=1;
```

```
for t=[0:tidsavstand:(tmax-1)*tidsavstand]                %time loop

   P(2,[1:R(1)-1],1)=...
       2*sin(2*pi*f*t)*ones(1,(R(1)-1),1);                %excitation

   for n=1:N
      for m=1:M
         PR(:,n,m)=0.5*S*P(:,n,m);
      end
   end

   Psum(p,:,:)=PR(1,:,:)+PR(2,:,:)+PR(3,:,:)+PR(4,:,:);

   p=p+1                                                  %writes to screen, test in
                                                          %case something hangs


   %for N=1, south border
   P(3,[1:R(1)-1],1)=PR(1,[2:R(1)],1);
   P(3,R(1),1)=PR(3,R(1),1);                              %reflection from east
   P(3,[R(1)+1:N-1],1)=PR(1,[R(1)+2:N],1);
   P(3,N,1)=0;%PR(3,N,1);

   P(1,1,1)=0;%PR(1,1,1);                                 %reflection from west
   P(1,[2:R(1)],1)=PR(3,[1:R(1)-1],1);
   P(1,R(1)+1,1)=PR(1,R(1)+1,1);
   P(1,[R(1)+2:N],1)=P(3,[R(1)+1:N-1],1);

   P(2,[R(1):N],1)=PR(4,[R(1):N],2);                      %the rest of P(2,:,1) is excitation

   P(4,[1:N],1)=0;                                        %absorption at south border
   %P(4,[1:N],1)=PR(4,[1:N],1);                           %reflection from south

   Rl=length(R);

   for w=2:(Rl-1)                                         %horn loop
                                                          %assumes M>length(R)

      sluttpunkt = R(w-1);

      P(3,[1:R(w)-1],w)=PR(1,[2:R(w)],w);
      P(3,R(w),w)=PR(3,R(w),w);                           %west wall


      P(1,1,w)=0;%PR(1,1,w);                              %east wall
      P(1,[2:R(w)],w)=PR(3,[1:R(w)-1],w);

      P(2,[1:sluttpunkt],w)=PR(4,[1:sluttpunkt],w+1);

      P(4,[1:sluttpunkt],w)=PR(2,[1:sluttpunkt],w-1);

      if R(w)==R(w+1)

             if R(w)==R(w-1)
```

```
          P(2,[R(w):R(w)+1],w)=PR(4,[R(w):R(w)+1],w+1);
          P(4,[R(w):R(w)+1],w)=PR(2,[R(w):R(w)+1],w-1);

        elseif R(w)==R(w-1)+1

          P(2,R(w),w)=PR(4,R(w),w+1);
          P(4,R(w),w)=PR(4,R(w),w);

            P(2,R(w)+1,w)=PR(4,R(w)+1,w+1);
          P(4,R(w)+1,w)=PR(2,R(w)+1,w-1);

       else

          P(2,[R(w-1)+1:R(w)+1],w)=PR(4,[R(w-1)+1:R(w+1)+1],w+1);
          P(4,[R(w-1)+1:R(w)],w)=PR(4,[R(w-1)+1:R(w)],w);

          P(4,R(w)+1,w)=PR(2,R(w)+1,w-1);

       end

    elseif  R(w+1)-R(w)==1

       if R(w)-R(w-1)==1

           P(2,R(w),w)=PR(4,R(w),w+1);
              P(4,R(w),w)=PR(4,R(w),w);

           P(2,R(w)+1,w)=PR(2,R(w)+1,w);
           P(4,R(w)+1,w)=PR(2,R(w)+1,w-1);

        else

          P(2,[R(w-1)+1:R(w)],w)=PR(4,[R(w-1)+1:R(w)],w);
          P(4,[R(w-1)+1:R(w)],w)=PR(4,[R(w-1)+1:R(w)],w);

          P(2,R(w)+1,w)=PR(2,R(w)+1,w);
          P(4,R(w)+1,w)=PR(2,R(w)+1,w-1);

      end

else

        P(2,[R(w-1)+1:R(w)],w)=PR(4,[R(w-1)+1:R(w)],w+1);
          P(4,[R(w-1)+1:R(w)],w)=PR(4,[R(w-1)+1:R(w)],w);

       P(2,[R(w)+1:R(w+1)],w)=PR(2,[R(w)+1:R(w+1)],w);
       P(4,[R(w)+1:R(w+1)],w)=PR(2,[R(w)+1:R(w+1)],w-1);



 end

P(3,[R(w)+1:N-1],w)=PR(1,[R(w)+2:N],w);
P(3,N,w)=0;                                          %reflection at west wall
```

```
      P(1,R(w)+1,w)=PR(1,R(w)+1,w);                                %reflection at instrument wall
      P(1,[R(w)+2:N],w)=PR(3,[R(w)+1:N-1],w);

      P(2,[R(w+1)+1:N],w)=PR(4,[R(w+1)+1:N],w+1);

      P(4,[R(w+1)+1:N],w)=PR(2,[R(w+1)+1:N],w-1);

    end

    P(3,[1:R(Rl)-1],Rl)=PR(1,[2:R(Rl)],Rl);
       P(3,R(Rl),Rl)= PR(3,R(Rl),Rl);% PR(1,R(Rl)+1,Rl);       %reflection at instrument wall
       P(3,[R(Rl)+1:N-1],1)=PR(1,[R(Rl)+2:N],1);
       P(3,N,1)=0;%PR(3,N,1);

       P(1,[2:R(Rl)],Rl)=PR(3,[1:R(Rl)-1],Rl);
       P(1,R(Rl)+1,Rl)=PR(1,R(Rl)+1,Rl);
       P(1,[R(Rl)+2:N],Rl)=P(1,[R(Rl)+1:N-1],Rl);

       P(2,[1:N-1],Rl)=PR(4,[2:N],Rl+1);
    P(2,N,Rl)=0;%PR(2,N,Rl);

    P(4,[1:R(Rl-1)],Rl)=PR(2,[1:R(Rl-1)],Rl-1);
     P(4,[R(Rl-1)+1:R(Rl)],Rl)=PR(4,[R(Rl-1)+1:R(Rl)],Rl);       %reflection at instrument wall
    P(4,[R(Rl)+1:N],Rl)=PR(2,[R(Rl)+1:N],Rl-1);

    %outside the instrument
    P(3,[1:N-1],[Rl+1:M])=PR(1,[2:N],[Rl+1:M]);
    P(1,[2:N],[Rl+1:M])=PR(3,[1:N-1],[Rl+1:M]);
    P(2,[1:N],[Rl+1:M-1])=PR(4,[1:N],[Rl+2:M]);
    P(4,[1:N],[Rl+1:M])=PR(2,[1:N],[Rl:M-1]);



       P(3,N,[Rl:M])=0;%PR(3,N,[Rl:M]);                            %east wall

       P(1,1,[Rl:M])=0;%PR(1,1,[Rl-1:M-1]);                        %west wall

       P(2,[1:N],M)=0;%PR(2,[1:N],M);

end

t1=1;

t2=tmax;

lengdet=t2-t1;

Nplot=N;
Mplot=M;
for T=t1:t2

for n=1:Nplot

  for m=1:Mplot
```

```
        sumplot(n,m)=Psum(T,n,m);%Ptest(T,n,m);

    end

end

    F=moviein(lengdet);
   figure(1);

   colormap('pink');

   surfl(sumplot)
   shading interp
   axis([1 Mplot 1 Nplot -5 5]);
   F(:,lengdet)=getframe;

end

surfl(sumplot)
shading interp
c2=clock;
```

A.2 Lur recordings analyzis

```
%Program to analyze recordings of the sound-field inside a lur. The
%microphone was moved out of the lur while the instrument was played. To
%find the first frequecency peak it is assumed that it is the strongest.
%That was always the case for the recordings inside the instruments with a
%frequency above 100 Hz. The amplitude of the three first harmonics inside
%and outside the instrument are found and the former is normalized through
%division with the later.

clear
close all
[y,fs]=wavread('dra12.wav');                    %reads wav-file

plot(y)

testint=100000:101000;                          %intervall to take fft
                                                %of to find 3 first harmonics
spektestinn=abs(fft(hann(length(testint))...
    .*y(testint,2)));                           %fft of signal outside the instrument
spektestut=abs(fft(hann(length(testint))...
    .*y(testint,1)));                           %fft of signal inside the instrument

frekvek=[0:fs/length(testint)...
    :fs*(1-1/length(testint))];                 %frequency vector to get
                                                %right axis in plot
figure
subplot(2,1,1),plot(frekvek,spektestinn)...
    ,axis([0 4000 0 max(spektestinn)])
subplot(2,1,2),plot(frekvek,spektestut)...
    ,axis([0 4000 0 max(spektestut)])

[amputtest(1),maksuttest(1)]=max(spektestinn);  %finds first frequency peak
                                                %(assumes that the first is the strongest)

lengde=length(testint);                         %length of intervall

antall=floor(length(y(:,2))/lengde);            %calculates number of fft windows

for n=1:antall

    spek=abs(fft(hann(lengde)...
    .*y(1+lengde*(n-1):lengde*n,2)));           %finds fft for a hann-time
                                                %window of signal inside
                                                %instrument

    spekut=abs(fft(hann(lengde)...
    .*y(1+lengde*(n-1):lengde*n,1)));           %finds fft for a hann-time
                                                %window of signal outside
                                                %instrument
    [amput(n,1),maksut(n,1)]=...
    max(spek(maksuttest-5:maksuttest+4));      %finds first harmonic inside
                                                %the instrument by searching
```

```
                                                %in area around the fundamental
    maksut(n,1)=maksut(n,1)+maksuttest-6;       %adds integer to get the right value
    [amput(n,2),maksut(n,2)]=...
    max(spek(maksuttest*2-5:maksuttest*2+5)); %finds second harmonic inside
                                                %the instrument by searching
                                                %in the area around 2 * the
                                                %fundamental already
    maksut(n,2)=maksut(n,2)+maksuttest*2-6;
    [amput(n,3),maksut(n,3)]=...
    max(spek(maksuttest*3-5:maksuttest*3+5)); %finds first harmonic inside the
                                                %instrument by searching in the
                                                %area around 3 * the fundamental
    maksut(n,3)=maksut(n,3)+maksuttest*3-6;

    [yamp(n,1),maksinn(n,1)]=...
    max(spekut(maksut(n,1)-5:maksut(n,1)+4)); %first harmonic outside the instrument
                                                %using the value of the
                                                %first harmonic inside the
                                                %instrument
    [yamp(n,2),maksinn(n,2)]=...
    max(spekut(maksut(n,2)-10:maksut(n,2)+10)); %finds amplitude and frequency of
                                                %second harmonic outside the instrument

    [yamp(n,3),maksinn(n,3)]=...
    max(spekut(maksut(n,3)-10:maksut(n,3)+10)); %finds amplitude and frequency of second
                                                %harmonic outside the instrument


    maksinn(n,1)=maksinn(n,1)+maksut(n,1)-6;
    maksinn(n,2)=maksinn(n,2)+maksut(n,2)-11;
    maksinn(n,3)=maksinn(n,3)+maksut(n,3)-11;

    amputnorm(n,:)=amput(n,:)./yamp(n,:);       %normalizes the amplitude of the
                                                %harmonics inside the instrument by
                                                %dividing the amplitude of
                                                %the ones outside the instrument
end

tidvektor=[1/fs:1/fs:length(y(:,1))/fs];        %makes timevector
ynorm=y(:,2)./y(:,1);
figure
subplot(2,1,1),plot(tidvektor,y(:,1))           %plots amplitude afa time
subplot(2,1,2),plot(tidvektor,y(:,2))
xlabel('Time [s]')
tidamput=([1:length(amputnorm(:,1))])*1000/fs+500/fs;
figure
subplot(3,1,1),plot(tidamput,amputnorm(:,1))    %plots amplitude of three
subplot(3,1,2),plot(tidamput,amputnorm(:,2))    %first harmonics afa time
subplot(3,1,3),plot(tidamput,amputnorm(:,3))
xlabel('Time [s]')
```

A.3 Instantaneous frequency

```
%Program that finds the instantaneous frequency of a signal by finding
%the maximum of each period in the time domain

[y,fs]=wavread('leppetrille1.wav');          %reads wav-file

%fest=200;                                   %estimated frequency
[amp(1),topp(1)]=max(y(17850:17950));        %finds amplitude and time
                                             %(in samples) of first period
                                             %in the lipthrill, whereabouts
                                             %of the first period are found
                                             %visualy


topp(1)=topp(1)+17850;                       %adds starting point to get right
                                             %number of samples for the first
                                             %period
midperiode=125;                              %average period
%midperiode=fs/fest;                         %found from visual examination
                                             %of signal or estimated
                                             %frequency
nmaks=2300;                                  %number of periods

for n=2:nmaks                                %finds amplitude and time (in samples)
                                             %til n-th period
    [amp(n),topp(n)]=max(y(topp(n-1)...
        +midperiode-40:topp(n-1)+midperiode+40));
    topp(n)=topp(n-1)+topp(n)+midperiode-41;
end

ll=length(topp)
maks=max(y);

plot(y)                                      %visualy tests that the
                                             %right times are found
hold
for n=1:2                                    %plots two first times
    line([topp(n):0.0001:topp(n)],...
        [0:0.0001:maks],'LineStyle','-','Color','r')
end
for n=ll-10:ll                               %plots 10 last times
    line([topp(n):0.0001:topp(n)],...
        [0:0.0001:maks],'LineStyle','-','Color','r')
end

periode=topp(2:length(topp))...
    -topp(1:length(topp)-1);                 %calculates periods in samples
middelperiode=mean(periode)/fs;              %mean period in seconds
middelfrekvens=1/middelperiode;              %mean frequency
frekvens=(periode/fs).^-1;                   %instantanoeus frequency in Hz

tidsvektor=topp(1:nmaks-1)/fs;               %time vector
```

```
tidsvektor=tidsvektor-tidsvektor(1);        %makes time vector start at 0

figure
plot(tidsvektor,frekvens)                   %plots instantaneous
                                            %frequency as a function of time
xlabel('Time [s]')
ylabel('Frequency [Hz]')
```

Appendix B

Material parameters

Table B.1 *Material parameters*

Material	Young's modulus Pa	Poisson's ratio	Density $\frac{kg}{m^3}$	Thermal expansion factor
American red oak	12.4e9	0.3	630	4.9e-6
Gold	70e9	0.44	19300	14.2e-6
Iron	200e9	0.29	7870	12.e-6
Lead	16e9	0.44	11340	28.9e-6
Brass	100e9	0.34	8500	12e-6

Appendix C

Comsol resolution

The accuracy of the solutions is important when deciding whether it is likely that a found difference is due to numerical discrepancies or physical differences. First the difference between solutions with different accuracy is examined, that show the difference between a simulation where the mesh is fine enough compared to frequency and one with maximum element size that is too big compared to the frequency. Then simulations with good enough accuracy are compared, they should ideally be the same but show differences that follow a frequency depended pattern. Last the accurate frequencies of two resonances are found to see how much the changing the mesh moves the frequency peak.

When creating an unstructured mesh for use with the default second order elements, the maximum element size should be set to 0.2 times the wavelength. For frequency of 600 Hz this equals about 0.11 m. In figure C.1(b) the pattern in the difference between the calculated impedances changes at around 300 Hz where the accuracy of the mesh with the biggest maximum element size starts to worsen. Before 300 Hz the maxima in the difference coincides with the maxima and minima of the impedance, suggesting that the frequency peaks are slightly skewed. The same pattern can be seen in figure C.2(a) where simulations from two different meshes that both have maximum element size under 0.2 * the minimum wavelength but different resolution of the narrow regions resulting in a different mesh size inside the cylinder. Figure C.2(b) shows that this difference can be quite big, figure C.3 show how the first resonance peak for the two meshes differs in amplitude and the fourth resonace peak differs in both amplitude and frequency.

Figure C.5 shows how the frequency of the resonance peaks differs for the different meshes in table C. A possible explanation is that the different meshes in the cylinders opening changes the acoustical length of the cylinder so that the wave sees a different opening for each mesh. Since the bigger frequency shifts don't occur at the same change in mesh for different frequencies, it seems likely that the end correction and its dependency on the mesh are dependent on the frequency.

It is important to compare solutions with equal meshes when possible, if not the main mesh parameters should be kept the same. Solutions that both can be considered correct when judged by the maximum element size are not always the same.

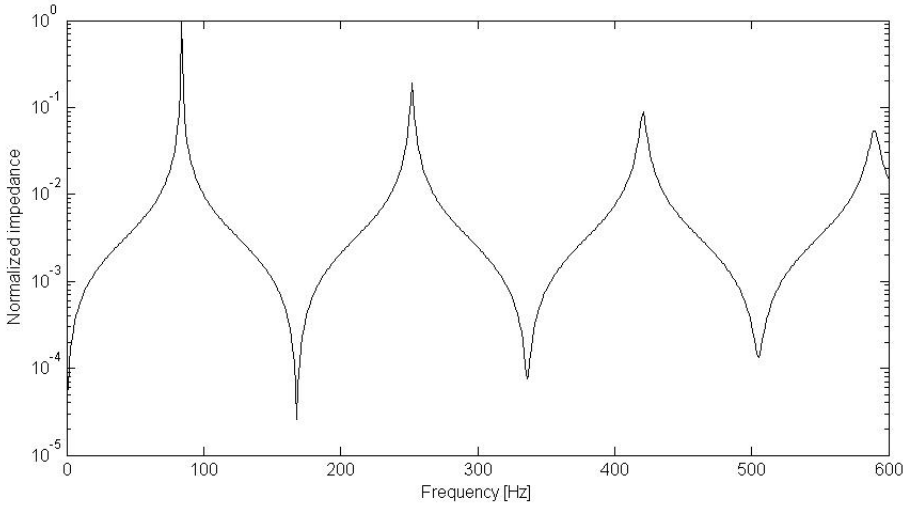

(a) Impedance

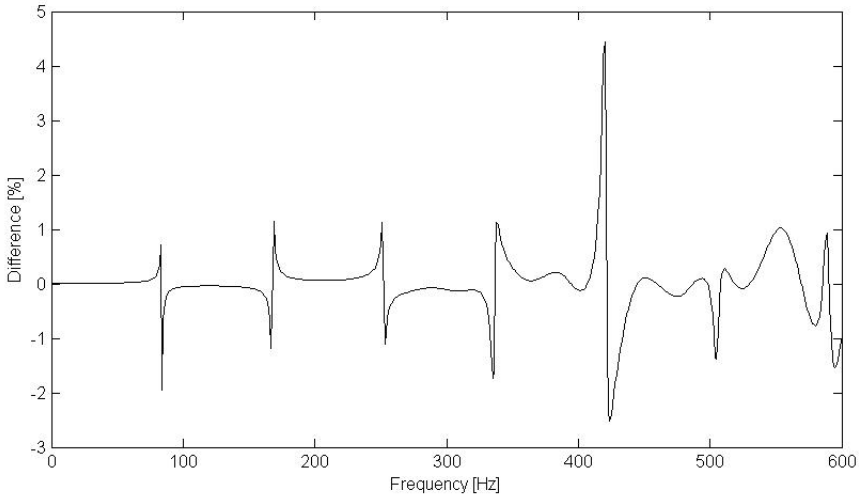

(b) Difference in impedance in %

Figure C.1 *The upper figure shows the impedance of a one meter long and 6 cm wide cylinder. The lower figure shows the difference in the impedance for the cylinder in the upper figure found from two different simulations with different meshes, one with a maximum element size of 0.11 m and the other with a maximum element size of 0.6 m. The other mesh parameters are the same for both meshes.*

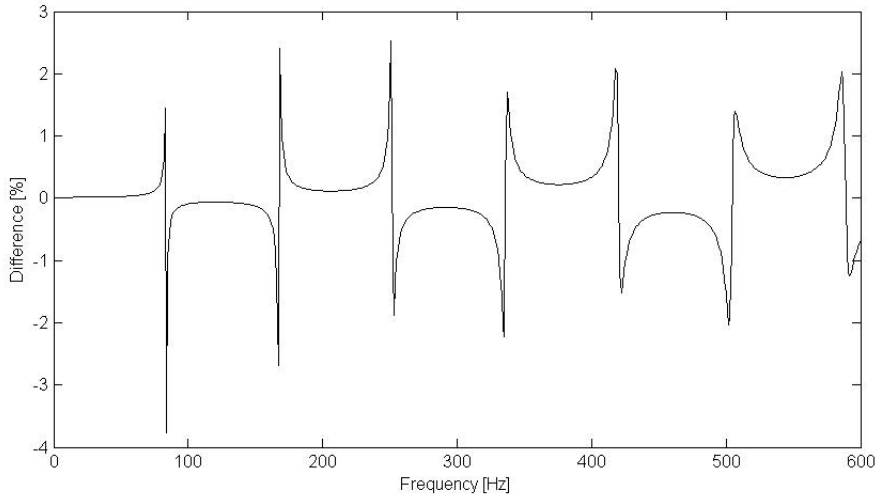

(a) Difference in impedance in %

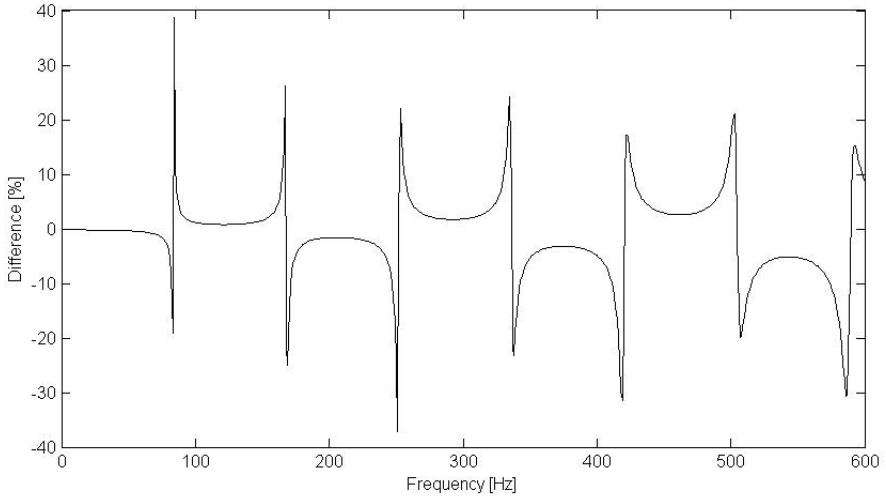

(b) Difference in impedance in %

Figure C.2 *The upper figure shows the difference in the impedance for the cylinder in figure C.1(b) found from two different simulations with different meshes, one with a maximum element size of 0.11 m and a resolution of narrow regions set to 5, the other with a maximum element size of 0.10 and a resolution of narrow regions of 10. The lower figure shows the difference in the impedance for the cylinder in figure C.1(b) found from two different simulations with different meshes, one with a maximum element size of 0.11 m and a resolution of narrow regions set to 1, the other with a maximum element size of 0.10 and a resolution of narrow regions of 10. The other mesh parameters are the same for all meshes.*

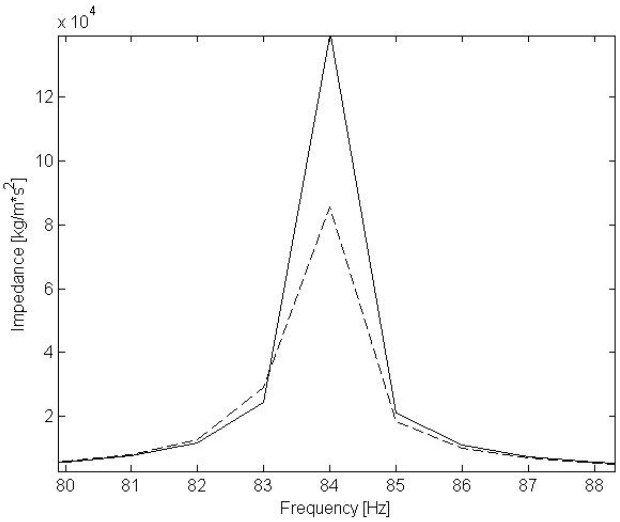

(a) Close-up of first harmonic

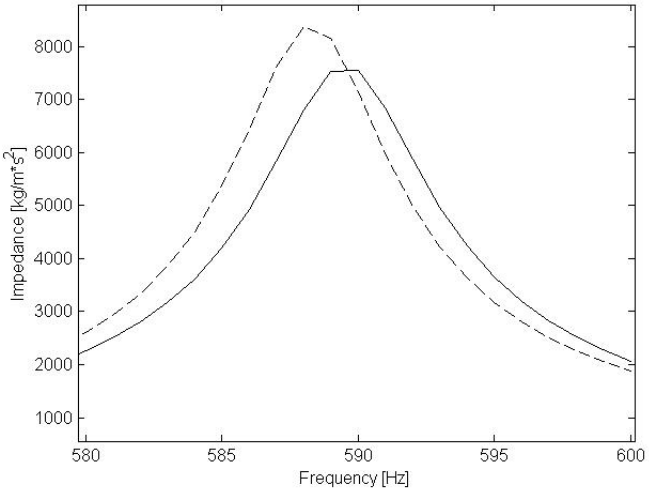

(b) Close-up of fourth harmonic

Figure C.3 *Close up of the impedance of the first and fourth peak for the two meshes from figure C.1(a), one with element size 0.11 and one with element size 0.10 and narrow region resolution 10 (dashed line)*

Table C.1 *Mesh parameters for the different resolutions, maximum element size scaling factor is kept constant at 1, the element growth rate at 1.3, the mesh curvature factor at 0.3 and the mesh curvature cutoff at 0.001.*

Mesh parameter	1	2	3	4	5	6	7	8
Maximum element size	0.3	0.3	0.11	0.11	0.11	0.10	0.10	0.9
Resolution of narrow regions	1	1	1	5	10	10	14	16
Number of elements	1069	2215	7062	8102	10540	11934	14485	17590

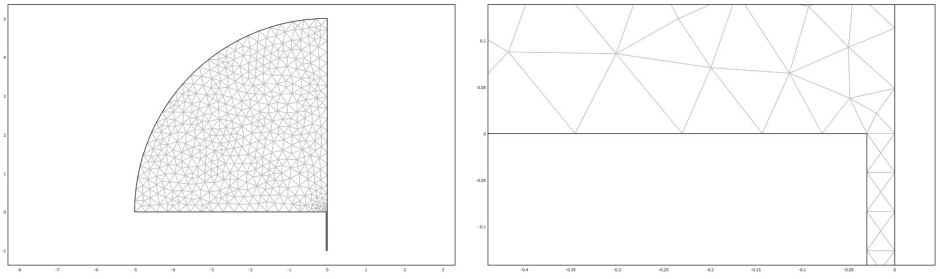

(a) Mesh number 1

(b) Mesh number 1,close-up

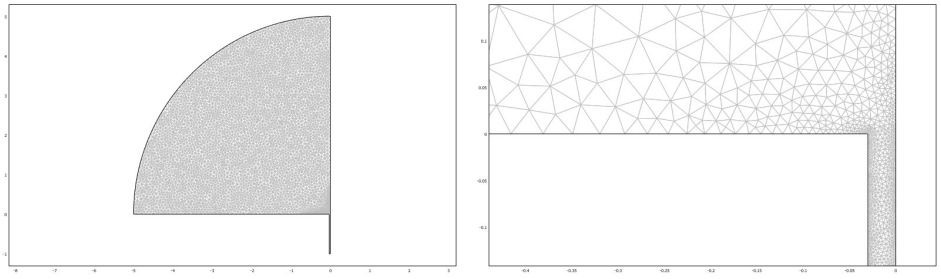

(c) Mesh number 8

(d) Mesh number 8,close-up

Figure C.4 *The mesh and close-up of the opening of the cylinder for mesh 1 and 8 from table C. When the resolution of narrow region is increased the size of the elements inside the cylinder decreases, also when the global maximum element size is kept constant.*

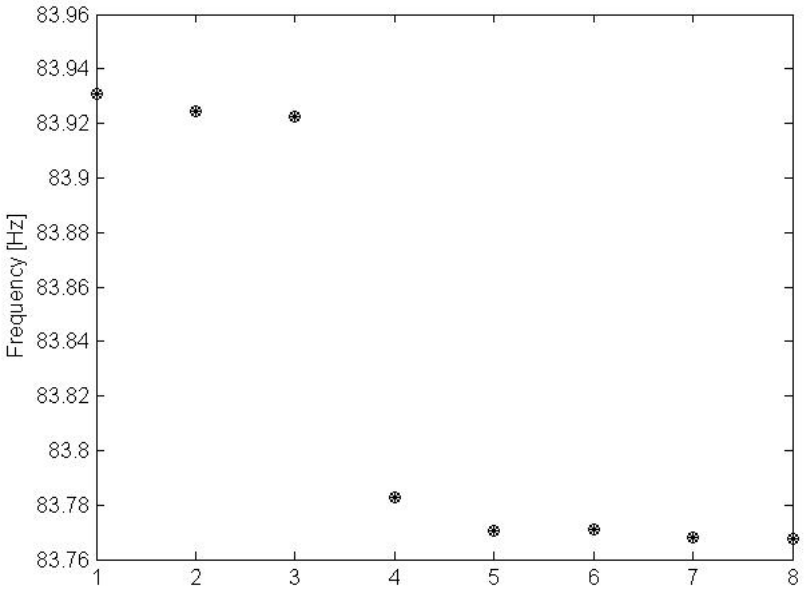

(a) First harmonic

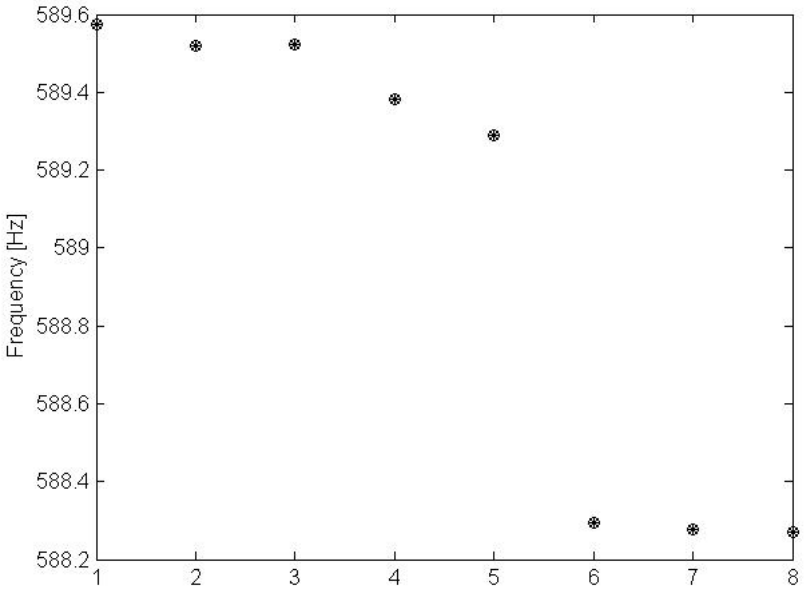

(b) Fourth harmonic

Figure C.5 *The frequency of the first and fourth impedance peak for the cylinder in figure C.1(a) with 8 different meshes from table C*